Characteristic Features of the Scattering of Elementary Particles Arising from their Spin and Electromagnetic Interaction

Geoffrey C. Fox

Trinity College
Cambridge

June 1967

A Dissertation submitted for the Degree of
Doctor of Philosophy at the University of Cambridge

PREFACE

The work presented here is claimed as original except where explicit reference is made to the work of others and no part has been submitted for any other degree or diploma.

I would like to thank both my supervisor, Dr. R.J. Eden, for his help and encouragement, and Dr. E. Leader, on whose original idea Chapter 4 is based. The further development of this chapter has benefited from many useful discussions with Terence W. Rogers. I am grateful to the Science Research Council for a grant, Trinity College for a Scholarship and the Cambridge University Mathematical Laboratory for use of their computer.

Geoffrey C. Fox

Geoffrey C. Fox

Trinity College
Cambridge

June 1967

CONTENTS

CHAPTER 1

Introduction

Most theoretical treatments of the dynamics of strongly interacting particles confine themselves to spinless particles and assume that the introduction of spin into the problem brings only inessential complications. Indeed in most cases spin acts simply as an extra label and may be taken into account by a multichannel formulation. However one must first choose which of the many possible amplitudes, differing by transformations on the spin indices, one will use. As shown in many papers, an unwise choice of amplitude can lead to long calculations and makes a simple generalization appear very complicated. This is particularly so when invariant amplitudes are used without considering whether the information thereby expressed is relevant to the problem at hand.

Recently Hara and Wang have suggested a new way of studying the analyticity of scattering amplitudes for particles with spin. The most important feature of their method is the observation that kinematic singularities arise from the singularities of the Lorentz transformations generating the chosen states. By relating our chosen amplitudes to those generated by Lorentz transformations without these singularities, one can expose the kinematic singularities. The Trueman-Wick crossing relation is a particular case of such a transformation. It is characteristic of this method that it only exposes the singularities locally, and not everywhere as can be done through a suitable choice of invariant amplitudes. However this is usually sufficient as will be seen from the examples considered in this thesis.

In Chapter 2 we give the theory of this method and compare it to the approach via invariant amplitudes. This will concentrate on the full amplitude, while in Chapter 3 we apply the theory to the residues of (fixed) poles in scattering amplitudes, partial wave amplitudes and form factors.

This is extended in Chapter 4 to a treatment of Regge poles. This necessitates a discussion of daughters and conspirators, but they are only considered in enough detail to enable one to apply the theory to the experimental situation. Preliminary results on some fits to the production of ρ, $N^*(1236)$, $K^*(890)$ at medium and high energy are presented.

Throughout this work we shall make the nontrivial restriction to non-zero mass particles and in the Regge section exclude the exchange of fermionic trajectories.

Finally in Chapter 5, which has no connection with the previous work, we consider two practical problems in combining electromagnetism and strong interactions. These are Dashen's calculation of the proton-neutron mass difference and the extraction of Coulomb-nuclear interference from experimental data on elastic scattering at high energies.

CHAPTER 2

The Analyticity of Scattering Amplitudes for Particles with Spin

2.1 General Principles

In this chapter, the theoretical background to the work of chapters 3 and 4 will be described.

First in Section 2.2, we will give a derivation of the Trueman-Wick (hereafter called TW) crossing relation which is sufficiently complete to obtain the unknown phase in their formula. To make this worthwhile, requires a rather careful definition of the states and amplitudes to be used. This has been given by Stapp[S1] and Taylor[T2] and I base my notation on their work. In the appendix to this chapter I have collected all definitions and conventions used in this thesis. Here, for instance, M functions and helicity amplitudes are defined.

The study of the analyticity of scattering amplitudes for particles with spin may be based on the principle

(P) M functions are analytic functions of momenta, and kinematic singularities occur through the choice of their arguments $p_i = p_i(s,t)$ $i = 1 \ldots 4$ to obtain a function of s and t.

From the relation (2.A.7), given in the appendix, between helicity amplitudes and M functions, we may derive[S2] the alternative form of (P) ...

(P') The helicity amplitudes $H_x^{\lambda_4\lambda_3:\lambda_2\lambda_1}(x,y)$ $\{$e.g. x=s, y=t$\}$, where x is energy and y is momentum transfer, are for fixed x, analytic functions of y, except at the physical region boundary where they behave like

$$H_x^{\lambda_4\lambda_3:\lambda_2\lambda_1} \propto \left[\frac{1-\cos\Theta_x}{2}\right]^{\frac{1}{2}|\lambda_i-\lambda_f|} \left[\frac{1+\cos\Theta_x}{2}\right]^{\frac{1}{2}|\lambda_i+\lambda_f|} \qquad (2.1.1)$$

This latter behaviour may for instance be derived from (2.A.7), and the corresponding behaviour for the s-channel c.m. M functions (by this we mean the M function with as arguments the s-channel c.m. momenta) which is given by

$$M_{abcd}(p_s^{c.m.}) \propto \left[\sin\Theta_s\right]^{\frac{1}{2}|a+b+c+d|} \qquad (2.1.2)$$

(2.1.2) may be proved as follows:

The principle (P) enables us to determine the behaviour of $M(p_s)$ at the points $s = (m_i \pm m_j)^2$ by transforming to a frame without this singularity. The singularity at the physical region boundary is however present in all frames but as $\sin\Theta_s \longrightarrow 0$ the c.m. vectors become invariant under rotations about the z-direction. So using the Lorentz transformation law (2.A.6) plus the principle (P) to enable us to expand M in powers of the x and y components of particles 3 and 4, immediately gives the result (2.1.2).

Using the principle (P'), the Trueman-Wick crossing relation (2.2.8) enables us to expose the nature of the singularity of H_s at $s = (m_i \pm m_j)^2$ in the d^{s_i} matrices, since H_t has no such singularity. By this means, Hara and Wang have derived simple linear combinations of H_s which are everywhere nonsingular. Compensating this advantage of simplicity, these amplitudes suffer the disadvantage of containing kinematic zeros. Thus their analyticity, proved from the TW crossing relation (2.2.8), is insufficient to enable us to invert (2.2.8) and prove the input information that H_t is non-singular at s-thresholds. We will meet this in chapter 4 when we consider partial wave residues. The analogous method to that of Hara and Wang will, for instance, say correctly that D waves are analytic functions of s at thresholds, but not that they vanish like $s - (m_1 + m_2)^2$.

In Section 2.3, we show how Hara and Wang's arguments may be extended to derive linear combinations without singularities or zeros (but more complicatedly related to H_s). Unfortunately this argument only works directly if but one particle has spin when only one angle χ_i appears in the TW crossing relation. An extension to more than one spinning particle has only proved possible by the use of M functions. Thus if only particle 1 has spin; H_s is essentially identical to the M function with particle 1 at rest and particle 2 along the z-axis, while H_t is similarly related to the M function with particle 3 along the z-axis. As can be seen from (2.A.6), all particles transform with the same rotation, so the extension to greater than one spinning particles only requires the C.G. series when using M functions. The invariant amplitudes obtained in Section 2.3 are identical with those given earlier by Hepp[H2)] and Williams[W2)]. Thus this section is not intended to be directly useful, but is included to illustrate the complete equivalence of the approach based on (P') and that on invariant amplitudes. The requirement of parity conservation is not simply expressible in terms of M functions, as is familiar from the 4 components necessary in the Dirac formalism to describe a parity conserving spin ½ theory. We conclude Section 2.3 with a brief discussion of how one may try to overcome this difficulty.

Finally in Section 2.4, we present a selection of the various types of amplitudes one can choose from when tackling a particular problem. Here we compare the analyticity structure of M functions; Wigner amplitudes; ordinary, parity-conserving and perpendicular[K1)] helicity amplitudes. Also we introduce a few new ones to compare the behaviour at $s = (m_1 - m_2)^2$ with that at $(m_1 + m_2)^2$.

2.2 Derivation of the Trueman-Wick Crossing Relation

The purpose of this section is to derive the results of Muzinich[M1)] and Trueman and Wick[T1)] with sufficient attention to detail to obtain the phase in their relation. This is largely academic except in the case of elastic reactions where crossing leads to the same reaction and the conventional phases cancel out.

The most elegant derivation is that of Trueman and Wick, who state that amplitudes that transform in the same way under a general Lorentz transformation are identical up to a phase. To be pedantic this is not true as, for instance, an amplitude and its parity conjugate transform in the same way but are not necessarily equal. Indeed in a rather careless application of this method Bialas and Svensson[B1)] manage to "prove" hermitean analyticity. Such a method is presumably unable to determine the phase. Muzinich, by using the M function formalism, has however introduced a method which is sufficient for our purpose here.

The calculation is rather tedious and so we simply outline the main steps and give the final result in (2.2.8).

We wish to determine the relation between the analytic continuation of H_s and H_t in the t physical region. From (2.A.3) and (2.A.7) we have the relation

$$H_s^{\lambda_3\lambda_4:\lambda_2\lambda_1} = e^{-\lambda_3\sigma_3^s} e^{-\lambda_4\sigma_4^s} e^{\lambda_2\sigma_2^s} e^{\lambda_1\sigma_1^s} (-1)^{s_1+s_2+\lambda_1-\lambda_2}$$

$$d^{s_3}_{\lambda_3\mu_3}(-\theta_s)\, d^{s_4}_{-\lambda_4\mu_4}(-\theta_s)\, M_{s\,\mu_3\mu_4:\lambda_2-\lambda_1}(p_s^{c.m.}) \qquad (2.2.1)$$

H_t is similarly expressed in terms of $M_t(p_t^{c.m.})$. M_s and M_t are essentially the same and the required factors in their relation is given in (2.A.8).

If we can find a Lorentz transformation A such that

$$\begin{aligned} p_{1s}^{c.m.} &= A\, p_{1t}^{c.m.} \\ p_{2s}^{c.m.} &= -A\, p_{2t}^{c.m.} \\ p_{3s}^{c.m.} &= -A\, p_{3t}^{c.m.} \\ p_{4s}^{c.m.} &= A\, p_{4t}^{c.m.} \end{aligned} \tag{2.2.3}$$

then we have

$$H_s^{\lambda_3\lambda_4:\lambda_2\lambda_1} = d_{\lambda_4\mu_4}\left[b^{-1}(p_{4s}^{c.m.})Ab(p_{4t}^{c.m.})\right] d_{\lambda_3\mu_3}\left[b^{-1}(p_{3s}^{c.m.})Ab(p_{3t}^{c.m.})C^{-1}\right]$$

$$d_{\lambda_2\mu_2}\left[Cb^{-1}(p_{2s}^{c.m.})Ab(p_{2t}^{c.m.})\right] d_{\lambda_1\mu_1}\left[Cb^{-1}(p_{1s}^{c.m.})Ab(p_{1t}^{c.m.})C^{-1}\right] .$$

$$\cdot\ \eta_{st}\ H_t^{\mu_2\mu_4:\mu_3\mu_1} \tag{2.2.4}$$

where η_{st} contains the conventional crossing phases, "particle 2" phases[J1] and particle re-ordering phases. It is therefore

$$\eta_{st} = \epsilon_{23}\,\epsilon_{34}\,\epsilon_{42}\ \lambda_3^*\,\lambda_2\ (-1)^{s_2-\lambda_2+s_4-\lambda_4} \cdot (-1)^{s_3-\mu_3+s_4-\mu_4} \tag{2.2.5}$$

The rotations in (2.2.3) are (almost) Wigner rotations and it is clearly desirable to use the geometric method introduced by Wick[W3] to evaluate them. In order to obtain the desired precision we first reduce A to a real Lorentz transformation, after which we may use geometry with a greater hope of getting the correct sign. We will treat particles 1 and 2 first and consider 3 and 4 later.

A is a complex Lorentz transformation. We write $A = A_2 A_1$, where A_2 is a trivial combination of a complex boost in the z-direction with parameter $\sigma = \pm i\pi/2$ and rotations through π about the y and z axes. The exact value of A_2 depends on the continuation adopted for H_s in travelling from the s to t physical region. A_1 is a fixed real Lorentz transformation such that $A_1 p_{it}^{c.m.}$ is the set of vectors

$$\begin{aligned}
q_1 &= \left(0,\ 0,\ \frac{-s - m_1^2 + m_2^2}{2\sqrt{-s}},\ \frac{\mathcal{S}_{12}}{2\sqrt{-s}} \right) \\
q_2 &= \left(0,\ 0,\ \frac{s + m_2^2 - m_1^2}{2\sqrt{-s}},\ \frac{\mathcal{S}_{12}}{2\sqrt{-s}} \right) \\
q_3 &= \left(-\frac{\mathcal{S}_{34}\sinh|\theta_s|}{2\sqrt{-s}},\ 0,\ \frac{s + m_3^2 - m_4^2}{2\sqrt{-s}},\ \frac{\mathcal{S}_{34}\cosh|\theta_s|}{2\sqrt{-s}} \right) \\
q_4 &= \left(-\frac{\mathcal{S}_{34}\sinh|\theta_s|}{2\sqrt{-s}},\ 0,\ \frac{-s - m_4^2 + m_3^2}{2\sqrt{-s}},\ \frac{\mathcal{S}_{34}\cosh|\theta_s|}{2\sqrt{-s}} \right)
\end{aligned} \qquad (2.2.6)$$

where $\cosh|\theta_s| = -\cos\theta_s$ is ≥ 1.

This is the set of vectors we would naturally have introduced if we had considered decomposing the scattering amplitude w.r.t. the 2 + 1 Lorentz group for $s<0$, as opposed to the 3 dimensional rotation group appropriate in the s-channel physical region. As is necessary for a negative mass squared representation the little vector $q_1 - q_2 = q_4 - q_3$ is $\propto (0, 0, 1, 0)$.

We split up the rotations in (2.2.4) as, for instance,

$$d\left[Cb^{-1}(p_{2s}^{c.m.})Ab(p_{2t}^{c.m.})\right] = d\left[Cb^{-1}(p_{2s}^{c.m.})A_2 b(q_2)b^{-1}(q_2)A_1 b(p_{2t}^{c.m.})\right]$$

Now both A_2 and A_1 have simple Wigner rotations for particles 1 and 2: that of A_1 may be evaluated geometrically to give the $d^{s_i}(\chi_i)$ (see figure 2.1 and Wick[W3] for the rules) and that of A_2 algebraically. We have now evaluated half of the expression (2.2.4).

To consider particles 3 and 4 we use a frame similar to (2.2.6) but with 34 rather than 12 along the z-axis. Thus we write

$$A = A_2 X^{-1}_{|\theta_s|}(X_{|\theta_s|}A_1) \tag{2.2.7}$$

where $X_{|\theta_s|}$ is a boost in the x-direction with parameter $|\theta_s|$ given after (2.2.6). In figure 1, $X_{|\theta_s|} A_1$ takes us from C_t to X', while $X'X$ represents the pure Lorentz transformation

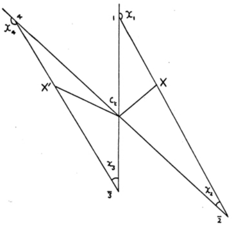

Figure 2.1: Momentum diagram[W3]:
χ_i are defined in (2.A.1d); C_t is the t-channel centre of mass frame; X is the frame (2.2.6); X' is the similar frame with 34 replacing 12; X and X' lie, as drawn, between the particle vectors for $s < -\max \begin{Bmatrix} |m_1^2 - m_2^2| \\ |m_3^2 - m_4^2| \end{Bmatrix}$.

$X_{|\Theta_s|}$. Figure 2.1 is accurate for s,t large and near u = 0, and by going to the physical region boundary the phases in relations such as (2.2.7) may be evaluated.

The $d^{s_1}(\Theta_s)$, in the s-channel boosts $b(p^{c.m.}_{3,4s})$, cancels with the $X^{-1}_{|\Theta_s|}$ to ensure that $A_2 X^{-1}_{|\Theta_s|}$ has a simple Wigner rotation for 3 and 4, while as before $X_{|\Theta_s|}$ A_1 give us the $d^{s_i}(\chi_i)$.

Thereby one obtains the T.W. crossing relation with a phase that depends on the route taken from the s to the t channel. Rather than give the general case we state the answer for the continuation used in Regge theory.

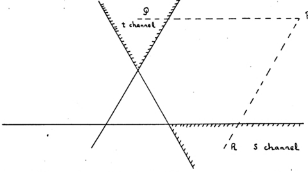

Figure 2.2: Route used for H_s in TW crossing relation. H_s is defined at R, continued at fixed s to P, and then continued at fixed large t to Q.

In the continuation, singularities are met at both the s and t physical region boundaries, and $s = (m_1 \pm m_2)^2$, and $(m_3 \pm m_4)^2$.

The route adopted around the physical region boundaries is such that from $R \to P$ $\phi^{\frac{1}{2}} \to i\ |\phi|^{\frac{1}{2}}$; and from $P \to Q$ $|\phi|^{\frac{1}{2}} \to -i\,|\phi|^{\frac{1}{2}}$, while the route around $s = (m_1 \pm m_2)^2$ is

and similarly for $s = (m_3 \pm m_4)^2$.

These conventions are consistent when in equal mass cases the singularities coincide.

Then finally the TW crossing relation is

$$
\begin{aligned}
H_s^{\lambda_3 \lambda_4 : \lambda_2 \lambda_1} &= \epsilon_{13}\, \epsilon_{34}\, \epsilon_{42}\, \lambda_3^{*}\, \lambda_2 \\
& d_{\lambda_1 \mu_1}(\chi_1)\ d_{\lambda_2 \mu_2}(\chi_2)\ d_{\lambda_3 \mu_3}(\chi_3)\ d_{\lambda_4 \mu_4}(\chi_4) \\
& e^{-i\pi[s_2 - s_3 + \mu_1 + \mu_2 + \mu_3 + \mu_4]} \quad H_t^{\mu_2 \mu_4 : \mu_3 \mu_1}
\end{aligned}
\tag{2.2.8}
$$

The result for other routes of continuation may be derived from this.

2.3 Derivation of Invariant Amplitudes

a) We take the TW crossing relation for a single particle (no.1) with spin. As pointed out in Section 2.1, the helicity amplitudes H_s and H_t are then essentially identical to the M functions, with particle 1 at rest and, respectively, particles 2 and 3 along the z-axis. In fact, independently of the TW crossing relation, it is obvious from figure 2.1 that $\pi - \chi_1$, is the rotation relating these rest frames.

We can trivially extend the treatment to any number of spinning particles by using the C.G. series. Let (j,m) label an irreducible state so formed. We have

$$M^{(j,m)}(p_s^{rest}) = (-1)^m M^{(j,\mu)}(p_t^{rest})\, d_{\mu m}(\chi_1) \qquad (2.3.1)$$

in the t physical region for the route of continuation such that $S_{12} \to |S_{12}|$, $\phi^{\frac{1}{2}} \to |\phi|^{\frac{1}{2}}$.

As described in Section 2.1 our statement of analyticity via the principle (P) implies that:

(i) At the physical region boundary $M(p^{rest}_{s\text{ or }t})$ is proportional to $\phi^{\frac{1}{2}|m|}$ times a function regular there.

(ii) While the other singularities in this case are: $M(p_s^{rest})$ is singular at $S_{12} = 0$; $M(p_t^{rest})$ is singular at $T_{13} = 0$.

We will now try to find some nonsingular linear combinations of $M(p_s^{rest})$, which are not only analytic at $S_{12} = 0$ but whose analyticity there enables one to deduce that $M(p_t^{rest})$ is analytic there. These linear combinations should also enable one to prove the physical region boundary behaviour of M and show that $M(p_s^{rest})$ is analytic at $T_{13} = 0$.

b) This problem is fortunately soluble in triangular fashion. Thus we consider the equation: for any θ and $\eta = \pm 1$

$$d^J_{Jm}(\theta) + \eta\, d^J_{-Jm}(\theta) = \left\{ d^J_{J\mu}(\theta - \chi_1) + \eta\, d^J_{-J\mu}(\theta - \chi_1) \right\} \cdot d^J_{\mu m}(\chi_1) \quad (2.3.2)$$

Then for

I) $\eta = (-1)^J$:

Operate on both sides of (2.3.2) with

$$\frac{\sin^{(J-\ell)}\chi_1}{\ell!} \quad \frac{d^\ell}{d^\ell(\cot\theta)} \quad \frac{1}{\sin^J\theta} \cdots \Bigg|_{\theta = \chi_1} \quad \text{for } \ell = 0 \ldots J$$

and write the resulting equation

$$A^{Jm}_\ell = B^{J\mu}_\ell \; d^J_{\mu m}(\chi_1) \quad (2.3.3)$$

We have

$$A^{Jm}_\ell = (-1)^{J-m} \; B^{Jm}_{(J-\ell)}$$

and (2.3.4)

$$A^{Jm}_\ell = 0 \qquad |m| < \ell$$

Now form

$$\sum_m A^{Jm}_\ell \; (-1)^m \; M^{(J,m)}(p_s^{rest}) = \sum_\mu B^{J\mu}_\ell \; M^{(J,\mu)}(p_t^{rest}) \quad (2.3.5)$$

where ℓ runs from 0 to j. Then from (2.3.4) we have a triangular structure with linear combinations of $M(p_s^{rest})$ (of one less in number each time) equal to linear combinations of $M(p_t^{rest})$ (of one more in number each time).

We must now multiply by some factors to remove the singularities, and so we form the invariant amplitudes:

$$I_\ell^j = \frac{\sum_{m\geq 0} A_\ell^{jm} (-1)^m \left\{ M^{(j,m)}(p_s^{rest}) + (-1)^m M^{(j,-m)}(p_s^{rest}) \right\} \quad [\times \tfrac{1}{2} \text{ if } m=0]}{(\sin^j \chi_1)\ S_{12}^{j-\ell}\ T_{13}^{\ell}} \qquad (2.3.6)$$

$$\text{for } \ell = 0 \ldots j$$

These are proved analytic at $T_{13} = 0$ from (2.3.6), and at $S_{12} = 0$ from the expression (2.3.5) in terms of $M(p_t^{rest})$, and at $\phi = 0$ from either (2.3.5) or (2.3.6).

But as they are triangular these relations may be inverted. Taking for example the $T_{13} = 0$ singularity we start at $m = \ell = j$ and work downwards in m, inverting to find $M^{(j,m)}(p_s^{rest})$ in terms of I_ℓ^j ($\ell \geq m$). At each stage the new $M^{(j,m)}(p_s^{rest})$ has a simple coefficient in $I_{\ell=m}^j$ proportional to $(\sin \chi_1)^{j-m}$, the $T_{13} = 0$ singularity of which is cancelled by the division factors in (2.3.6). Thus we may prove $M(p_s^{rest})$ analytic at $T_{13} = 0$. We can consider S_{12} and $\phi = 0$ similarly and hence find that I_ℓ^j are the desired singularity free amplitudes.

II) $\eta = -(-1)^j$ gives the remaining j invariant amplitudes.

This time we operate on both sides of (2.3.2) with

$$\frac{\sin^{(j-\ell)}\chi_1}{(\ell-1)!} \; \frac{d^{\ell-1}}{d^{\ell-1}(\cot\theta)} \; \frac{1}{\sin^{j-1}\theta} \cdots \Big|_{\theta = \chi_1}$$

for $\ell = 1 \ldots j$

and write the resulting equation

$$\bar{A}_\ell^{jm} = \bar{B}_\ell^{j\nu} \; d^j_{\nu m}(\chi_1) \tag{2.3.7}$$

where

$$\bar{A}_\ell^{jm} = (-1)^{j-m} \; \bar{B}^{jm}_{(j-\ell+1)} \tag{2.3.8}$$

Then, similarly to the previous method, we find the invariant amplitudes

$$\bar{I}_\ell^j = \sum_{m>0} \bar{A}_\ell^{jm} \frac{(-1)^m \left\{ M^{(j,m)}(p_s^{rest}) - (-1)^m M^{(j,-m)}(p_s^{rest}) \right\}}{\sin^j \chi_1 \; S_{12}^{j-\ell+1} \; T_{13}^{\ell}} \tag{2.3.9}$$

c) We can now compare these results with those from other methods. Firstly the method of Hara and Wang would form

$$HW_m^j(s) = \frac{M^{(j,m)}(p_s^{rest}) + (-1)^m M^{(j,-m)}(p_s^{rest})}{S_{12}^j \; \phi^{\frac{1}{2}m}} \qquad \text{for } m \geq 0 \tag{2.3.10}$$

$$\overline{HW}_m^j(s) = \frac{M^{(j,m)}(p_s^{rest}) - (-1)^m M^{(j,-m)}(p_s^{rest})}{S_{12}^{j-1} \; \phi^{\frac{1}{2}m}} \qquad \text{for } m > 0$$

which are indeed nonsingular. We start off with $I^j_j \propto HW^j_j(s)$, but in an endeavour to avoid kinematic zeros, we are forced to take in I^j_{j-1} a linear combination of $HW^j_j(s)$ and $HW^j_{j-1}(s)$ and so on, eventually ending in I^j_0, which contains all $HW^j_m(s)$ and is in fact identical to $HW^j_j(t)$.

Secondly in our paper[F1)] we have shown that the invariant amplitudes I^j_ℓ, $\bar{I}^j_\ell$ are identical to those given earlier by Hepp[H2)] and Williams[W2)]. We do not give the details here as it requires an excess of definitions and they do not appear to be very useful in the problems of interest in this thesis. Thus the Lorentz transformation law (2.A.6) of the M functions is the same whatever the number of spinning particles involved, but the constraint of parity conservation re-introduces a dependence on, for instance, the masses of the particles. In particular, it does not preserve the C.G. series that we constructed at the beginning of this section. Thus, in general, conservation of parity implies

$$M(\underline{p}) = \otimes\, \eta_p \; D\left[\frac{\sigma . p}{m}\right] \; M(-\underline{p}) \tag{2.3.11}$$

or, restricting ourselves to the case when only two particles have spin,

$$P_{\lambda_1\lambda_2}(p) = \otimes\, \eta_p \; M_{\lambda_1\lambda_2}(p) \, ,$$

where P is the parity conjugate M function defined by following

(2.3.11) with a rotation through π about the y axis to take $-\underline{p}$ back to $\underline{p}$.

$$P_{\lambda_1\lambda_2}(p) = (-1)^{s_1+s_2-\lambda_1-\lambda_2} M_{-\lambda_1-\lambda_2}(p) e^{-2\lambda_2\sigma} \qquad (2.3.12)$$

and $\sigma = \sigma_1^s + \sigma_2^s$, where σ_1^s and σ_2^s are defined in the appendix.

We may apply the principle (P) to $P_{\lambda_1\lambda_2}$ just as to M and thereby derive a new set of invariant amplitudes, which are the same linear combinations of P as I and $\bar{I}$ were of M. We must now choose a linearly independent subset of the new invariant amplitudes plus I and $\bar{I}$ for which parity takes a simple form. Fortunately this may also be done triangularly (I am only able to invert such matrices to show no singularities have been introduced!) and the results are given in our paper[F1)]. For this special case - namely when only two particles have spin - Williams and Guertin have also derived invariant amplitudes. These seem more elegant and also achieve the discrete symmetry of particle identity if $s_1 = s_2$, which is not done by my method. However if $s_1 \neq s_2$ my method seems easier to invert. Thus although the general problem of obtaining parity-conserving invariant amplitudes for arbitrary spins has not been solved, in any problem of practical interest the initial writing down of a parity-conserving set is not difficult. The major portion of the work lies in obtaining both formulae for H_s in terms of invariant amplitudes and inversely the invariant amplitudes in terms of H_s. Either direction is easy but having chosen one the other is difficult.

We end this section with two disconnected comments. Firstly Hepp[H2] has shown that the non-singularity of the transformation (2.3.11) implies that it may always be diagonalized to find a singularity-free set of parity-conserving amplitudes. So our quest above to find their explicit form was not doomed to failure from the start. Secondly we have tried to apply the triangular method used in the beginning of this section to the full TW crossing with more than one angle. It produced an elegant set of invariant amplitudes for the case $s_1 = s_2 = 1$, $s_3 = s_4 = 0$, $\otimes \eta_p = 1$ (which is soluble by classical methods anyway) but failed in the case of the same spins but $\otimes \eta_p = -1$ (even though this has fewer independent amplitudes, i.e. four, against five in the former case).

2.4 Comparison of the various Amplitudes used for Spinning Particles

We describe and compare the properties of various types of amplitude that are found to be useful when considering particles with spin.

i) M functions

These are functions of momenta whereas the physical scattering amplitudes are properly regarded as functions of the boosts. They are therefore used in field theory, where integrals over all momenta occur. If we substitute for the argument $p = p_s^{c.m.}$, we find a function which is singular at $s = 0$; $s = (m_1 \pm m_2)^2$ when 1 and 2 are along the z axis; and on the physical region boundary as given in (2.1.2). The M functions behave in the same way at $s = (m_1 - m_2)^2$ as they do at $s = (m_1 + m_2)^2$ because the momenta have similar behaviour at those two points. This contrasts with the helicity and Wigner amplitudes which will be considered later. The singularity at $s = (m_1 \pm m_2)^2$ is easily exposed by rotating the vectors to put 3 and 4 along the z axis. If parity is conserved, the singularity at $s = (m_1 \pm m_2)^2$ is such that it may be removed by an overall factor in the manner of Hara and Wang. If $m_1 \neq m_2$, the singularity at $s = 0$ is exhibited by taking particle 1 to rest.

ii) Wigner Amplitudes

These may, for instance, be found in Goldberger and Watson[G1] who justly claim them to be valid relativistically. Taking those corresponding to 1 and 2 along the z axis, they are related to helicity amplitudes by

$$W_{s:(12)}{}^{\mu_3\mu_4:\mu_2\mu_1} = d^{s_4}_{\mu_4-\lambda_4}(\Theta_s)\; d^{s_3}_{\mu_3\lambda_3}(\Theta_s)\; H_s^{\lambda_4\lambda_3:-\mu_2\mu_1} \qquad (2.4.1)$$

They are singular at the physical region boundary, where they are proportional to $\left[\sin \Theta_s\right]^{\frac{1}{2}\,|\mu_i-\mu_f|}$ (where $\mu_i = \mu_1 + \mu_2$, $\mu_f = \mu_3 + \mu_4$). The other singularities are at $s = 0$, which is not easily dealt with, and at the three thresholds $s = (m_1 \pm m_2)^2$ and $s = (m_3 - m_4)^2$. If parity is conserved these latter singularities may be removed by an overall factor. Wigner amplitudes behave nonrelativistically like M functions. Thus comparing (2.2.1) and (2.4.1) we see the only essential difference between $M(p_s^{c.m.})$ and $W_{s:(12)}$ lies in the boosts $e^{\sigma_i^s}$. These tend to 1 at $s = (m_3 + m_4)^2$, but at $s = (m_3 - m_4)^2$, for instance, $\mathrm{sh}\,\sigma_3^s \to 0$ but $\mathrm{ch}\,\sigma_3^s \to 1$ or -1, if $m_3 > $ or $< m_4$ respectively. This mass dependence and difference between $(m_3 - m_4)^2$ and $(m_3 + m_4)^2$ is characteristic of physical scattering amplitudes, as it is a singularity of the boost not the momenta. The e^{σ} associated with M functions give them the same behaviour at $s = (m_3 \pm m_4)^2$ but destroy the parity transformation law. This is another general feature: the tedious calculations associated with form factors have little effect except achieving the correct behaviour at both $s = (m_3 \pm m_4)^2$.

Wigner amplitudes are usually expanded in terms of orbital angular momenta states,

$$W_{s:(12)}^{\mu_3\mu_4:\mu_2\mu_1} = \sum_{s_i s_f} C(s_1 s_2 s_i : \mu_1 \mu_2)\; C(s_3 s_4 s_f : \mu_3 \mu_4)$$
$$\sum_{\ell_i \ell_f J} (2\ell_i + 1)^{1/2}\, (2\ell_f + 1)^{1/2}\; C(\ell_f\, s_f\, J : \mu_i - \mu_f, \mu_f) \qquad (2.4.2)$$
$$C(\ell_i\, s_i\, J : 0, \mu_i)\; T^{J:s_f s_i}_{\ell_f \ell_i}\; d^{\ell_f}_{\mu_i - \mu_f, 0}(\theta_s)$$

from which we find as usual $T^J_{\ell_f \ell_i} \propto \left[s - (m_3 + m_4)^2\right]^{\frac{1}{2}\ell_f} \cdot \left[s - (m_1 + m_2)^2\right]^{\frac{1}{2}\ell_i}$ but that this behaviour is not in general achieved at $s = (m_i - m_j)^2$. To discuss the behaviour there we define.

iii) <u>W' and H' Amplitudes</u>

As discussed in ii) the only difference in behaviour of helicity amplitudes at $(m_i - m_j)^2$ and at $(m_i + m_j)^2$ lies in the e^{σ} factors in (2.2.1). We thus define quantities to be identical with these factors at $(m_i - m_j)^2$ rather than at $(m_i + m_j)^2$. Namely put

$$H'^{\,\lambda_3\lambda_4:\lambda_2\lambda_1}_s = e^{i\pi(\lambda^i_{lighter} - \lambda^f_{lighter})}\, H_s^{\lambda_3\lambda_4:\lambda_2\lambda_1} \qquad (2.4.3)$$

where, for instance, $\lambda^i_{lighter} = \lambda_k$ where k is the lighter particle of 1 and 2.

Similarly define W' and $T^{J:s'_f s'_i}_{\ell'_f\, \ell'_i}$ by (2.4.1) and (2.4.2) with primes added to all quantities. The $T^J_{\ell'_f \ell'_i}$ are in general completely different from $T^J_{\ell_f \ell_i}$ and behave like $\left[s - (m_1 - m_2)^2\right]^{\frac{1}{2}\ell_i'} \times \left[s - (m_3 - m_4)^2\right]^{\frac{1}{2}\ell_f'}$. If parity is conserved one can however say that the singularity at the lower thresholds in $T^J_{\ell_f' \ell_i}$ may be removed by an overall factor. Notice that for the primed states the effective parity of the lighter particle of 1 and 2 is changed by $(-1)^{2s_{\text{lighter}}}$. This has to be borne in mind when calculating the allowed values of ℓ'. It is illustrated in Chapter 4 when we consider the $N\bar{N}^*$ vertex.

Notice, as a particular case of the difference between primed and unprimed states, that the total spin s_f is not equal to s_f', showing there is no significance of s_f away from the physical region. Thus acting on H or W, s_f states are formed from

$$\sum_{\mu_3+\mu_4=\mu_f} C\,(s_3\ s_4\ s_f : \mu_3\ \mu_4)$$

and s_f' states from

$$\sum_{\mu_3+\mu_4=\mu_f} C\,(s_3\ s_4\ s_f' : \mu_3\ \mu_4)\ (-1)^{s_4 - \mu_4}.$$

This also occurs at s = 0 in equal mass cases and has been remarked upon by Freedman and Wang[F2)].

iv) Helicity Amplitudes J1)

These are the most generally useful amplitudes, whose analyticity has been given in the principle (P'). They are also singular at all the thresholds and this may be exposed, either by the TW crossing relation, or more easily by the relation (2.2.1) to M functions, with either 12 or 34 along the $\hat{z}$ axis. If $m_1 \neq m_2$ and $m_3 \neq m_4$, they are nonsingular at s = 0, which is useful advantage over M or W functions. However the latter are simpler at the thresholds.

v) Parity-conserving Helicity Amplitudes

Hara[H1)] and Wang[W1)] form

$$HW_{s:(\eta_f)}^{\lambda_3\lambda_4:\lambda_2\lambda_1}(s,t) = \bar{H}_s^{\lambda_3\lambda_4:\lambda_2\lambda_1}(s,t) + \eta_f\, \bar{H}_s^{-\lambda_3-\lambda_4:\lambda_2\lambda_1}(s,t) \quad (2.4.4)$$

where

$$\bar{H}_s = \frac{H_s}{B_s^{\lambda_f\,\lambda_i}} \quad ,$$

and the physical region boundary function is given by

$$B_s^{\lambda_f\,\lambda_i} = \left[\frac{1+\cos\theta_s}{2}\right]^{\frac{1}{2}|\lambda_i+\lambda_f|} \left[\frac{1-\cos\theta_s}{2}\right]^{\frac{1}{2}|\lambda_i-\lambda_f|} \qquad (2.4.5)$$

It is important to note that "parity-conserving" is not used in the same sense as in our Section 2.3 on invariant amplitudes and here means that a Regge pole of definite τP contributes to the amplitude. (τ = signature occurs because plain parity would require $z \to -z$). The singularities of these amplitudes may be removed by overall factors as described by Wang[W1], whose results are correct except in the Boson-Fermion case, where she takes the fermion heavier than the boson. (See 2.4 (ii) and (iii) for this mass dependence). These results are not obviously useful because of the kinematic zeros both at thresholds and at $s = 0$, where the original helicity amplitudes were nonsingular. They are certainly not useful for Regge theory as it is much easier and more accurate to study the partial wave residues rather than the full amplitude.

The kinematic zeros at thresholds may be removed by the use of perpendicular helicity amplitudes.

vi) Perpendicular Helicity (or Wigner) Amplitudes

These were introduced by Kotanski[K1] and correspond to quantizing the spin along the y not the z axis. They are related to ordinary helicity amplitudes by:

$$P_s^{p_3p_4:p_2p_1}(s,t) = X_{p_3\lambda_3}(\pi/2)\, X_{p_4-\lambda_4}(\pi/2)\, H_s^{\lambda_3\lambda_4:\lambda_2\lambda_1}(s,t)$$

$$X_{-\lambda_2 p_2}(-\pi/2)\, X_{\lambda_1 p_1}(-\pi/2) \qquad (2.4.6)$$

where $X(\theta)$ is a rotation through θ about the x axis and $X(\pi/2)$ carries the y into the z axis.

The TW crossing relation becomes diagonal when expressed in terms of these amplitudes. This means the non-singularity at s thresholds of P_t is easily expressed without kinematic zeros in terms of P_s.

Unfortunately this is countered by the grave disadvantage that P_s and P_t are both singular at the physical region boundary. Thus it seems that they are only useful locally for expressing the threshold conditions on H_s in terms of simpler linear combinations than the original TW crossing relation and H_t gave.

We finish by listing the behaviour of P_s at the thresholds in more detail. This requires a separate discussion for the three mass types. In Leader's notation, these are denoted,

$$\begin{array}{lll} m_1 \neq m_2, & m_3 \neq m_4 & \text{U U} \\ m_1 = m_2, & m_3 \neq m_4 & E_i U_f \\ m_1 = m_2, & m_3 = m_4 & \text{E E} \end{array} \qquad (2.4.7)$$

a) U U

We will need a phase to describe the route taken round the physical region boundary singularity to reach the thresholds, and suppose $\tan \Theta_s \to i\chi$, $\chi = \pm 1$ at thresholds. Then at the top thresholds $s = (m_i + m_j)^2$

$$P_s^{p_3 p_4 : p_2 p_1} \sim s_{12}^{\chi(p_1 + p_2)} \, s_{34}^{\chi(p_3 + p_4)} \qquad (2.4.8a)$$

while at the bottom thresholds the result is the same, except the index of the lighter particle in each pair (12), (34) is reversed in sign.

At $s = 0$, P_s is nonsingular.

b) $\underline{E_i U_f}$

The results at $(m_3 \pm m_4)^2$ and $(m_1 + m_2)^2$ are as in (a).

At $s = 0$ we have

$$P_s^{p_3 p_4 : p_2 p_1} \sim (\sqrt{s})^{\epsilon (p_1 - p_2)}, \qquad (2.4.8b)$$

where the new phase ϵ is defined by

$$\phi^{\frac{1}{2}} \rightarrow m_1 (m_3^2 - m_4^2)\, i\, \epsilon \qquad \text{as } s \rightarrow 0 .$$

c) $\underline{E\ E}$

The result at the top thresholds is as in (a). $s = 0$ is now a physical region boundary and P_s are no longer well-behaved there. However the TW crossing angles $\rightarrow \pi/2$, and so one can use $d(\pi/2)$ rather than $X(\pi/2)$ to express conditions on H_s, i.e. we have (independent of the route of continuation of H_s)

$$d_{p_3 \lambda_3}(-\pi/2)\, d_{p_4 -\lambda_4}(-\pi/2)\, H_s^{\lambda_3 \lambda_4 : \lambda_2 \lambda_1} d_{-\lambda_2 p_2}(\pi/2)\, d_{\lambda_1 p_1}(\pi/2)$$

$$\sim \sqrt{s}^{\,|p_1 + p_4 - p_2 - p_3|} \qquad (2.4.8c)$$

Appendix: Notation T2), S1)

i) Particles are labelled $i = 1 \dots 4$ and have mass m_i and spin s_i.

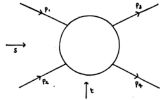

Mandelstam invariants are defined as usual

$$s = (p_1 + p_2)^2 \quad t = (p_1 - p_3)^2 \quad u = (p_1 - p_4)^2$$

ii) Rotations are labelled by Euler angles α, β, γ and written $r(\alpha, \beta, \gamma)$. Their matrix elements $D^j(r(\alpha, \beta, \gamma))$ are defined as in Jacob and Wick[J1] and $d^j_{mm'}(\theta) = D^j_{mm'}(r(0,\theta,0))$. This differs by $(-1)^{m-m'}$ from the definition used in the useful reference[A1] for complex j. We thus define our second type functions $e^j_{mm'}(z)$ to be $(-1)^{m-m'}$ times those in Gunson and Andrews[A1].

Pure Lorentz transformations from rest up to $\underline{p}$ are written $h(\underline{p})$, and $b(\underline{p})$ is a general boost up to $\underline{p}$.

Vector components are written in the order (x, y, z, t).

iii) The kinematic definitions are[W1]

$$\mathcal{S}^2_{ij} = \left[s - (m_i+m_j)^2\right] \cdot \left[s - (m_i-m_j)^2\right] \quad (ij) = (12) \text{ or } (34) \qquad (2.A.1a)$$

and similarly for t and u.

The c-m frames are defined as usual (see section (v) of the appendix), and the s-channel c.m. vectors are denoted $p_{is}^{c.m.}$ $i = 1 \ldots 4$ and we take p_s^{rest} to be the system generated from this by a pure Lorentz transformation reducing particle 1 to rest.

The c.m. scattering angle is given by

$$S_{12}\, S_{34} \cos \theta_s = s(t - u) + (m_1^2 - m_2^2)\,(m_3^2 - m_4^2) \qquad (2.A.1b)$$

$$S_{12}\, S_{34} \sin \theta_s = 2\sqrt{s}\, \phi^{1/2} \quad \text{defines } \phi$$

The boost parameters are defined by

$$\operatorname{ch} \sigma_i^s = E_i^s / m_i \,, \qquad (2.A.1c)$$

where E_i^s are the c.m. energies.

The TW crossing angles are defined by

$$\begin{aligned} S_{12}T_{13} \cos\chi_1 &= (s+m_1^2-m_2^2)\,(t+m_1^2-m_3^2) + 2m_1^2\,\Delta \\ S_{12}T_{24} \cos\chi_2 &= -\,(s+m_2^2-m_1^2)\,(t+m_2^2-m_4^2) + 2m_2^2\,\Delta \\ S_{34}T_{13} \cos\chi_3 &= -\,(s+m_3^2-m_4^2)\,(t+m_3^2-m_1^2) + 2m_3^2\,\Delta \\ S_{34}T_{24} \cos\chi_4 &= (s+m_4^2-m_3^2)\,(t+m_4^2-m_2^2) + 2m_4^2\,\Delta \end{aligned} \qquad (2.A.1d)$$

where

$$\Delta = m_3^2 + m_2^2 - m_1^2 - m_4^2$$

iv) Single Particle States

Particles are described by invariantly normed states

$|\underline{p}, \lambda\rangle$, which have Lorentz transformation law

$$U(\Lambda)\, |\underline{p}, \lambda\rangle = \sum_{\lambda'} |\Lambda \underline{p}, \lambda'\rangle\, D_{\lambda'\lambda}(\omega(\Lambda, \underline{p}))$$

for $\Lambda \in SL(2, \mathbb{C})$ where the Wigner rotation

$$\omega(\Lambda, \underline{p}) = b^{-1}(\Lambda \underline{p})\, \Lambda\, b(\underline{p}) \qquad (2.A.2)$$

Here the boost $b(\underline{p})$ is a Lorentz transformation taking us from rest to momentum $\underline{p}$. Different choices of $b(\underline{p})$ correspond to the different type of spin amplitudes. For

$$\text{Helicity States:} \quad b(\underline{p}) = h(\underline{p})\, r(\varphi, \theta, -\varphi) = r(\varphi, \theta, -\varphi)\, h(|\underline{p}|\ \underline{z}) \qquad (2.A.3)$$

$$\text{Wigner States:} \quad b(\underline{p}) = h(\underline{p}) \qquad (2.A.4)$$

where $\underline{p}$ is in direction (θ, φ).

Spinor states are obtained by extending D to be a representation of the homogeneous Lorentz group and splitting (2.A.2) into its constituent parts. We will only need lower spinor states defined by

$$|\underline{p}, \alpha\rangle = \sum_{\lambda} |\underline{p}, \lambda\rangle\, D_{\lambda\alpha}(C\, b^T(\underline{p})) \qquad (2.A.5)$$

which is independent of b. Thus we have simplified the Lorentz transformation law at the cost of a non-unitary transformation. Here

$$C = \begin{bmatrix} \cdot & -1 \\ 1 & \cdot \end{bmatrix} \in SL(2, \mathbb{C}) .$$

v) Scattering Amplitudes

As usual, define the T matrix by

$$S_{fi} = \delta_{fi} + i(2\pi)^4 \delta^4(P_f - P_i) T_{fi}$$

We can take matrix elements of the T matrix between any of the above type of states. Choosing spinor states, we find M functions which have the Lorentz transformation law

$$M(p) = \otimes D(\Lambda) \quad M(\Lambda^{-1} p) \tag{2.A.6}$$

This can be simplified by use of the C.G. series, thereby reducing the study of the M function describing many particles to that describing one.

The relation between M functions and physical scattering amplitudes is

$$M(p) = \underset{\text{outgoing}}{\otimes D(b)} \quad \underset{\text{incoming}}{\bullet D(b\ c^{-1})} \quad T^{\lambda_4 \lambda_3 : \lambda_2 \lambda_1} \tag{2.A.7}$$

where b are given by (2.A.3), (2.A.4) for Wigner or helicity amplitudes. It is also customary[J1)] to insert an extra factor $(-1)^{s_2 - \lambda_2} (-1)^{s_4 - \lambda_4}$ in (2.A.7) when dealing with helicity amplitudes.

In (2.A.7) we substitute the usual c.m. momenta for the arguments of M and T. In this thesis we shall always take the c.m. frame of $\langle cd | T | ab \rangle$ to be that with the positive y axis along $\underline{a} \times \underline{c}$, and with $0 \leqslant \theta_{s,t,u} \leqslant \pi$.

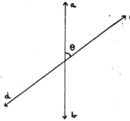

We define the s-channel as $\langle 34 \mid T_s \mid 21 \rangle$ and the t-channel as $\langle \bar{2}4 \mid T_t \mid \bar{3}1 \rangle$, where the ordering of labels defines both the momenta as above and the order of creation operators.

We will call Wigner amplitudes $W^{\mu_4 \mu_3 : \mu_2 \mu_1}$ and helicity amplitudes $H^{\lambda_4 \lambda_3 : \lambda_2 \lambda_1}$ adding a subscript s, t, u to distinguish the various channels.

Also we put $\lambda_i = \lambda_1 - \lambda_2$, $\lambda_f = \lambda_3 - \lambda_4$.

vi) Crossing

In terms of M functions this means we must add a label s, t, u to M in (2.A.7) and introduce a crossing phase λ_a, so that $|a\rangle \to \lambda_a \langle \bar{a}|$ on crossing, where $\bar{a}$ is the antiparticle of a.

λ_a corresponds to the relative phase of the particle annihilation operator a_α and anti-particle creation operator $b_\alpha^\dagger$ in the field theory approach of Weinberg[W4] and Carruthers[C1].

For example

$$\chi_\alpha = \frac{1}{(2\pi)^{3/2}} \int \frac{d^3 p}{2 p_0} \left(a_\alpha \, e^{-i p.x} + \lambda^* \, b_\alpha^\dagger \, e^{i p.x} \right)$$

where α is a spinor index. This is useful if one wishes to use Carruther's[C1] SU_2 crossing relations.

Then, taking account of the change in the ordering of states, we have, on crossing 2 and 3,

$$M_t(p_1,p_2,p_3,p_4) = \epsilon_{23}\, \epsilon_{34}\, \epsilon_{42}\, \lambda_2^*\, \lambda_3\, M_s(p_1,-p_2,-p_3,p_4) \qquad (2.A.8)$$

where $\epsilon_{ij} = +1$, unless i,j are both fermions when it is -1.

When we leave the subscript s, t, u off M, we will mean M_s.

vii) The Crossing Phase λ

Let η_P η_C η_T be the phase factors in the transformations of the single particle states under the discrete transformations of parity, charge conjugation and time reversal respectively.

That is, for Wigner states:

$$P\,|\,\underline{p},\lambda\rangle = \eta_P \quad |-\underline{p},\lambda\rangle$$

$$T\,|\,\underline{p},\lambda\rangle = \eta_T \quad |-\underline{p},\lambda'\rangle \; d_{\lambda'\lambda}(\pi)$$

$$C\,|\,a\rangle = \eta_C \quad |\,\bar{a}\rangle$$

Then $\lambda_a = \lambda_{\bar{a}}$, and the PCT theorem says

$$\lambda_a = \eta_P \eta_C \eta_T \quad \text{for bosons}$$

$$\lambda_{\bar{a}} = i \eta_P \eta_C \eta_T \quad \text{for fermions}$$

ignoring possible superselection rules. The i occurs for fermions because the physical PCT symmetry differs from the crossing relation known as the "PCT theorem" by a complete reversal in the order of all states in the scattering amplitude.

Finally we note that we will take $\eta_T = 1$ in this thesis.

CHAPTER 3

Partial Wave Amplitudes, Pole Residues and Form Factors

3.1 Introduction

In this chapter we describe some applications of the previous chapter to partial wave amplitudes for physical j.

Section 3.2 is devoted to a discussion of the kinematic singularities of partial wave amplitudes. This is necessary if, for instance, one wishes to include the N^*_{1236} in an N/D calculation, and from the spinless case we know how important it is to enforce threshold behaviour to obtain successful results in approximate calculations.

Section 3.3 is devoted to pole residues. It is well known[T3)] that to evaluate one-particle exchange diagrams, instead of using a specific Lagrangian, it is sufficient to put a pole in the crossed partial wave series. We spell this out showing how one may cope with the three pieces of information we think are contained in a phenomenological Lagrangian. These are analyticity, crossing for the $2 \rightarrow 1$ amplitudes and positive definite hamiltonian. These are all easily expressed in an helicity formalism.

Finally in our last physical j application we discuss form factors and the solution they offer for the behaviour at $s = 0$.

We also evaluate the helicity amplitudes for some well known form factors[J2].

Chapter 4 on Regge theory will be an extension of Section 3.4 and the work in Section 3.2 on threshold conditions.

3.2 Partial Wave Amplitudes

We define our helicity partial waves by

$$T^J_{\lambda_3\lambda_4:\lambda_2\lambda_1}(s) = \frac{1}{2}\int_{-1}^{+1} d(\cos\theta)\; d^J_{\lambda_i\lambda_f}(\theta_s)\; H_s^{\lambda_3\lambda_4:\lambda_2\lambda_1}(s,t) \qquad (3.2.1)$$

Kinematic singularities occur at thresholds and at $s = 0$ and we deal with the two cases separately.

(i) The Thresholds

This is the easier case, and we have already shown in Chapter 2 how one can define orbital angular momentum states in terms of which there is an exact statement of the behaviour at $s = (m_i + m_j)^2$. We also defined primed states that behave similarly at $(m_i - m_j)^2$. Namely:

$$T^{J:s_f s_i}_{\ell_f \ell_i} = \frac{(2\ell_i+1)^{1/2}\,(2\ell_f+1)^{1/2}}{(2J+1)} \sum_{\lambda_1\lambda_2\lambda_3\lambda_4} \qquad (3.2.2)$$

$$C(\ell_f\, s_f\, J : 0\, \lambda_f)\quad C(\ell_i\, s_i\, J : 0\, \lambda_i)$$

$$C(s_3\, s_4\, s_f : \lambda_3, -\lambda_4)\; C(s_1\, s_2\, s_i : \lambda_1, -\lambda_2) \qquad T^J_{\lambda_3\lambda_4:\lambda_2\lambda_1}$$

while $T^{J:s_f^{\prime}s_i^{\prime}}_{\ell_f^{\prime}\ell_i^{\prime}}$ is given by the same equation with the extra phase

$$e^{i\pi(\lambda^i_{\text{lighter}} - \lambda^f_{\text{lighter}})},$$

(See (2.4.3) for notation), and

$$T^{J:s_f s_i}_{\ell_f \ell_i} \propto \left[s - (m_3+m_4)^2\right]^{\frac{1}{2}\ell_f} \left[s - (m_1+m_2)^2\right]^{\frac{1}{2}\ell_i}$$

$$T^{J:s_f^{\prime}s_i^{\prime}}_{\ell_f^{\prime}\ell_i^{\prime}} \propto \left[s - (m_3-m_4)^2\right]^{\frac{1}{2}\ell_f^{\prime}} \left[s - (m_1-m_2)^2\right]^{\frac{1}{2}\ell_i^{\prime}}$$

Alternatively one can take "parity-conserving" linear combinations in the manner of Hara and Wang.

Thus form

$$T^{J:(\eta)}_{\lambda_3\lambda_4:\lambda_2\lambda_1} = T^{J}_{\lambda_3\lambda_4:\lambda_2\lambda_1} + \eta\, T^{J}_{\lambda_3\lambda_4:-\lambda_2-\lambda_1} \tag{3.2.3}$$

Then at $s = (m_1 + m_2)^2$ if

$$(-1)^{J-s_1-s_2}\eta = +1 : T^J \propto \left[s - (m_1+m_2)^2\right]^{\frac{1}{2}} \text{ minimum even } \ell_i$$

$$= -1 : T^J \propto \left[s - (m_1+m_2)^2\right]^{\frac{1}{2}} \text{ minimum odd } \ell_i$$

where ℓ_i runs from the $\min\left[0, J-s_1-s_2\right]$ to $J+s_1+s_2$.

Some kinematic zeros can easily be removed by forming total spin linear combinations.

$$\sum_{\lambda_1-\lambda_2=\lambda_i} C(s_1 s_2 s_i : \lambda_1, -\lambda_2)\ T^{J:(\eta)}_{\lambda_3\lambda_4:\lambda_2\lambda_1}$$

for which ℓ_i runs up from $\min\left[0,\ J - s_i\right]$.

At $s = (m_3 + m_4)^2$ we have similar results with $\eta \to \eta$ times the product of intrinsic parities of the particles $(-1)^{s_1+s_2-s_3-s_4}$.

At $s = (m_1 - m_2)^2$ we should replace η by $\eta(-1)^{2s^i_{\text{lighter}}}$.

In boson fermion cases it is customary to regard the amplitude as a function of $\sqrt{s}$. In the results for $\sqrt{s} = -|m_1 \pm m_2|$, as from the argument leading to primed states, we pick up phase factors $e^{\pm i\pi\lambda_k}$ from the e^{σ_k} in (2.2.1) whenever $\text{ch}\sigma_k = -1$.

For example, if $m_1 > m_2$

The correct behaviour for $\sqrt{s} < 0$ may also be obtained from the MacDowell symmetry relation[F4),T3)].

Only in simple cases such as $\pi N \to \pi N$ is it possible to satisfy all these conditions simultaneously without introducing kinematic zeros. A possible approach is to take ordinary orbital angular momentum states to ensure the correct behaviour at the top thresholds, removing the singularity at the bottom threshold with an overall factor, thereby introducing the usual kinematic zeros.

An alternative method is suggested by Regge theory and is rather surprisingly applicable to physical j, with an important proviso to be mentioned later. If one expands asymptotically the Trueman-Wick crossing relation, one finds,

$$\mathcal{G}_{\mu_3\mu_4:\mu_2\mu_1} = \bigotimes_i d_{\mu_i\lambda_i}(\chi_i^{\infty}) \frac{e^{i\pi/2(\lambda_i-\lambda_f)}\, T^J_{\lambda_3\lambda_4:\lambda_2\lambda_1}}{\sqrt{\Gamma(J+\lambda_f+1)\,\Gamma(J-\lambda_f+1)\,\Gamma(J+\lambda_i+1)\,\Gamma(J-\lambda_i+1)}} \cdot \left[\frac{s}{\mathcal{S}_{12}\mathcal{S}_{34}}\right]^J \tag{3.2.4}$$

is nonsingular at s-thresholds. Here χ_1^{∞} is given by (2.A.1d) with t taken to ∞, e.g.

$$\cos\chi_1^{\infty} = \frac{s+m_1^2-m_2^2}{S_{12}} \qquad \sin\chi_1^{\infty} = \frac{2m_1\sqrt{-s}}{S_{12}}$$

The Γ functions come from the asymptotic coefficient of the d^J function.

It is perhaps not obvious that this is the full kinematic condition, but this may be proved by using the method of Kotanski[K1)] to write (3.2.4)

$$P^J_{\gamma_3\gamma_4:\gamma_2\gamma_1} \sim S_{34}^{J+\gamma_3+\gamma_4} \quad S_{12}^{J+\gamma_1+\gamma_2} \tag{3.2.5}$$

As usual the index of lighter particle is reversed at the lower threshold, and

$$P^J_{\gamma_3\gamma_4:\gamma_2\gamma_1} = \sum_{\lambda_3\lambda_4\lambda_2\lambda_1} T^J_{\lambda_3\lambda_4:\lambda_2\lambda_1} \tag{3.2.6}$$

(to be continued)

$$X^{s_4}_{\gamma_4 -\lambda_4}(\pi/2)\ X^{s_3}_{\gamma_3\lambda_3}(\pi/2)\ X^{j}_{j\lambda_f}(\pi/2)\ X^{j}_{\lambda_i j}(-\pi/2)\ X^{s_2}_{-\lambda_2\gamma_2}(-\pi/2)$$

$$X^{s_1}_{\lambda_1\gamma_1}(-\pi/2) \qquad \text{(3.2.6 continued)}$$

We can now easily prove the equivalence of the orbital angular momentum conditions and (3.2.5) by acting the C.G. coefficients in (3.2.2) on the rotations by $\pi/2$ about the x axis in (3.2.6).

(3.2.4) are splendid states except that for $j < \max(s_1 + s_2, s_3 + s_4)$ the "nonsense conditions" imply that not all the states are linearly independent. There seems no easy way round this, and we will comment on it later in Regge theory, where these conditions occur when the trajectory passes through physical values of j and not for all s.

We end by remarking that in our analysis at $s = (m_i - m_j)^2$ we excluded the case - which occurs in elastic (e.g. πN) scattering - where the threshold condition is spoilt by a singularity $u = (m_i + m_j)^2$ entering the region of integration. If this happens it is best to split the amplitudes into two parts - the major part without the singularity to which our theory applies, and a small portion treated separately.

(ii) <u>s = 0</u>

Finally we discuss the behaviour at s = 0. According to Freedman and Wang[F3),F4)], this is dominated by the leading Regge pole and one should remove a factor s^{α}. We do not believe this is always the correct approach to N/D equations. Writing a fixed s dispersion relation for $H_s^{\lambda_3\lambda_4:\lambda_2\lambda_1}$ namely

$$H_s^{\lambda_3\lambda_4:\lambda_2\lambda_1}(s,t) = B_s^{\lambda_f\lambda_i}(z_s)\left\{ \frac{1}{\pi}\int^{\infty}\frac{dt'}{t'-t}\; D_{t'}^{\lambda_3\lambda_4:\lambda_2\lambda_1} + \frac{1}{\pi}\int^{\infty}\frac{du'}{u'-u}\; D_{u'}^{\lambda_3\lambda_4:\lambda_2\lambda_1}\right\} \tag{3.2.7}$$

where $B_s^{\lambda_f\lambda_i}$ is defined in (2.4.5), we write T^J in Froissart-Gribov form

$$\pi\, T^J_{\lambda_3\lambda_4:\lambda_2\lambda_1} = \int^{\infty} D_{t'}^{\lambda_3\lambda_4:\lambda_2\lambda_1}\, e'^{J}_{\lambda_i\lambda_f}(z_s(t'))\, dz_s(t') + (-1)^{J+\lambda_i}\int^{\infty} D_{u'}^{\lambda_3\lambda_4:\lambda_2\lambda_1}\, e'^{J}_{\lambda_i-\lambda_f}(\bar{z}_s(u'))\, d\bar{z}_s(u') \tag{3.2.8}$$

where $\bar{z}_s(u') = -\, z_s(\Sigma m^2 - s - u')$ in the second integral while $e'^{J}_{\lambda_i\lambda_f} = e^{J}_{\lambda_i\lambda_f}\, B_s^{\lambda_i\lambda_f}(z)$ and e^J is defined in the appendix to Chapter 2.

We must now remove a function of s from T^J so that its left-hand cut discontinuity comes from the cut of e' for $z_{t'} \in [-1\ 1]$ rather than kinematic singularities of $D_{t'}$ or u'.

For the case of UU scattering (see (2.4.7) for this notation) the structure of the physical region near s = 0 is

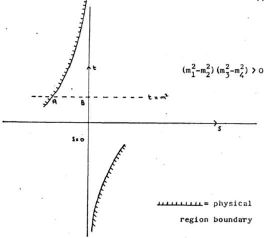

A δ-function contribution to D_t at $t = m^2$ gives rise to, among other things, a left hand cut in T^J between A and B. In particular if we take the discontinuity arising from a Regge pole for large t (and integrate up to $t = \infty$), we will find an $s^{-\alpha}$ behaviour near s = 0. Hence, to enforce this behaviour is both unnecessary and an inferior approximation, as it replaces the cut from A to B by one from $s = -\infty$ to B.

In the case of spin, the Regge contribution is not always the most important near s = 0. We deal with the three mass types separately.

(a) Thus in the UU case the Regge contribution to T^J is proportional to the residue β of the leading Regge pole, where the constant may be evaluated in the same way as[F3] using the Bateman manuscript[B2] and the hypergeometric form of $e^j_{\lambda_i \lambda_f}(z)$[A1].

Putting $\epsilon = \text{sign}\,(m_1^2 - m_2^2)(m_3^2 - m_4^2)$, β must $\sim \sqrt{s}^{\,|\lambda_i + \epsilon \lambda_f|}\, s^{-\alpha(0)}$ and if factorization holds it $\sim \sqrt{s}^{\,|\lambda_i| + |\lambda_f|}\, s^{-\alpha(0)}$. (See Chapter 4).

Meanwhile a general contribution from a finite part of the discontinuity $t = m^2$

$$\sim \quad \frac{s}{\sqrt{s}^{\,|\lambda_i - \epsilon \lambda_f|}} \left\{ \text{finite} + \sqrt{s}^{\,|\lambda_i - \epsilon \lambda_f|} \ln(\pm s) \right\} \tag{3.2.9a}$$

It is this last form which enables one to determine the factor $(\sqrt{s}^{\,(|\lambda_i - \epsilon \lambda_f| - 2)})$ that multiplies T^J, and ensures that the left hand cut comes only from $e'^J_{\lambda_i \lambda_f}(z)$.

(b) In the $U_f E_i$ case we are faced with a kinematic zero difficulty. In terms of the amplitudes of (3.2.3) we have ($s_1 = s_2$)

$$T^{J:(\eta)}_{\lambda_3 \lambda_4 : \lambda_2 \lambda_1} \sim s^{-s_1} \quad \text{if} \quad \eta(-1)^{J+\lambda_f+\lambda_1+\lambda_2} = 1$$

$$\text{or} \qquad \sqrt{s}\,.\,s^{-s_1} \quad \text{if} \quad \eta(-1)^{J+\lambda_f+\lambda_1+\lambda_2} = -1 \tag{3.2.9b}$$

It is possible to do better than this by defining yet another type of orbital angular momentum state, by taking (2.2.1) and replacing the boosts for particles 1 and 2 by their values at s = 0. Unfortunately this produces an $e^{i\pi/2\lambda_i}$ and gives difficulty with parity, so I will not pursue it here.

(c) In the EE case it is well known from the NN example[G2] that the conditions (2.4.8c) on H_s require relations between the partial wave amplitudes of different J. The relation (2.4.8c) separates on forming total spin s' states (section 2.4), and in the NN case we have:

$$s_i' = s_f' = 0 \ : \ \text{no condition}$$

$$s_i' = 0 \quad s_f' = 1 : T^J{}^{0'\,0'}_{0\ \pm1} \sim \sqrt{s} \ ,$$

However if $s_i' = s_f' = 1$ all amplitudes are constant at s = 0 but satisfy

$$-\sqrt{J(J+1)}\ A^{J-1} + (J-1)\sqrt{\frac{J+1}{J}}(C^{J-1} - B^{J-1}) + \frac{2J+1}{\sqrt{J(J+1)}}(B^J + C^J)$$

$$+\sqrt{J(J+1)}\ A^{J+1} + (J+2)\sqrt{\frac{J}{J+1}}(B^{J+1} - C^{J+1}) \quad \sim \ s$$

$$\begin{aligned} \text{where}\quad A^J &= T^J{}^{1'\,1'}_{0\ 0} = f_0^J \\ B^J &= T^J{}^{1'\,1'}_{1\ -1} = \tfrac{1}{2}(f_1^J - f_{22}^J) \\ C^J &= T^J{}^{1'\,1'}_{1\ 1} = \tfrac{1}{2}(f_1^J + f_{22}^J) \end{aligned} \qquad (3.2.10)$$

in more usual (and better!) notation.

In general one must satisfy

$$\sum_{\lambda_f \lambda_i} d^{s_f'}_{p_f \lambda_f}(-\pi/2)\; H_s^{\lambda_f:\lambda_i}\; d^{s_i'}_{\lambda_i p_i}(\pi/2) \sim \sqrt{s}^{\,|p_f - p_i|} \qquad (3.2.11)$$

where

$$H_s^{\lambda_f:\lambda_i} = \sum_J (2J+1)\; T^J {}^{s_f'\, s_i'}_{\lambda_f:\lambda_i}\; d^J_{\lambda_i \lambda_f}(\theta_s)$$

I will content myself by noting a method of generating relations such as (3.2.10) in general. It will take no account of the special form of (3.2.11) and simply consists in finding a set of functions f^{ℓ}, independent of λ_i and λ_f, in terms of which we may expand $d^J_{\lambda_i \lambda_f}$. This is a generalization of the method used in[G2], and a suitable set of f^{ℓ} is

α) $\underline{\lambda_i + \lambda_f \text{ even}}$

$$f^{\ell} = \frac{d^{\ell}_{x0}(\theta_s)}{\sin^x \theta_s} \qquad \ell = x \ldots \infty$$

where $x = (s_i' + s_f')/2$ if $s_i' + s_f'$ even

or $x = (s_i' + s_f' - 1)/2$ if $s_i' + s_f'$ odd

β) $\underline{\lambda_i + \lambda_f \text{ odd}}$

$$f^{\ell} = \frac{d^{\ell}_{x+1,0}(\theta_s)}{\sin^x \theta_s} \qquad \ell = x+1, \ldots \infty$$

where $x = (s_i' + s_f' - 2)/2$ if $s_i' + s_f'$ even

$x = (s_i' + s_f' - 1)/2$ if $s_i' + s_f'$ odd

This may be proved by repeated use of the C.G. series and gives relations like (3.2.10) involving in general $2x + 1$ values of j.

3.3 Pole Residues

We consider in decreasing order of importance and complication: analyticity, crossing and the conditions following from a positive definite Hamiltonian.

(i) Analyticity

If T^J, as defined by (3.2.1), has a pole at $s = m^2$, then near there

$$H_s \sim \frac{(2J+1)}{m^2 - s} \quad \gamma^J_{\lambda_4 \lambda_3} \quad \gamma^J_{\lambda_2 \lambda_1} \quad d^J_{\lambda_i \lambda_f}(\theta_s) \qquad (3.3.1)$$

The residue at the pole in H_s is uniquely (and simply) specified, but as usual there is an ambiguity in the off-mass shell continuation. In a dispersion approach this means there is no such thing as the continuation of a pole to an amplitude as it depends on the direction dispersed in and the assumed behaviour at infinity. One could put the pole in invariant amplitudes but as I do not know a generally useful form for these, I will only describe the method of Hara and Wang, which is sufficient as long as one only disperses in one direction at a time. This method has already been described by Trueman T4),01) for treating superconvergence relations and as this is an elegant application I will review his work.

Here we write a dispersion relation at fixed t, and so we can invoke the principle (P') to say

$$f_t = \bar{H}_t \,(\sqrt{-t})^{\left|\lambda_i^t - \epsilon \lambda_f^t\right|}$$

has no singularities in $s(\lambda_i^t = \lambda_1 - \lambda_3,\ \lambda_f^t = \lambda_2 - \lambda_4)$. For convenience I have multiplied by a factor

$$\sqrt{-t}^{\left|\lambda_i^t - \epsilon \lambda_f^t\right|}$$

($\epsilon = \mathrm{sign}[\,(m_1^2 - m_3^2)(m_2^2 - m_4^2)\,]$) to ensure that in the UU case f_t is analytic in t at t = 0.

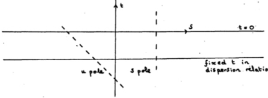

So we can define residues by (3.3.1) for any poles that are present, and evaluate their residue in f_t from the TW crossing relation (2.2.8) at $s = m^2$. This is written down for large s, and one must analytically continue (2.2.8) in s for poles which lie below the s-thresholds. (Notice we have reversed s and t compared with Chapter 2). A similar procedure works for poles in H_u.

The advantage of this application is that it is clearly superior to invariant amplitudes, in that to write down superconvergence relations we need to know the behaviour as $s \to \infty$ of f_t. In Regge theory this is very simple, being

$$f_t \sim s^{\alpha_{\text{leading}}(t) - \Lambda}$$

where $\Lambda = \max\left(|\lambda_i^t| , |\lambda_f^t| \right)$.

We can then decide whether the superconvergence relations of the form $\int_{-\infty}^{\infty} s^n \, \mathrm{Im}\, f_t \, ds$ converge. As usual, if $(-1)^{\Lambda - v}\, \tau = + (-1)^n$, Regge poles of signature τ do not contribute to this relation in leading order. ($v = 0$ except for boson-fermion reactions in the t-channel when it is ½). Also as $t \to 0$ if there is no conspiracy, the contribution of any Regge pole in leading order vanishes like

$$(\sqrt{-t})^{\left\{ |\lambda_i^t| + |\lambda_f^t| - |\lambda_i^t + \epsilon \lambda_f^t| \right\}},$$

which will help the convergence of some relations.

(ii) <u>Crossing</u>

Writing

$$\tilde{\gamma}^{J}_{\lambda_2 \lambda_1} = \sqrt{2J+1} \;\; \gamma^{J}_{\lambda_2 \lambda_1} \tag{3.3.2}$$

the relation (3.3.1) becomes

$$H_s \sim \sum_m \left(\tilde{\gamma}^{J}_{\lambda_4 \lambda_3} \, D^{J}_{\lambda_f m} (R_f^{-1}) \right) \cdot \frac{1}{m^2 - s} \cdot \left(\tilde{\gamma}^{J}_{\lambda_2 \lambda_1} \, D^{J}_{m \lambda_i} (R_i) \right) \tag{3.3.3}$$

where we have split up $\Gamma_{0\,\theta_s\,0} = R_i^{-1} R_f$, where R_i and R_f are rotations relating the initial and final states, respectively, to some standard set of axes.

We can identify

$$T^J_m \begin{matrix} s_2 & s_1 \\ \lambda_2 & \lambda_1 \end{matrix} = d^J_{m\lambda_i}(R_i)\ \tilde{\gamma}^J_{\lambda_2\lambda_1} \qquad (3.3.4)$$

as the helicity amplitude for the reaction $1 + 2 \to 5$, putting $J = s_5$ and $m = \lambda_5$. In particular $\tilde{\gamma}^J_{\lambda_2\lambda_1}$ corresponds to a transition from a state with 1 and 2 along the z axis to particle 5 at rest, with $\lambda_5 = \lambda_i = \lambda_1 - \lambda_2$.

We can now define an M function as in (2.A.7) and then cross particle 5 with 1 or 2 getting a very simple result.

To be definite, take all particles stable so that for instance $(m_1 + m_2)^2 > m_5^2 > (m_1 - m_2)^2$. Then $\tilde{\gamma}^J_{\lambda_2\lambda_1}$ has to be continued past the threshold $s = (m_1 + m_2)^2$ from $s > (m_1+m_2)^2$ where it is real (see part (iii) of this section). Let all amplitudes be continued above the top threshold, i.e.

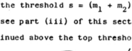

Then on crossing 2 and 5

$$\tilde{\gamma}^J_{\lambda_2\lambda_1} = e^{-i\pi(s_2+s_5)}\ \eta_1^p\, \eta_2^p\, \eta_5^p\, \eta_{25}\ \tilde{\gamma}^J_{\lambda_5\lambda_1} \qquad (3.3.5)$$

where $\eta_{25} = \epsilon_{25} \; \lambda_2 \lambda_5^*$ in terms of the quantities in the appendix to Chapter 2 (here λ is a crossing phase, not an helicity!).

(3.3.5) enables one to express conditions on $\widetilde{\gamma}$ if some of the particles are the same or if they are different, simply to relate poles in different reactions. In this latter case it is usually sufficient to know that the phase in (3.3.5) is independent of helicities.

If one of the particles is unstable, say particle 2, we are in a dilemma as (3.3.5) relates a quantity with $s = m_5^2 < (m_1 - m_2)^2$ to one with $s = m_2^2 > (m_1 + m_5)^2$, and it would imply that the former has a dynamical cut at $s = (m_1 - m_2)^2$ to correspond to the latters unitarity cut at $s = (m_1 + m_5)^2$.

(iii) Positive Definite Hamiltonian

The real analyticity of the full scattering amplitude gives a definite prediction as to the reality of the product of two $\widetilde{\gamma}^J$'s. However the reality of the $\widetilde{\gamma}^J$'s themselves is still undetermined up to a possible factor i. From field theory we can obtain this factor and thereby give a definite sign to the residue of poles in elastic scattering amplitudes. In order to translate this result into the helicity formalism, we temporarily place particle 5 of section (ii) on a Regge trajectory which we suppose to be the leading one. Then taking s above threshold we can make the "narrow resonance approximation" to 2-particle unitarity and assume unitarity is saturated by this one Regge pole. This gives at once the desired sign and shows that for my definitions $\widetilde{\gamma}^{J}_{\lambda_2\lambda_1}$ is real above threshold (in accordance with the approximation the small dynamical imaginary part is neglected). But our residues occur at $s = m_5^2$ below threshold, and we say that the reality conditions can be taken below threshold by expressing them in terms of states, e.g. of orbital angular momentum, which are nonsingular at $s = (m_1+m_2)^2$.

This then says for $(m_1 - m_2)^2 < m_5^2 < (m_1 + m_2)^2$

$$\widetilde{\gamma}^{J}_{\lambda_2\lambda_1} \text{ is real if } \eta_1^P \eta_2^P \eta_5^P = 1$$

$$\text{is pure imaginary if } \eta_1^P \eta_2^P \eta_5 = -1$$

It may be proved algebraically, in case the above argument is unconvincing, that this is identical to the prediction obtained from Weinberg's Feynman rules[W4].

3.4 Form Factors

This may be regarded as an introduction to our work on Regge theory. In Section 3.2 we considered the analyticity of partial wave amplitudes. The analysis of form factors is precisely the same at the thresholds $s = (m_i \pm m_j)^2$ as that given earlier where the conditions are factorizable, and so it is immediately applicable to $\widetilde{\gamma}^{J}_{\lambda_2\lambda_1}$. Therefore, in this section, we will only consider the behaviour at $s = 0$ and give some examples.

(i) $s = 0$

As in Section 3.3(ii), we introduce the 3-particle M function. Written explicitly we have

$$M_{\nu_1 \nu_2 \nu_5} = (-1)^{s_2 - \nu_2} (-1)^{s_1 - \nu_1} e^{\nu_1 \sigma_1^S} e^{-\nu_2 \sigma_2^S} \tilde{\gamma}^{J}_{\nu_2 - \nu_1} \qquad (3.4.1)$$

where $s = m_5^2$, $\nu_1 + \nu_2 + \nu_5 = 0$ and M has arguments

$$p_1 = m_1(0, 0, \operatorname{sh} \sigma_1^S, \operatorname{ch} \sigma_1^S)$$
$$p_2 = m_2(0, 0, -\operatorname{sh} \sigma_2^S, \operatorname{ch} \sigma_2^S)$$
$$p_5 = m_5(0, 0, 0, 1)$$

In field theory we would assume that M obeys the principle (P). This was a satisfactory assumption before, and contained the same information whatever spinor states were used. Thus a lower-dotted spinor state is given in terms of the lower states, that we have previously used, by:

$$|p, \dot{\ell}\rangle = |p, \ell'\rangle \, D_{\ell' \dot{\ell}} \left(C^{-1} \frac{p.\sigma}{m} \right) \qquad (3.4.2)$$

Normally the D matrix gives a polynomial in $\frac{p.\sigma}{m}$ and the principle (P) (analyticity in p) is valid for all spinor states together. Unfortunately in our 3-particle case $s = 0$ corresponds to $m_5 = 0$ and a singularity in (3.4.2). Thus we will find different predictions as to the behaviour at s = 0 of $\tilde{\gamma}^{J}_{\lambda_2\lambda_1}$, corresponding to the infinite number of representations of the homogeneous Lorentz group in which we may place particle 5. All of these results will however be consistent with the analyticity of the full amplitude calculated as

$$\langle \ell_3 \ell_4 | m | \ell_2 \ell_1 \rangle = \langle \ell_3 \ell_4 | m | \ell_5' \rangle \; C^{-1}_{\ell_5' \ell_5} \cdot \frac{1}{m^2 - s} \cdot \langle \ell_5 | m | \ell_2 \ell_1 \rangle \tag{3.4.3}$$

We will consider first the predictions of the lower M function. When $m_1 \neq m_2$ we have

$$\tilde{\gamma}^{J}_{\lambda_2\lambda_1} \sim \sqrt{s}^{\;-\epsilon_i \lambda_i} \tag{3.4.4}$$

where $\epsilon_i = \text{sign}\,(m_1^2 - m_2^2)$.

But parity relates λ_i to $-\lambda_i$ and so we end up with

$$\tilde{\gamma}^{J}_{\lambda_2\lambda_1} \sim \sqrt{s}^{\;|\lambda_i|} \tag{3.4.5}$$

The contradiction with parity (and time-reversal) of (3.4.4) could have been expected as the condition of parity conservation (2.3.11) has a $1/m_5$ in it.

In Regge theory we need only guarantee the analyticity of the amplitude to leading orders as we allow daughters to take care of the nonasymptotic behaviour. Then we find the behaviour

$$\widetilde{\gamma}^{J}_{\lambda_2\lambda_1} \sim \frac{\sqrt{s}^{\,|\lambda_1|}}{\sqrt{s}^{\,J}} \tag{3.4.6}$$

and as expected the form factor predicts a far more dramatic vanishing at $s = 0$.

In the case $m_1 = m_2$, we get results like (3.4.4) but with rotations by $\pi/2$ acting on the indices (see (4.2.9b)). As mentioned at the end of Section 3.2, we may introduce some new orbital angular momentum states, ℓ'' say:

$$\widetilde{\gamma}^{s_i' \ell''} = \sum_{\lambda_1\lambda_2} \widetilde{\gamma}^{J}_{\lambda_2\lambda_1} \; (-1)^{s_2-\lambda_2} \; e^{i\pi/2\,\lambda_i}$$

$$C(s_1 s_2 s_i' : \lambda_1, -\lambda_2) \;\; C(J\, s_i'\, \ell'' : -\lambda_i, \lambda_i)$$

which behave like $\sqrt{s}^{\,\ell''}$. Notice we have the familiar total spin s' linear combinations (Section 2.4).

I have not examined what happens when one places particle 5 in a more general Lorentz group representation, but it is of some interest to consider the case when $s_5 = 1$ and one describes particle 5 by a Lorentz vector A_μ. Then, an application of the principle (P) gives, if $m_1 \neq m_2$,

$$\begin{aligned} \widetilde{\gamma}^{J}_{\lambda_2\lambda_1} &\sim \sqrt{s} & \lambda_i &= 0 \\ &\sim 1 & \lambda_i &= \pm 1 \end{aligned} \tag{3.4.7}$$

We see that the behaviour of the spin-flip and spin non-flip contributions have been exactly reversed, as compared with the prediction (3.4.5) of the lower M-function. Comparing with the Regge prediction (3.4.6), they are the same for the spin-flip but the non-flip has an extra vanishing in (3.4.7).

If $m_1 = m_2$ a similar reversal of flip and non-flip behaviour occurs, when expressed in terms of amplitudes rotated by the usual equal-mass $\pi/2$ w.r.t. $\tilde{\gamma}^J_{\lambda_2\lambda_1}$. This has obvious relevance for the photon preferring to populate states of helicity one, and presumably one can prove a similar theorem to Weinberg's[W5] on the physically acceptable Lorentz representations for the photon.

When doing form factor calculations of ρ exchange, it is customary to use an A_μ field for the ρ and invoke the ρ - photon analogy to pick out a particular form of coupling. In fact only this choice ($G_1 = G_2$ at $s = 0$ see part (ii) for notation) guarantees the analyticity of the amplitude! We will comment further on this when dealing with the reaction $\pi N \to \pi N^*$ in Chapter 4.

(ii) Examples

Here we calculate $\tilde{\gamma}^J_{\lambda_2\lambda_1}$ for some of the form factors used in Jackson and Pilkuhn[J2], whose notation is used. (See also[G3] for some useful information).

This will be useful when comparing their coupling constants and those obtained in Regge theory where $\tilde{\gamma}^J_{\lambda_2\lambda_1}$ is parameterized.

Put $\lambda(a,b,c) = \left[a^2 + b^2 + c^2 - 2(ab + bc + ca)\right]^{\frac{1}{2}}$.

Then

a)

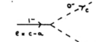

$1^- \rightarrow 0^- \, 0^-$

$$\widetilde{\gamma}_{00} = g' \, \frac{\lambda(m_a^2, m_c^2, m_e^2)}{m_e}$$

b)

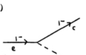

$1^- \rightarrow 0^- \, 1^-$

$$\widetilde{\gamma}_{01} = -\widetilde{\gamma}_{0-1} = \frac{f}{2m_c} \lambda(m_a^2, m_c^2, m_e^2)$$

c)

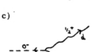

$0^- \rightarrow \frac{1}{2}^+ \, \overline{\frac{1}{2}^+}$

$$\widetilde{\gamma}_{\frac{1}{2}\frac{1}{2}} = -\widetilde{\gamma}_{-\frac{1}{2}-\frac{1}{2}} = G\left[(m_b - m_d)^2 - m_e^2\right]^{\frac{1}{2}}$$

d)

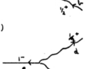

$1^- \rightarrow \frac{1}{2}^+ \, \overline{\frac{1}{2}^+}$

$$\widetilde{\gamma}_{\frac{1}{2}\frac{1}{2}} = \widetilde{\gamma}_{-\frac{1}{2}-\frac{1}{2}} = (g_V + g_T)\,\frac{(m_b + m_d)}{m_e}\,\sqrt{(m_b - m_d)^2 - m_e^2} - g_T\,\frac{\left[(m_b + m_d)^2 - m_e^2\right]}{m_e\,(m_b + m_d)}\,\sqrt{(m_b - m_d)^2 - m_e^2}$$

$$\widetilde{\gamma}_{\frac{1}{2}-\frac{1}{2}} = \widetilde{\gamma}_{-\frac{1}{2}\frac{1}{2}} = \sqrt{2}\,\sqrt{(m_b - m_d)^2 - m_e^2}\,(g_V + g_T)$$

e)

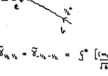

$$0^- \rightarrow \tfrac{1}{2}^+ \; \overline{3/2^+}$$

$$\tilde{\gamma}_{\frac{1}{2}\frac{1}{2}} = \tilde{\gamma}_{-\frac{1}{2}-\frac{1}{2}} = g^* \, \frac{\left[(m_b+m_d)^2 - m_e^2\right]}{\sqrt{6}\, m_d m_e} \sqrt{(m_b-m_d)^2 - m_e^2}$$

f)

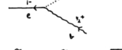

$$1^- \rightarrow \tfrac{1}{2}^+ \; \overline{3/2^+}$$

$$\tilde{\gamma}_{\frac{1}{2}-\frac{1}{2}} = -\tilde{\gamma}_{-\frac{1}{2}\frac{1}{2}} = \frac{\sqrt{(m_b-m_d)^2 - m_e^2}}{\sqrt{3}} \left\{ g_1 - g_2 \frac{\left[(m_b+m_d)^2 - m_e^2\right]}{m_d\,(m_b+m_d)} \right\}$$

$$\tilde{\gamma}_{\frac{1}{2}\frac{1}{2}} = -\tilde{\gamma}_{-\frac{1}{2}-\frac{1}{2}} = \frac{\sqrt{(m_b-m_d)^2 - m_e^2}}{\sqrt{6}\, m_d m_e} \left\{ g_1 \left(m_d^2 + m_e^2 - m_b^2 \right) + g_2 \frac{(m_b-m_d)\left[(m_b+m_d)^2 - m_e^2\right]}{(m_b+m_d)} \right\}$$

$$\tilde{\gamma}_{\frac{1}{2}\frac{3}{2}} = -\tilde{\gamma}_{-\frac{1}{2}-\frac{3}{2}} = \sqrt{(m_b-m_d)^2 - m_e^2} \;\; g_1$$

Our crossing relation (3.3.5) enables one to extend these results to cases found by permuting any of the three particles.

CHAPTER 4

Regge Theory of Resonance Production

4.1 Introduction

In the previous chapters we have studied the inter-relation of the various formalisms that can be used in studying higher spin particles. In this chapter we apply our techniques to the Regge theory of resonance production and make a direct comparison of our calculations with experimental results. The general methods that we have presented for dealing with higher spin can also be applied within the framework of other theories and problems. These include, for example, the use of the Mandelstam representation in the strip approximation. Another possible application is given by the attempt to calculate the neutron-proton mass difference by perturbing a multichannel N over D system of equations in which the proton is represented as a πN and πN^* bound state. Some aspects of the latter problem are considered in Chapter 5.

We begin this application of Regge theory by giving some essential formalism. In Section 4.2, we work to leading order and consider conspiracy briefly. In Section 4.3 we present a very limited treatment of daughters and nonasymptotic corrections. Then we turn to the problem of fitting experiment. In Section 4.4 we make some general comments on the experimental situation and list some technical points on the fitting procedure. After this we deal with some particular reactions: in Section 4.5, $\pi N \to \pi N^*_{1236}$ and $KN \to KN^*_{1236}$, in Section 4.6, $\pi N \to \rho N$ and $KN \to K^*_{890}N$, while in Section 4.7 we briefly consider double resonance production, $(KN \to K^*N^*)$.

This part of the work has been developed jointly with T. W. Rogers, who has considered the last case in more detail and also $\pi N \to f^0 N$, $\pi N \to f^0 N^*_{1236}$ and $NN \to NN^*_{1236}$. I am grateful to C. Froggatt for discussions on Section 4.6.

The diagrams and a table of the data used are given at the end of the chapter. Here I have indicated the number of data points available and estimated the number of events so that one can gauge the statistical accuracy.

4.2 Regge Theory in Leading Order

In order to consider the analyticity of the residue functions in t (in this chapter t is momentum transfer and $\sqrt{s}$ is energy), we asymptotically expand a suitable full amplitude. Taking the leading order, and assuming the presence of only one (or more if we have conspiracy) pole at $j = \alpha$, gives conditions on the residue functions. These conditions occur at $t = 0$ and $t \doteq (m_i \pm m_j)^2$. We must then see if the full amplitude has the required analyticity to all orders in s. As in the spinless case the contribution of a single pole gives this correct analyticity at the thresholds, but at $t = 0$ we will need daughters in order to render the nonasymptotic terms consistent with analyticity.

In this section we will be solely concerned with the leading order contribution. There are two possible approaches. The leading order contribution of a single pole at $j = \alpha$ to H_t is very simple and may be written

$$H_t^{\lambda_2\lambda_4:\lambda_3\lambda_1} \sim \frac{-(e^{-i\pi\alpha}+\tau)}{2\sin\pi\alpha}\, e^{-i\pi/2(\lambda_i-\lambda_f)}\, \gamma'_{\lambda_3\lambda_1}\gamma'_{\lambda_4\lambda_2}(s/s_0)^{\alpha} \qquad (4.2.1)$$

where (a) we have specialized at once to Boson-Boson or Fermion-Fermion reactions in the t-channel,

(b) our Regge pole has signature τ and scale factor s_0,

(c) H_t has been continued from the t-channel by the same route as in (2.2.8) (with s and t swopped),

(d) partial wave amplitudes are defined by (3.2.8) for complex j and have residue $\beta_{\lambda_2\lambda_4:\lambda_3\lambda_1}$ factored as $\gamma_{\lambda_4\lambda_2}$ $\gamma_{\lambda_3\lambda_1}$. Finally we have put

$$\gamma'_{\lambda_3\lambda_1} = \sqrt{\frac{\pi\,\Gamma(2\alpha+2)}{\Gamma(\alpha+\lambda_i+1)\,\Gamma(\alpha-\lambda_i+1)}}\left[\frac{\sqrt{ts_0}}{T_{13}}\right]^{\alpha}\gamma_{\lambda_3\lambda_1} \qquad (4.2.2)$$

Asymptotically the result is in fact equally simple in terms of H_s[F5], and in order give a treatment which is independent of the masses we first consider the analyticity of $\gamma'_{\lambda_3\lambda_1}$ using H_s.

(i) Direct Channel Approach (H_s)

Recently it has become apparent that the interpretation of Regge theory for unequal mass scattering requires some care due to the singularity of the mapping $(s,t) \rightarrow (s, \cos\theta_t)$ as $t \rightarrow 0$. There have been two main approaches to this problem. The first[F3)] assumes the amplitude has a smooth asymptotic behaviour in a pair of variables, such as (s,t) themselves, which are not afflicted by this singular mapping. The second [L1),G4)] writes a dispersion relation in t, at fixed s, for the Regge term expressing it as an integral over its discontinuity for $t > 4m^2$. The integrand is then asymptotically expanded in s and the integral over the leading order term done explicitly. Ignoring the possibility of fixed poles in the J plane which are suggested by the second method (these may be regarded as a special case of moving daughter poles) both methods lead to the same conclusion[F6)] and to the existence of subsidiary (i.e. daughter) trajectories, intercepting for t = 0 at $\alpha - 1$, $\alpha - 2$ ... (these will be considered in Section 4.3).

In the case of spin an appropriate generalization is to make the same assumptions about an amplitude which has no kinematic singularities or zeros in t. So a suitable candidate is $\bar{H}_s$, into which we put a smooth (in t) asymptotic behaviour. This gives in leading order for the customary route of continuation.

$$H_s^{\mu_3\mu_4;\mu_2\mu_1} = \frac{(e^{-i\pi\alpha}+\tau)}{-2\sin\pi\alpha}\; g_{\mu_3\mu_1}\; g_{\mu_4\mu_2}\; \left[\frac{s}{s_0}\right]^{\alpha}$$

$$\cdot\; \epsilon_{13}\;\epsilon_{34}\;\epsilon_{42}\;\lambda_1\lambda_3^{*}\;(-1)^{s_2+\mu_2}\;(-1)^{s_4-\mu_4}\;\eta_2^{P}\;\eta_4^{P}\;\tau P \qquad (4.2.3)$$

Notice that the s-channel η_2^P not η_I^P is used

where the Regge pole has parity P and as in (3.2.4)

$$g_{\mu_3\mu_1} = \sum_{\lambda_1\lambda_3} e^{i\pi/2(\lambda_1+\lambda_3)}(-1)^{s_3+\lambda_3}\;\gamma'_{\lambda_3\lambda_1}$$

$$\cdot\; d^{s_3}_{\lambda_3\mu_3}(-\chi_3^{\infty})\;\; d^{s_1}_{\lambda_1\mu_1}(-\chi_1^{\infty}) \qquad (4.2.4)$$

and

$$\cos\chi_1^{\infty} = \frac{t+m_1^2-m_3^2}{T_{13}} \qquad \cos\chi_3^{\infty} = -\frac{(t+m_3^2-m_1^2)}{T_{13}}$$

are the Trueman-Wick crossing angles with s taken to ∞.

Asymptotically the physical region boundary is $t = 0$ (we consider corrections to this in the next section) and so we must have

$$g_{\mu_3\mu_1}\; g_{\mu_4\mu_2} \sim (\sqrt{-t})^{|\mu_i + \mu_f|} \qquad (4.2.5)$$

and on using parity which relates $g_{\mu_4\mu_2}$ and $g_{-\mu_4-\mu_2}$ we also have

$$g_{\mu_3\mu_1}\; g_{\mu_4\mu_2} \sim (\sqrt{-t})^{|\mu_i - \mu_f|}\,.$$

and hence

$$g_{\mu_3\mu_1} \sim (\sqrt{-t})^{|\mu_1|} \qquad (4.2.6)$$

So $g_{\mu_3\mu_1}$ is free of all kinematic singularities apart from its behaviour at t = 0 which is given by (4.2.6).

Although the contribution of a Regge pole is asymptotically as simple in H_s as in H_t it will turn out to be more convenient to parameterize $\gamma'_{\lambda_3\lambda_1}$ directly and so we now go on to consider this.

(ii) Crossed Channel Approach (H_t)

The amplitudes g of (4.2.4) gave a very simple expression of the kinematic structure, but as discussed in subsection 3.2(i) they do not simply satisfy the nonsense conditions, which, in potential theory, are

$$\gamma'_{\lambda_3\lambda_1} \sim (\alpha - J) \qquad |\lambda_i| > J \qquad (4.2.7a)$$
$$\sim \text{const} \qquad |\lambda_i| \leq J$$

if the Regge pole chooses sense, while if it should choose nonsense

$$\gamma'_{\lambda_3\lambda_1} \sim \sqrt{\alpha - J} \qquad \text{for all } \lambda_i \, . \qquad (4.2.7b)$$

This holds for J integral $\geq$ 0, while if J is a negative integer, only the possibility (4.2.7b) remains. ~~with J replaced by -J-1.~~
~~we apply the same rules (4.2.7) with J replaced by - J - 1.~~

There have been many discussions lately of the status of these results in a relativistic theory.

If the pole chooses sense, these give nontrivial conditions on the g, which are not easy to satisfy and must be imposed as extra constraints. An alternative method which we will use, is to take γ' in terms of which the rules of (4.2.7) are easily stated and impose the threshold behaviour as extra conditions.

$e^{i\pi/2(\lambda_1+\lambda_3)}\gamma'_{\lambda_3\lambda_1}$ is real for $t < 0$, and more exactly we may divide out its singularities in the manner of Hara and Wang as follows.

(a) Top Threshold

$$\gamma'_{\lambda_3\lambda_1} \sim \frac{1}{\left[t-(m_1+m_3)^2\right]^{\frac{1}{2}(s_1+s_3-\eta)}} \tag{4.2.8a}$$

$$\eta = 0 \quad \text{if} \quad \tau P \eta_1^P \eta_3^P \ (-1)^{s_1+s_3} = 1$$

$$\eta = 1 \quad \text{if} \quad \tau P \eta_1^P \eta_3^P \ (-1)^{s_1+s_3} = -1$$

(b) Bottom Threshold $m_1 \neq m_3$

$$\gamma'_{\lambda_3\lambda_1} \sim \frac{1}{\left[t-(m_1-m_3)^2\right]^{\frac{1}{2}(s_1+s_3-\eta)}} \tag{4.2.8b}$$

$$\eta = 0 \quad \text{if} \quad \tau P \eta_1^P \eta_3^P \ (-1)^{s_1-s_3} = 1$$

$$\eta = 1 \quad \text{if} \quad \tau P \eta_1^P \eta_3^P \ (-1)^{s_1-s_3} = -1$$

(c) $\underline{t = 0 \quad m_1 \neq m_3}$

$$\gamma'_{\lambda_3\lambda_1} \sim (\sqrt{t})^{|\lambda_1 - \lambda_3|} \tag{4.2.8c}$$

(d) $\underline{t = 0 \quad m_1 = m_3}$

$$\gamma'_{\lambda_3\lambda_1} \sim (\sqrt{t})^{\eta} \tag{4.2.8d}$$

$$\eta = 0 \quad \text{if} \quad \tau P \eta_1^P \eta_3^P \quad (-1)^{\lambda_1+\lambda_3} = 1$$
$$\eta = 1 \quad \text{if} \quad \tau P \eta_1^P \eta_3^P \quad (-1)^{\lambda_1+\lambda_3} = -1$$

Only in the unequal mass case at t = 0 does (4.2.8) represent the full conditions and in the other cases we must supplement (4.2.8) with further constraints to remove the kinematic zeros. Those at the thresholds may be most easily expressed, as in the full amplitude, in terms of the perpendicular amplitudes of Kotanski [(3.2.5)] . This gives

$$\sum_{\lambda_1 \lambda_3} d^{s_3}_{\gamma_3 - \lambda_3}(\pi/2) \quad d^{s_1}_{\gamma_1 \lambda_1}(\pi/2) \quad \gamma'_{\lambda_3\lambda_1} \sim T_{13}^{\pm \gamma_1 \pm \gamma_3} \tag{4.2.9a}$$

and as usual the negative sign is taken for the lighter particle at $t = (m_1 - m_3)^2$.

In the equal mass case at t = 0 (4.2.4) immediately gives

$$\sum_{\lambda_1 \lambda_3} d^{s_3}_{\mu_3 - \lambda_3}(\pi/2) \; d^{s_1}_{\mu_1 \lambda_1}(\pi/2) \; e^{i\pi/2(\lambda_1 + \lambda_3)} (-1)^{s_3 + \lambda_3} \cdot \gamma'_{\lambda_3 \lambda_1} \sim (\sqrt{-t})^{|\mu_1 - \mu_3|} \tag{4.2.9b}$$

as $\chi_1^\infty = \chi_3^\infty = \pi/2$ at $t = 0$ in this case.

Finally we give the conditions on γ' following from invariance under the various discrete symmetries.

Time reversal has already been taken into account in using the same symbol for the coupling at each vertex. Parity implies

$$\gamma'_{\lambda_3 \lambda_1} = \eta_1^P \eta_3^P \; \tau P \; (-1)^{s_1 + s_3} \; \gamma'_{-\lambda_3 - \lambda_1} \tag{4.2.10a}$$

and if particle 1 = particle $\bar{3}$

$$\gamma'_{\lambda_{\bar{3}} \lambda_1} = \tau \; \gamma'_{\lambda_1 \lambda_{\bar{3}}} \tag{4.2.10b}$$

and if we have formed states of definite isospin I in the t-channel, (4.2.10b) has an extra phase $(-1)^{I - 2I_3}$.

Similarly if particle 1 = 3

$$\gamma'_{\lambda_3 \lambda_1} = G \; (-1)^I \; \tau \; \gamma'_{\lambda_1 \lambda_{\bar{3}}} \tag{4.2.10c}$$

where the Regge pole has G parity G.

(iii) Conspiracy [P1),L3)]

The result (4.2.6), following from factorization or parity, implies that, however many Regge poles contribute to the scattering amplitude, $H_s \sim \sqrt{-t}^{\,|\mu_i| + |\mu_f|}$ asymptotically rather than the expected $\sqrt{-t}^{\,|\mu_i - \mu_f|}$. This leads one to predict a certain behaviour of the density matrix elements as $t \to 0$, which is not particularly well satisfied experimentally. So we may try to remove this theoretical prediction by allowing two or more poles to collide at the same value of α at $t = 0$. There are of course many ways of doing this but a particularly interesting case is found by taking just two poles of opposite values of τP. We must satisfy

$$g^{(1)}_{\mu_3\mu_1} \; g^{(1)}_{\mu_4\mu_2} + g^{(2)}_{\mu_3\mu_1} \; g^{(2)}_{\mu_4\mu_2} \sim \sqrt{-t}^{\,|\mu_i + \mu_f|}$$

which may be done by taking

$$g^{(k)}_{\mu_3\mu_1} \sim \frac{\sqrt{-t}^{\,|\mu_i|}}{\sqrt{-t}} \qquad |\mu_i| \neq 0$$

$$\sim \sqrt{-t} \qquad \mu_i = 0 \qquad k = 1,2$$

and

$$g^{(1)}_{\mu_3\mu_1} = i\, g^{(2)}_{\mu_3\mu_1} \qquad \text{for} \quad \mu_i > 0$$

to leading order in t as $t \to 0$ while the coefficients of $\sqrt{-t}$ for $\mu_i = 0$ are arbitrary.

We will apply this with Regge pole 1 as the π and g as the amplitudes at the $N\bar{N}$ and $\pi\rho$ vertices. In the first case we have $|\mu_i| = 1$ only but in the second $|\mu_i| = 0$ and 1. But in either case before conspiracy we have

$$g^{\pi}(|\mu_i| = 1) \sim \sqrt{-t} \qquad g^{\pi}(\mu_i = 0) \sim \text{const.}$$

but after conspiracy .

$$g^{\pi}(|\mu_i| = 1) \sim \text{const.} \qquad g^{\pi}(\mu_i = 0) \sim \sqrt{-t}$$

So before conspiracy, the dominant (i.e. that containing the particle pole) π contribution to $NN \to NN$, $\pi N \to \rho N$ and $\pi N \to \rho N^*$ behave like t, $\sqrt{-t}$, 1, while after conspiracy, like 1, $\sqrt{-t}$, t. We will only consider the middle case, $\pi N \to \rho N$, quantitatively, where $d\sigma/dt$ is unaltered in shape but conspiracy alters the expected t-variation of the density matrix elements.

4.3 Regge Theory including Nonasymptotic Corrections

In the previous section, we have chosen the t-dependence of our residues to ensure that suitable amplitudes were consistent with analyticity in leading order. We now consider whether this still holds when non-asymptotic corrections are included. Non-leading terms may be classified into three types.

a) $s^{\alpha} \rightarrow z_t^{\alpha}$

b) Threshold effects.

c) t = 0 and the physical region boundary. This has a part near u = 0 and another asymptotically t = 0. Both are quite important.

i) $s^{\alpha} \rightarrow z_t^{\alpha}$ (See Erratum)

As we are treating the Regge formula with some suspicion, we must consider whether to use s^{α} or z_t^{α} in our formulae. If we wish to avoid Regge poles with parallel trajectories α and $\alpha - 1$ ... , we must use z_t. Also z_t puts the cut in s associated with the Regge form at $z_t = 0$, i.e.

$$2s = \sum m^2 - t - (m_1^2 - m_3^2)\ (m_2^2 - m_4^2)\ /\ t$$

which is more satisfactory than one at s = 0 (indicated by the asymptotic form). We have therefore used this correction in our fitting. A proper treatment of this requires the explicit subtraction of the unwanted discontinuity, and has been given for unequal mass scattering by Goldberger and Jones[G4].

ii) Thresholds

As long as one uses the trick due to Mandlestam of dropping the part of $P^J \propto Q^J$ and keep only the Q^{-J-1} portion, (this is necessary to apply Regge theory below Rej = $-\frac{1}{2}$) the nonasymptotic terms of the usual Regge form give a full amplitude with the correct analyticity, as long as the residue functions have the form determined asymptotically. This statement is only exactly true at the lower threshold, as unitarity is well known to require a condensation of poles at $\ell = -1$ at the top threshold. This appears rather high in the j plane (i.e. $j = \max(s_1 + s_3, s_2 + s_4) - 1$) for spinning particles but we will ignore it.

The thresholds become rather more interesting when in part iv) of this section we add daughter trajectories with residues determined at $t = 0$.

iii) $t = 0$ and the Physical Region Boundary: Direct Channel Method

An asymptotic behaviour which is consistent with analyticity, for fixed s, and all t is obtained by placing

$$H_s^{\mu_3\mu_4:\mu_2\mu_1} = B_s^{\mu_i\mu_f} \left\{ \frac{1}{B_s^{\mu_i\mu_f}\Big|_{\text{asymptotic form}}} \cdot \text{equation (4.2.3)} + \text{any corrections of } O(s^{\alpha-1}) \text{ which are nonsingular in } t \right\} \quad (4.3.1)$$

This is unsatisfactory for two reasons:

(a) It gives Regge poles with J differing by integral values for all t which would not be sensible in some potential theory limit (and relativistically summing ladder graphs does not give parallel trajectories[S3),S4)]).

(b) It does not give the correct analyticity in s. This is probably not usually important, but becomes so if the Regge pole creates a particle at $t = m^2$. Then the formula (4.3.1) by no means ensures that at $t = m^2$ the residue in H_t has an s dependence $\propto d^j(\theta_t)$. This enhancement of the nonanalyticity in s becomes particularly apparent for the π Regge pole and I have verified on the computer that, whereas at $s = 5$ Gev^2 the natural non-asymptotic corrections are quite small (see Section 4.3), formula (4.3.1) gives results differing by 50% from the asymptotic value.

A more sensible method, which answers the first objection, may be found in the O_4 symmetry approach developed by Freedman and Wang[F2)]. This model is only applicable naturally to equal mass scattering but may have a more general use as in a Wick rotated Bethe-Salpeter equation the masses become equal in pairs as $t \to 0$. It seems more complicated to apply than a simple Regge model, other than just at $t = 0$, as it only applies without symmetry-breaking to the coefficient of $\sqrt{-t}^{\,|\mu_i - \mu_f|}$ in $H_s^{\mu_3\mu_4:\mu_2\mu_1}$. for equal mass scattering. One must await experimental tests on its predictions on the ratios of residue functions at $t = 0$, following from placing the particle Regge poles in definite O_4 representations, before deciding whether it has any fundamental significance.

The second objection may be overcome by using invariant amplitudes as these remove the singularities in s and t simultaneously. However we saw in Chapter 2 that they contained no more information on the analyticity at t = 0 than the principle (P') and so there is no need to use them in a theoretical treatment of daughters and the behaviour at t = 0. As no general simple formula is known for them they are not even useful as a convenient phenomenological device.

iv) <u>t = 0 and the Physical Region Boundary: Crossed Channel Method</u>

The method of the previous subsection generated results which were non-singular at t = 0. However as we discussed there, they had certain disadvantages and so we will now study the same problem keeping rather closer to the natural Regge form. For all mass values, $\bar{H}_s$ is a suitable amplitude to study analyticity at t = 0 and on the physical region boundary. However in the case of UU scattering we can use (cf. Section 3.3)

$$f_t = \bar{H}_t^{\lambda_2\lambda_4:\lambda_3\lambda_1} (\sqrt{-t})^{\left|\lambda_i - \epsilon\lambda_f\right|} \tag{4.3.2}$$

where

$$\epsilon = \text{sign}\left[(m_1^2 - m_3^2)(m_2^2 - m_4^2)\right]$$

which is non-singular at these two points and more convenient for Regge theory.

We will say something later about UE and EE scattering. The full contribution of a Regge pole to f_t is

$$f_t = f_t \Big|_{asymptotic} \cdot \left[\frac{T_{13}T_{24}}{st}\right]^{\alpha-\Lambda} \left[\tfrac{1}{2} z - \tfrac{\epsilon}{2}\right]^{\alpha-\Lambda} \qquad (4.3.3)$$

$$\cdot \ {}_2F_1 \left(\Lambda - \alpha, \lambda - \alpha, -2\alpha ; \ \frac{2}{1-\epsilon z}\right)$$

where the second term is just 1/the asymptotic value of the third term and

$$\Lambda = \max\left\{|\lambda_i| \ , \ |\lambda_f|\right\}$$
$$\lambda = \epsilon \ \mathrm{sign}\left\{\lambda_i \lambda_f\right\} \quad \min\left\{|\lambda_i| \ , \ |\lambda_f|\right\}.$$

Because $z \to \epsilon$ as $t \to 0$ for all s, $z - \epsilon$ is a satisfactory quantity to appear and $(\frac{z-\epsilon}{t})$ and t are a pair of variables non-singularly related to s and t as $t \to 0$.

Working to $O(s^{\alpha-1})$ the hypergeometric function becomes

$$1 + \frac{(\Lambda - \alpha)(\lambda - \alpha)}{-\alpha t} \cdot \frac{t}{(1 - \epsilon z)} \qquad (4.3.4)$$

which has a 1/t pole as $t \to 0$. This must be cancelled by one or more daughter trajectories. In order to make the study nontrivial we will suppose there is but one daughter trajectory (at $j = \alpha - 1$) which has factorizable residues. It therefore must contribute to f_t a term which is proportional to the 1/t part of the ${}_2F_1$ and hence adds to (4.3.4) a term

$$- \frac{(\Lambda - \alpha)(|\lambda| - \alpha)}{- \alpha t} \quad \frac{t}{(1 - \epsilon z)}$$

where from factorization we have $|\lambda|$ and not λ . So the joint contribution of parent and daughter at t = 0 may be obtained by replacing (4.3.4) by

$$1 + \frac{(\Lambda - \alpha)(\lambda - |\lambda|)}{- \alpha t} \cdot \frac{t}{1 - \epsilon z} \qquad (4.3.5)$$

f_t must be non-singular and there is still a 1/t in (4.3.5) if λ negative. However factorization of the parent trajectory implies from (4.2.6) that as $t \to 0$,

$$f_t \Big|_{\text{asymptotic}} \sim \text{const} \quad \text{if } \lambda \text{ positive}$$
$$\sim t^{|\lambda|} \quad \text{if } \lambda \text{ negative}$$

This behaviour when multiplied into (4.3.5) gives a non-singular form to f_t.

In terms of γ' the parameters of the daughter are given by:

$$\alpha^{(d)}(0) = \alpha^{(p)}(0) - 1$$
$$\tau P \Big|^{(d)} = \tau P \Big|^{(p)} \qquad (4.3.6)$$
$$\tau^{(d)} = - \tau^{(p)}$$

(to be continued)

(4.3.6 continued)

$$\gamma'^{(d)}_{\lambda_3\lambda_1} = \gamma'^{(p)}_{\lambda_3\lambda_1} \frac{(|\lambda_1| - \alpha)}{\sqrt{-2t\alpha s_0}} \cdot T_{13} \cdot \epsilon_1 \quad (\text{as } t \to 0)$$

where $\epsilon_1 = \text{sign}\,(m_1^2 - m_3^2)$ (and we have given the parent and daughter the same scale factor s_0).

T_0 work to order $s^{\alpha-2}$ and lower is only well defined for the most singular part in t, as the other singular terms are affected by the difference between the daughter and parent parameters away from t = 0. Thus (4.3.6) cannot hold for all t as it contradicts the threshold behaviour at $T_{13} = 0$. (This occurs even in the spinless case when γ' is non-singular at thresholds). However one can easily give a formal extension of the analysis to all orders in s by using the identity. (Andrews and Gunson[A1], equation (13.1)).

$$1 = \sum_{r=0}^{\infty} \frac{1}{r!} \frac{(\Lambda-\alpha)_r(\lambda-\alpha)_r}{(r-1-2\alpha)_r} (-x)^r \; {}_2F_1\,(\Lambda-\alpha+r, \lambda-\alpha+r,$$

$$-2\alpha + 2r : x)$$

which is simply a complex form of the C.G. series **for**

$$d^{j_a}_{\Lambda-j_b, j_a}(\theta_t) \quad d^{j_b}_{j_b, \lambda-j_a}(\theta_t) \qquad (j_a + j_b = \alpha)$$

Putting $x = 2/(1-\epsilon z)$ and then multiplying through by $(-1/x\epsilon)^{\alpha-\Lambda}$ we get the sum of parent pole and daughters on the right hand side equal to the, well-behaved as $t \to 0$, function $(\frac{1}{2}z - \frac{1}{2}\epsilon)^{\alpha - \Lambda}$. This, as for the first daughter, only works exactly for the positive λ but, as before, the asymptotic vanishing of f_t ensures that the daughter residues determined for $\lambda > 0$ are sufficient to ensure analyticity for $\lambda < 0$.

We had to use the above device rather than expand (4.3.3) further as the residue of the second daughter is determined by terms from both the parent and the first daughter.

So the residues of the daughter at $\alpha^{(p)}(0) - r$ are given by

$$\gamma'^{(d)}_{\lambda_3\lambda_1} = \gamma'^{(p)}_{\lambda_3\lambda_1} \frac{(|\lambda_i| - \alpha)_r}{\sqrt{r!\,(r-1-2\alpha)_r}} \cdot \left[\frac{T_{13}\,\epsilon_i}{\sqrt{ts_0}}\right]^r . \qquad (4.3.7)$$

Again we have one and only one daughter trajectory at $\alpha - r$ (r integral) and if (4.3.7) held as identity in t (and the daughter trajectories were parallel to the parent away from $t = 0$) this would ensure that f_t had no singular terms. However as discussed above this is impossible and the above analysis only holds for the most singular term in t.

We will now consider UE and EE scattering. UE scattering seems the most difficult but a treatment to order $s^{\alpha - 1}$ may be given as follows.

We now state our analyticity in terms of the Trueman-Wick crossing relation and the non-singularity of $\bar{H}_s$. As we are only interested in $t = 0$ and the physical region boundary and not the other t thresholds we may introduce the total spin s', which as mentioned before (Section 2.4) always diagonalizes the behaviour we want here, and simplify the statement of analyticity by putting

$$m_1 = m_3 : \quad H_t^{\lambda_2 \lambda_4 : \lambda_i}{}_{s_i'} = \sum_{\lambda_1 - \lambda_3 = \lambda_i} C\,(s_1\, s_3\, s_i' : \lambda_1, -\lambda_3)\,(-1)^{s_3 - \lambda_3}\, H_t^{\lambda_2 \lambda_4 : \lambda_3 \lambda_1}$$

which satisfies (4.3.8)

$$\sum_{\lambda_i} H_t^{\lambda_2 \lambda_4 : \lambda_i}{}_{s_i'}\; d^{s_i'}_{\lambda_i \mu_i} \quad (\chi)$$

has only the physical region boundary behaviour $\left[1+\cos\theta_t\right]^{\frac{1}{2}|\lambda_f + \epsilon_f \mu_i|}$ where χ may be taken as χ_1 or χ_3 (or $\frac{\chi_1 + \chi_3}{2}$ for that matter). Because in UE scattering, the physical region boundary differs from t = 0 by terms proportional to $1/s^2$, $\left[1 + \cos\theta_t\right]^{\frac{1}{2}|\lambda_f + \epsilon_f \mu_i|}$ may be replaced by $t^{\frac{1}{2}|\lambda_f + \epsilon_f \mu_i|}$ for the purposes of our analysis to $O(s^{\alpha - 1})$.

From (4.2.9b) it is useful to introduce, at the equal mass vertex, the perpendicular amplitudes

$$P^{\mu_i}_{s_i'} = \sum_{\lambda_1 \lambda_3} C\,(s_1 s_3 s_i' : \lambda_1, -\lambda_3)\,(-1)^{s_3 - \lambda_3}\, e^{-i\pi/2\,\lambda_i}\, \gamma'_{\lambda_3 \lambda_1}\, d^{s_i'}_{\lambda_i \mu_i}\,(\pi/2) \qquad (4.3.9)$$

which $\sim t^{\frac{1}{2}|\mu_i|}$ as $t \to 0$.

Instead of $z - \epsilon$ which was an appropriate variable in the UU case, it is now sensible to expand in terms of z. Then if we assume that there is again only one daughter whose residue at the unequal mass vertex is given from factorization by (4.3.6), we can show that the daughter residues at the equal mass vertex are given by

$$\rho_{s_i'}^{\mu_i\,(d)} = \frac{m_1}{\sqrt{2\alpha s_0}} \left(s_i' - |\mu_i| + 1\right)^{\frac{1}{2}} \left(s_i' + |\mu_i|\right)^{\frac{1}{2}} \operatorname{Sign}(\mu_i) \; \rho_{s_i'}^{[(|\mu_i|-1)\,\operatorname{Sign}(\mu_i)]}\,(\text{parent}) \quad \text{as } t \to 0 \quad \text{for } |\mu_i| > 0 \tag{4.3.10}$$

while for $\mu_i = 0$ the daughter can have any residue as long as it vanishes like $\sqrt{t}$ to cancel the $1/\sqrt{t}$ in $\gamma'^{(d)}_{\lambda_4\lambda_2}$.

It may be verified that the equal mass conditions ((3.2.11)) are also satisfied to $O(s^{\alpha-1})$ by the same daughter with factorized residues given by (4.3.10).

As an example we can take the well known case of nucleon-nucleon scattering. In terms of the perpendicular and s' notation, which is rather cumbersome in this special case, we have three types of couplings:

I $\quad$ $\underline{\tau P = + : G(-1)^I\ P = +}$

$s' = 0$ $\quad$ one coupling $\quad$ which is irrelevant here

$s' = 1$ $\quad$ one coupling $\quad$ $p^0 = 0$ $\quad$ (4.3.11)

$$p^1 = p^{-1} = -i\,\gamma_1'$$

II $\underline{\tau P = - \; : \; G(-1)^I P = +}$

$s' = 1$ one coupling $p^0 = i\sqrt{2}\, \gamma_1'$

$p^1 = p^{-1} = 0$

$$\text{(4.3.11)}$$

III $\underline{\tau P = - \; : \; G(-1)^I P = -}$

$s' = 1$ one coupling $p^0 = 0$

$p^1 = -p^{-1} = \gamma_0' / \sqrt{2}$

Here γ'_{λ_i} stands for

$$\sum_{\lambda_1 - \lambda_3 = \lambda_i} C(s_1 s_3 s_i' : \lambda_1, -\lambda_3)\; (-1)^{s_3 - \lambda_3}\; \gamma'_{\lambda_3 \lambda_1}$$

for $s_i' = 1$ and so are directly the residues to be inserted in the standard relation (3.2.10).

Our rules (4.3.10) show that only one type has a daughter at $j = \alpha - 1$ with singular residues. This is type II (associated with the A_1 or D mesons) with a type III (π, η) daughter. This is a particular case of many solutions known to (3.2.10). Our assumption that there is only one daughter covering all reactions has picked out a unique solution.

This method of tackling the UE and EE cases seems incapable of easy extension to $O(s^{\alpha-2})$ and lower. Also it makes it appear rather miraculous that the daughter has factorizable residues, while in fact this should have been expected. Thus the only reason UE and EE reactions are different from the general UU case is that the thresholds $(m_1 - m_3)^2$, $(m_2 - m_4)^2$ move down and coalesce with $t = 0$. Now the threshold conditions in the UU case required no extra daughters and so one would not expect extra ones to be produced when $t = 0$ happens to coincide with $t = (m_1 - m_3)^2$. This can be made the basis of a quantitative study of EE and UE reactions as follows. Thus take the UU expressions for the daughter residues and write them in terms of amplitudes which have no kinematic singularities or zeros at the thresholds. As emphasized before, even in the spinless case, this is not automatic from the natural factors of (4.3.6) and (4.3.7). Then letting $m_1 \rightarrow m_3$ we would achieve the correct results for UE and EE scattering. This is straightforward for the most singular term in t and although one does not know an explicit general solution it is not very difficult in practice for $N\bar{N}$ when we only need $s' = 0$ and 1.

The above analysis may seem rather complicated but in practice it would probably be sufficient to include non-asymptotic terms only if they were singular compared with the parent, and destroyed the asymptotic vanishing of f_t. In our model which makes the arbitrary assumption of one daughter at each $\alpha - r$, this destruction occurs in a controlled way. Namely a term asymptotically proportional to $t^{|\lambda|}$ loses one factor of t each time you go down one power in s until you reach $s^{\alpha-|\lambda|}$ after which the further non-asymptotic terms are not more singular. In analysing the experimental situation one can bear in mind that non-asymptotic terms may be more singular than the above model suggests.

Finally we note that the simple prescription of just dividing out the physical region boundary behaviour

$$f_t = f_t \Big|_{\text{asymptotic}} \qquad (4.3.12)$$

although consistent with analyticity at t = 0 would lead to non-asymptotic contradictions with analyticity at the thresholds. As experiments are conducted nearer the physical region boundary than the thresholds this may not be important. The natural Regge non-asymptotic terms restore consistency at thresholds and in fact make the corrections away from the physical region boundary smaller. Thus (4.3.12) gives corrections of O(1/s) relative to leading order in physical quantities but as

$$d^{\alpha}_{\lambda_i \lambda_f}(z) = \text{Asymptotic form} \left\{1 + \frac{\lambda_i \lambda_f}{\alpha z} + \dots \right\}$$

(where asymptotic means asymptotic in z not s, here see subsection (i)) the non-asymptotic correction behaves like a pole of opposite τP to the leading order and so does not interfere with it in calculating physical quantities. So the only 1/s correction is the daughter-leading order interference.

4.4 Experimental Fitting

(i) The quantities which we must try to fit are:

$$\frac{d\sigma}{dt} = \frac{0.3893}{16\,\pi\, S_{12}^2} \sum_{\substack{\text{sum over final and}\\ \text{average over initial}\\ \text{spins}}} \left| H_t^{\lambda_2\lambda_4:\lambda_3\lambda_1} \right|^2 \qquad (4.4.1)$$

and the density matrix elements. These are usually referred to a set of axes popularized by Jackson, and

$$\rho_{mm'} = \frac{\hat{\rho}_{mm'}}{\mathrm{Tr}\,\hat{\rho}_{mm'}} \qquad (4.4.2)$$

where

$$\hat{\rho}_{mm'} = \sum_{\lambda_1\lambda_2\lambda_4} (-1)^{m-m'}\, H_t^{\lambda_2\lambda_4:m\lambda_1}\, H_t^{\lambda_2\lambda_4:m'\lambda_1\,*}$$

for particle 3 decaying while for particle 4 the formula is the same with $3 \leftrightarrow 4$ but without the factor $(-1)^{m-m'}$. We must be careful about the definition of our y axis. I have taken it along $p_1^{c.m.} \times p_3^{c.m.}$ for both particles 3 and 4. Everybody follows this procedure for particle 3 but for particle 4 (which will be the N^*_{1236}) there appears to be some confusion. The KN^* C.E.R.N. experiment and Jackson and Pilkuhn[J2)] make the opposite choice but I have assumed that the other experiments have made my choice. The sign of Re ρ_{31} is altered on changing the direction of the y axis and as this is small, little qualitative difference will be made to the fits if my assumption is not correct.

As $\rho_{mm'}$ is given by t channel amplitudes it is strongly affected by their kinematic singularities (especially for the N^*) which may obscure the dynamical information. This may be an argument against using this particular set of axes. Thus we saw earlier in Section 4.2 that the simplicity following from a single Regge pole exchange was as easily stated in terms of H_s as H_t.

(ii) The reactions we will be interested in and some of the Regge poles which may be expected to dominate are given in the table below.

Reaction	$\tau P = +$	$\tau P = -$	
$\pi N \to \pi N^*$	ρ (ρ')	not allowed	
$KN \to KN^*$	ρ (ρ') A_2	not allowed	
$\pi N \to \eta N^*$	A_2	not allowed	
$\pi N \to \rho N^*$	A_2	A_1, π	
$\pi N \to \omega N^*$	ρ	B	
$KN \to K^*N^*$	ρ , A_2	A_1, B, π	
	Type I	Type II	Type III
$\pi N \to \rho N$	A_2, ω	A_1	π
$KN \to K^*N$	A_2, ρ, P, P', ω	A_1, D	B, π

The division into the two values of τP is useful as from (4.2.10a) we see that in leading order poles of opposite τP do not interfere in either $d\sigma/dt$ or density matrix elements. Also when there is an $N\bar{N}$ vertex the three types of (4.3.11) do not interfere.

We notice that, except for the π, the poles of high intercept α_0 have $\tau P = +$. Experimentally this is born out in our reactions except at the lowest energies where we definitely need more $\tau P = -$ than the π provides. This could either be due to a failure of Regge pole theory (e.g. the background integral is important) or that the A_1, D and B mesons with probably somewhat lower intercepts are becoming important. I will usually consider all data above $p_{lab} = 2$ Gev, which is an unfortunately low limit but the most reliable experiments lie in the 2 to 3 Gev region. The errors on the density matrix elements are especially large at high energies and fits involving only the high energy data are largely determined by $d\sigma/dt$. At lower energies we have much more accurate density matrix giving large contributions to χ^2 as they are very sensitive to the exchanged τP.

In the non-charge exchange reactions such as $\pi^{\pm}p \rightarrow \rho^{\pm}p$ there is the well known forward scanning bias, which means that $d\sigma/dt$ and the density matrix elements are unreliable for small t. I have deleted all such suspicious points although it would appear that some experiments have made the necessary corrections.

(iii) Characteristics of the Exchanged Poles

The density matrix elements for $\pi N \rightarrow \rho N$ and $KN \rightarrow K^*N$ are especially sensitive to the value of τP of the exchanged pole as will be described in more detail in Section 4.6. For N^* production the density matrix elements are not so critically dependent on τP. (See Section 4.7). Also the density matrix elements will enable one to detect if a pole chooses sense or nonsense when it goes through zero near t = 0.

However there is one general comment that may be made about the shape of $d\sigma/dt$ produced by these poles. Thus π has a nearby pole; and ρ a reasonable slope α_0', quite a near pole and a strong spin-flip vanishing at t = - .6. So these two poles produce $d\sigma/dt$'s which fall off rapidly with t. ω may be similar but the evidence is less conclusive. These conclusions will be somewhat modified for ρ and ω in $KN \rightarrow K^*N$ and $\pi N \rightarrow \rho N$ where we have only a spin-flip coupling at the meson vertex and the associated t = 0 vanishing can give a broader $d\sigma/dt$. A_2 and P' however produce a characteristic broad cross section, as the lack of dips in their reactions may be because they choose nonsense at $\alpha = 0$ so that the vanishing (4.2.7) cancels the ghost and there is no residual spin-flip vanishing.

(iv) I have written programs which fit the experimental $d\sigma/dt$'s and density matrix elements to the leading order formulae for an arbitrary number of poles in the reactions of interest here.

The residue functions $\gamma'_{\lambda_3\lambda_1}$ were parameterized as polynomials with an overall exponential dependence in t being given by a choice of s_0. χ^2 was minimized with respect to the coefficients of the polynomials by evaluating the derivatives in the usual way. The threshold constraints (4.2.9a) gave linear relations among these coefficients which were conveniently incorporated using Lagrange multipliers. The parameters α_0, α_0' and s_0 for each pole were fixed during each fit.

In the next three sections we will describe the results of these fits for the three classes of reactions. We can summarize the conclusions by saying then is in general reasonable agreement for any given reaction. The strong correlation in the determination of parameters from any one reaction renders tests of factorization difficult. However there appear to be some significant differences in the parameters necessary in different reactions (especially for the π) which may indicate the presence of cuts in the j plane.

Lastly I should say that there have been several Regge pole analyses[T5)] of the reactions of interest. I can add no more to this work on the energy variation of σ_{total} (see Morrison[M2)]) and $d\sigma/dt$. However the previous work seems to contain technical errors especially in the treatment of density matrix elements.

4.5 $\pi N \to \pi N^*_{1236}$ and $KN \to KN^*_{1236}$

(i) General

There are four couplings at the $\bar{N}N^*$ vertex into which we may coalesce the single $\pi\pi$ coupling. At $t = (m_N - m_{N*})^2 \simeq .09\ \mathrm{Gev}^2$, there are from (4.2.9a) four constraints while we will ignore the two further constraints at $t = (m_N + m_{N*})^2$. The closeness of the threshold and the number of the conditions would seem to make them quite important. In order to illustrate the constraints, suppose that the helicity double-flip term $\gamma'_{-3/2\ \frac{1}{2}} = 0$. Then the remaining residues $\sim$ constants at $(m_N - m_{N*})^2$ (previously they $\sim 1/[t - (m_N - m_{N*})^2]$) and satisfy the one relation

$$\sqrt{3}\ (\gamma'_{\frac{1}{2}\frac{1}{2}} - \gamma'_{-\frac{1}{2}\frac{1}{2}}) = \gamma'_{3/2\ \frac{1}{2}} \tag{4.5.1}$$

This clearly indicates that although the helicity-flip terms vanish at t = 0 they are related in magnitude to the non-flip term at t = .09. Thus we should not be surprised to find evidence for strong spin flip terms in the density matrix elements.

There are three density matrix elements measured experimentally: ρ_{33}, Re ρ_{3-1} and Re ρ_{31} (where the index is 2m not m).

If we take $\gamma'_{\frac{1}{2}\frac{1}{2}} = 0$ and assume the other residues are sufficiently constant to be able to apply (4.5.1) away from t = .09 we find

$$\rho_{33} = 3/8 \qquad \rho_{3-1} = \sqrt{3}/8 \qquad \rho_{31} = 0 \qquad (4.5.2)$$

which is the well known Stodolsky-Sakurai distribution which we see is to some extent determined solely by kinematic effects. In particular this distribution and a turn over in $d\sigma/dt$ as $t \to 0$ (i.e. $\gamma'_{\frac{1}{2}\frac{1}{2}} = 0$) are kinematically realted.

As pointed out by Bialas and Kotanski if only one pole is exchanged, we have

$$\rho_{33}\ \rho_{11} = (\mathrm{Re}\ \rho_{31})^2 + (\mathrm{Re}\ \rho_{3-1})^2 \qquad (4.5.3)$$

This is well satisfied in both reactions although there is insufficient published information to evaluate the error properly.

Finally we note that non-asymptotic corrections are expected to be quite small because one vertex is spinless and the daughters have residues which are no more singular than the leading term. Also, even at $p_{lab} = 1.59$, the physical region boundary differs from t = 0 by only .001 Gev, (for $\pi N \to \pi N^*$).

(ii) $\pi^+ p \to \pi^0 N^{*++}$

Of the data used only that at 4 Gev has reasonable statistics.

In this reaction we only have one important pole exchanged; the ρ pole with $\alpha_0 \doteq .58$ and $\alpha'_0 \doteq 1$. The density matrix elements show an increasing and large amount of spin flip terms as t moves away from the physical region boundary, which we expect from the arguments in (i). Thus one might expect the Stodolsky-Sakurai assumption $\gamma'_{\frac{1}{2}\frac{1}{2}} \equiv 0$ to be unnecessary and that the situation could be described by simple constancy assumptions subject to (4.5.1) (or more correctly, the full conditions with $\gamma'_{-3/2\ \frac{1}{2}} \neq 0$). However the data show a dip in $d\sigma/dt$ in the forward direction which is extremely difficult to fit due to the sharp fall off of the ρ exchange contribution. Thus all my fits needed $\gamma'_{\frac{1}{2}\frac{1}{2}}$ to be much smaller than kinematically expected and gave theoretically a fractionally larger ρ_{33} than the experimental value for low t.

The strong spin flip terms lead one to predict a dramatic dip in the cross section at $t \simeq -.6$ where the ρ trajectory passes through zero. Unfortunately the best dip in the data occurs at $t \simeq -.35$. We can improve the agreement here by invoking the ρ' trajectory, which is already needed in one model of πN charge exchange, to fill in the predicted dip. The ρ parameters were insensitive to the introduction of the ρ' as long as you kept the intercept $\alpha^{\rho'}_0 \leq .2$ so that the energy dependence of the data determined the ρ as the dominant contribution.

The 4 and 8 Gev data had 37 data points and with 3 degrees of freedom for the ρ and 1 for the ρ' we found a χ^2 between 40 and 50 (depending on s_0 and the ρ' parameters). Figure 4.1 shows a typical fit to the 4 Gev data.

From the energy variation of σ_{tot} the lower energy data appears of suspect normalization. Allowing $d\sigma/dt$ scale factors determined at 3.54 Gev to be $\simeq$ 2 and at 2.75 Gev to be $\simeq$ 1.5 we had a χ^2 from 80 $\rightarrow$ 100 on a grand fit, to all 80 data points, using the same number of theoretical parameters as above. This is a measure of the poor statistics of the lower energy data rather than the applicability of the theory at low energies.

The important nature of the four kinematic constraints might lead one to expect a dependence on the mass of the N^* used. On altering m_{N*} to 1.15 Gev (so that $(m_N - m_{N*})^2 \simeq .05$) we found no change in χ^2 as there were no density matrix elements for small enough t for this shift to be significant. However it may be significant that the kinematically expected value of $\gamma^{\prime}_{\frac{1}{2}\frac{1}{2}}$ goes down, after this mass change.

(iii) $K^+p \rightarrow K^0N^{*++}$

In this reaction ρ and A_2 are expected to be the dominant poles but from SU_3 and the $\pi N \rightarrow \pi N^*$ cross section the A_2 is expected to be dominant. So we can first try a fit with just A_2, and as discussed in Section 4.4 we have an immediate qualitative explanation of why $KN \rightarrow KN^*$ has a much broader $d\sigma/dt$ than $\pi N \rightarrow \pi N^*$. The experimentalists have already done an analysis of the energy variation of this and found $\alpha_0 = .4 \pm .22$, which is excellent, but obtain also the unfortunate result that $\alpha_0^{\prime} = 1.72 \pm .33$. So we found for the A_2 parameters

$\alpha_0 = .35$ $\alpha_0' = .34$ rather bad agreement but for $\alpha_0' = .6$ (the density matrix elements imply that A_2 must choose nonsense at $\alpha = 0$ for this large slope) there is a great improvement, although the $t = -.3$ $p_{lab} = 5$ Gev data point was still too large theoretically (by three standard deviations). Thus on 50 data points and 3 degrees of freedom for the A_2 we found a $\chi^2 \simeq 130$ in the first case and $\chi^2 \simeq 90$ in the second.

We then added ρ exchange with parameters determined from my $\pi N \to \pi N^*$ analysis and with its SU_3 ratio. This leads to roughly equal ρ and A_2 contributions near $t = 0$ but with the rapid ρ fall off and broad A_2, the A_2 dominates away from $t = 0$. This reduced χ^2 by about 10 but it did not alter the systematic disagreement discussed above. Increasing the contribution led to a rise in χ^2 due to the theory being too large for small t. So one may say the data is consistent with a ρ contribution ranging from nothing up to 1.5 times the SU_3 prediction.

If the rapid fall off with t of the 5 Gev experiment is confirmed at higher energies it would suggest that the amount of ρ exchange has been underestimated in the above analysis. In this respect we may note that the similar reaction $\pi N \to \eta N^*$ which only has A_2 exchange shows the characteristic broad cross section in the data[M2] at 8 Gev.

The data was consistent with A_2 parameters rather similar to the ρ (i.e. small $\gamma'_{\frac{1}{2}\frac{1}{2}}$ $\gamma'_{-3/2\,\frac{1}{2}}$ in agreement with the

Stodolsky-Sakurai prediction) but reasonable fits can be obtained without this feature. Whereas the ρ can have a sensible $s_0 \approx 1$ the A_2 needs a small value $s_0 \approx .1$ in order to pull its $d\sigma/dt$ down for large t. The exact value of s_0 depends on α_0' and whether the A_2 chooses sense or nonsense when it goes through zero (either was consistent with the density matrix elements for the small slope $\alpha_0' = .34$).

Figure 4.2 gives the results of one of the fits, using A_2 only, for the 2.97 Gev experiment.

4.6 $\pi N \rightarrow \rho N$ and $KN \rightarrow K^* N$

(i) General

This class of reactions have the following features:

(a) Three charge states of which the charge exchange reaction picks out I = 1 exchange. In both examples the two non-charge exchange reactions, e.g. $\pi^{\pm} p \rightarrow \rho^{\pm} p$, have cross-sections which are compatible with equality.

(b) There is a large amount of data although not over a wide range of energies.

(c) The coupling structure at the two vertices is summarized below.

τP	$G(-1)^{T}P$	Type	Nonconspiracy		Conspiracy	
			Meson Vertex	$N\bar{N}$ Vertex	Meson Vertex	$N\bar{N}$ Vertex
+	+	I	$\gamma'_1 = -\gamma'_{-1} \sim \sqrt{t}$ $\gamma'_0 = 0$	$\gamma'_{++} = \gamma'_{--} \sim \text{const}$ $\gamma'_{+-} = \gamma'_{-+} \sim \sqrt{t}$	$\gamma'_1 \sim \text{const}$ $\gamma'_0 = 0$	$\gamma'_{++} \sim \sqrt{t}$ $\gamma'_{+-} \sim \text{const}$
-	+	II	$\gamma'_1 = \gamma'_{-1} \sim \sqrt{t}$	$\gamma'_{++} = \gamma'_{--} = 0$ $\gamma'_{+-} = -\gamma'_{-+} \sim \text{const}$		
-	-	III	$\gamma'_0 \sim \text{const}$	$\gamma'_{++} = -\gamma'_{--} \sim \sqrt{t}$ $\gamma'_{+-} = \gamma'_{-+} = 0$	$\gamma'_1 \sim \text{const}$ $\gamma'_0 \sim \sqrt{t}$	$\gamma'_{++} \sim \text{const}$ $\gamma'_{+-} = 0$

The structure of two couplings at the $N\bar{N}$ vertex for a type I pole can be ignored initially as we have no polarization data and always sum over the $N\bar{N}$ indices.

(d) There are again three density matrix elements measured experimentally: ρ_{00}, Re ρ_{1-1}, Re ρ_{10}.

From (4.4.2) we find the usual results

$$\tau P = + \ : \ \rho_{10} = \rho_{00} = 0 \qquad \rho_{11} = \rho_{1-1} > 0$$
$$\tau P = - \ : \ \rho_{00} \propto \gamma_0'^2 > 0 \qquad \rho_{11} = -\rho_{1-1} \propto \gamma_1'^2 > 0 \qquad (4.6.1)$$

This implies that if we form ρ_{00}, $\rho_{11} - \rho_{1-1}$ and $\rho_{11} + \rho_{1-1}$ we pick out the relative (leading order) contributions of the $\tau P = -, \gamma_0'^2$, $\tau P = -, \gamma_1'^2$ and $\tau P = +, \gamma_1'^2$ couplings respectively. The higher energy data have too large errors to make this very useful at the present although plotting these out does not contradict one's expectation of their energy dependence (e.g. $\tau P = +$ having a higher intercept than $\tau P = -$).

The above holds however many mesons are exchanged but if only one $\tau P = -$ Regge pole is present we have analogously to (4.5.3)

$$\rho_{00} (\rho_{11} - \rho_{1-1}) = 2 \rho_{01}^2 \qquad (4.6.2)$$

The experiments satisfy this to within their internal inconsistencies. (The 2.72 Gev $\rho^0 n$ data badly violates it but the 2.7 Gev data agrees well).

Now let us consider the expected t behaviour of the density matrix elements. As usual we take t = 0 and the thresholds separately and begin with t = 0. As we have an UE case H_t is singular at t = 0 but we can overcome this as the equal mass indices are summed over. Thus we can introduce the Trueman-Wick crossing matrices into (4.4.2), so that $\hat{\rho}_{mm'}$ is given by the same expression but with the $N\bar{N}$ indices belonging to the s not the t channel. (We also used this partial rotation in (4.3.8)). The hybrid amplitudes now appearing in the formula for $\hat{\rho}_{mm'}$ have the advantage of only having the physical region boundary singularity in t. So we find the following behaviour of the density matrix elements at t = 0 and the physical region boundary.

	Exact	← Asymptotic →				
		General Result	Nonconspiracy Regge Result	π nonconspiracy	conspiring π	conspirator
$\hat{\rho}_{00}$	const	const	const	$t/(t-m_\pi^2)^2$	$t/(t-m_\pi^2)^2$	0
$\hat{\rho}_{01}$	$\sin^{1/2}\theta$	$t^{1/2}$	$t^{3/2}$	$t^{3/2}/(t-m_\pi^2)$	$t^{1/2}/(t-m_\pi^2)$	0
$\hat{\rho}_{1-1}$	$\sin\theta$	t	t	t	const	$= -\pi$ contribution at t = 0
$\hat{\rho}_{11}$	const	const	t	t	const	$= +\pi$ contribution at t = 0

I have appended the nonconspiring and conspiring behaviour for the π and put in its pole as this occurs at essentially t = 0. The observed density matrix elements are of course

$\rho = \hat{\rho}/\mathrm{Tr}\,\hat{\rho}$.

We notice that the behaviour in the presence of conspiracy is the most singular allowed while in the nonconspiratorial case we have an extra vanishing in $\hat{\rho}_{01}$ and $\hat{\rho}_{11}$, and would expect ρ_{01} to be small and $\rho_{00} = 1 - 2\rho_{11}$ to be large near $t = 0$.

Now consider the thresholds. There are no conditions at the meson vertex for the $\tau P = +$ Regge poles to satisfy. Let us parameterize the π couplings at the meson vertex by

$$\gamma_0' = \frac{A}{T_{13}}$$
$$\gamma_1' = \frac{B\,\alpha_\pi\,\sqrt{t}}{T_{13}} \qquad (4.6.3)$$

We have thresholds $t = (m_1 \pm m_3)^2$ which are in our reactions

$\pi N \rightarrow \rho N$ $\qquad t = .4\ ,\ .8\ \mathrm{Gev}^2$

$KN \rightarrow K^* N$ $\qquad t = .16\ ,\ 1.9\ \mathrm{Gev}^2$

The amplitudes of (4.6.3) must satisfy there

$$A = \sqrt{2}\ \alpha\ t^{\frac{1}{2}}\ B \qquad (4.6.4)$$

where

$$\hat{\rho}_{01} \propto -\sqrt{-t}\ \ \alpha\ \ AB \qquad (4.6.5)$$

(4.6.4) is interesting as it relates the sign of A and B which on making minimal constancy assumptions and substituting into (4.6.5) gives a definite sign for ρ_{01}.

Taking just $t = (m_1 - m_3)^2$ gives as $\alpha_\pi < 0$ in the physical region, $\rho_{01} > 0$. If you allow A a linear variation in t and apply (4.6.4) at both thresholds you find $\rho_{01} < 0$ but in any case it is small being proportional to $\sqrt{-t}\,(t-m_\pi^2) \sim (-t)^{3/2}$.

However if the π suffers conspiracy ρ_{01} is proportional to $(t-m_\pi^2)/\sqrt{-t}$ and for small t is large and predicted from (4.6.4) to be negative whether one includes $t = (m_1 \pm m_3)^2$ or just $t = (m_1 - m_3)^2$. Of course by allowing the π residues extra variation one can obtain either sign in this case as well.

Finally we note that the conspirator itself played little role in the above discussion of ρ_{01} to which it does not contribute as it has no helicity 0 coupling. Indeed it does not interfere with the π and only shows up in ρ_{11}, where it adds constructively to the π to make ρ_{00} smaller in the forward direction, and in ρ_{1-1}, where it adds destructively to the π to ensure ρ_{1-1} has the necessary vanishing at t = 0. Also note that the conspirator has its dominant contribution as spin flip at the $N\bar{N}$ vertex and so we may ignore its interference with other $\tau P = +$ mesons, such as the ω, whose most important coupling is non-flip.

(ii) $\pi N \to \rho N$

Here we have so much data that I have been forced to choose between those at similar energies. Also to save time on the computer in large fits I have combined successive bins to get ones about .1 Gev in width. This reduces χ^2 as it reduces statistical fluctuations but increases the ratio χ^2/degrees of freedom. Also the width of the ρ meson produces much greater systematic differences in σ_{total} than the statistical accuracy of the experiment would suggest. Thus it proved necessary to allow $d\sigma/dt$ scale factors in about one fifth of the experiments.

I tried three types of fit:

(a) First I took all the data with $p_{lab} \geqslant 4$ Gev which gave 120 data points. One difficulty is the 8 Gev $\rho^0 n$ experiment which has in two experiments σ_{total} varying from .24 to .39. Theoretically we do not expect the total cross section to be greater than .18 and so this data had to be allowed a scale factor which turned out to be rather large. The π dominates this reaction, e.g. at 8 Gev for $\pi^{\pm}p \rightarrow \rho^{\pm}p$ it is 2/3 of the cross section in $0 > t > -.1$ and ½ that in $0 > t > -1$. So we must decide on what to add to the π and I tried fits with π, A_2 ; π, ω ; π, ω, A_2 ; π, ω, c ; and π, ω, c, A_2 where c stands for conspirator. The first two fits were unsatisfactory giving $\chi^2 > 180$. The 3 and 4 pole fits (although of course the conspirator parameters are determined at t = 0 and so do not represent much extra freedom) were all satisfactory with χ^2 from 140 → 150. There is insufficient data to get conclusive evidence for conspiracy from the density matrix elements although ρ_{10} is always negative and the data agrees well with the conspiracy predictions. The nonconspiratorial fits were also good but did not represent a smaller number of parameters as the π residues required extra variation. I have always made the conspirator choose nonsense at $\alpha^c = 0$ so as not to produce a particle, and usually given it a slope of .5 although fits without the A_2 preferred a smaller one.

One point of interest is the ω parameters. Although this is the dominant $\tau P = +$ contribution the data is most insensitive to its energy dependence. However, whether it chooses sense or nonsense, its contribution should vanish when $\alpha^\omega = 0$. There is no particular dip in the data until $t \simeq -.4$ when there is some levelling off of $d\sigma/dt$ and ρ_{1-1} which is suggestive of a ω dip leavened by a conspirator or A_2 background. (This dip made fits with only π and ω unsatisfactory). I have tried fits without compelling the ω to vanish where $\alpha^\omega = 0$ but allowing the residue function a linear variation in t. In many of these fits the residue function chose to vanish at $t \simeq -.4$ and so I have taken $\alpha_0^\omega = .4$ and $\alpha_0^{'\omega} = 1$. (This goes through the ω pole and has an intercept in agreement with the t = 0 πN and KN elastic scattering analyses). But see the erratum.

One unfortunate feature of all the fits was the small scale factor (.1) preferred by the π.

(b) Encouraged by the above results it was decided to include the lower energy data. But first the three charge states were considered separately. This produced the expected results. $\rho^- p$ and $\rho^+ p$ needed similar parameters but $\rho^0 n$ needed much less $\tau P = +$ exchange. The small value of ρ_{00} in the $\rho^0 n$ data seems to indicate conspiracy but the agreement with the density matrix elements is inferior in all models (although there are serious discrepancies between the 2.7 and 2.72 Gev data). Unfortunately I have ignored ϵ^0 contamination which might be expected[J3] to produce some difference in normalization near $t = 0$. These runs weeded out experiments of inconsistent normalization and equipping these with scale factors we then combined all the data.

(c) On the combined data over all energies we found good agreement with $d\sigma/dt$. Unfortunately there is quantitative disagreement in the experimental density matrix elements at 2.7 and 2.72 Gev. In the $\rho^- p$ state the theory agrees best with the 2.72 Gev data which shows ρ_{1-1} increasing with t but dropping away for $t \simeq -.4$ in agreement with the ω dip. The 2.7 Gev data shows a consistently lower ρ_{1-1}. However in the $\rho^0 n$ state we agreed better with the 2.7 Gev data.

Fits were better with conspiracy as they gave a lower ρ_{00} and a better shape for ρ_{01}. However as the high energy data was consistent with no conspiracy this could be the effect of non-asymptotic terms which may be expected, from our earlier discussion, to destroy the predicted extra vanishing of ρ_{01}. Our model did not give an $s^{\alpha^\pi - 1}$ term capable of this but the

A_1 daughter has singular residues and is of type III and can interfere with the π. Still one must say that the data is consistent at present over all energies with conspiracy.

As the theoretical ρ_{1-1} was too high at 2.7 Gev (although satisfactory at 2.72 Gev) it may be that we are wrong in attributing all the deviations from π exchange to $\tau P = +$ mesons. The inclusion of the A_1 improved χ^2 somewhat and gave a better ρ_{1-1}; the A_1 daughter will also lower ρ_{1-1}.

On 270 data points typical values of χ^2 were 540 for π, ω,c and 460 for π, ω,c,A_2,A_1. Apart from ρ_{1-1} there were no systematic differences between theory and experiment and bearing in mind the increased statistics of the lower energy data the agreement between theory and experiment seems as good at low as at high energies. This is perhaps because non-asymptotic corrections to π exchange are small.

In figures 4.3 to 4.5 we give typical fits to $d\sigma/dt$ and the density matrix elements at 2.7 and 8 Gev.

(iii) $KN \rightarrow K^*N$

In $\pi N \rightarrow \rho N$ we have a fit which is very similar to the absorptive model. Thus we use the same dominant poles and possibly our conspirator represents the cut given by absorptive corrections. However $KN \rightarrow K^*N$ is more interesting in that the dominant pole is not that used in the absorptive model which has π and ω exchange. In both models π exchange is a much smaller fraction of the total cross section than in

$\pi N \to \rho N$ but in Regge theory the ω cannot have a large contribution as the experimental $d\sigma/dt$ shows no evidence at present for a dip at $t \simeq -.4$. Also SU_3 would suggest the ω is small but if the ω decides both to violate SU_3 and not to vanish when $\alpha^{\omega} = 0$ (this does not contradict analyticity), I have verified it gives as good a fit as the model to be described and it certainly has a more satisfactory energy dependence. Thus one would expect P and P' to be the other important poles. From exact SU_3 P exchange is forbidden while P' (associating it with f^0) has a reasonable coupling which ought to be larger (from the $N\bar{N}$ vertex) than the P" (associated with the f'(1500)) which has a lower intercept. The $d\sigma/dt$ distribution is rather broad suggesting a P' choosing nonsense but unfortunately the energy variation of σ_{total} shows a $1/s^2$ behaviour.

Now let us consider the three charge states separately as in contrast to $\pi N \to \rho N$ they show significant differences.

(a) $\underline{K^+p \to K^{*+}p}$

The experimentalists have done a Regge type fit to their data finding an effective $\alpha_0 = .26 \pm .27$ but this includes the π-contribution which is, for example, at 2.97 Gev one half the total cross section in $0 > t > -.1$ and one quarter that in $0 > t > -1$.

An interesting feature is ρ_{10} which is even positive in some experiments and so in accordance with our previous discussion fits with a conspiring π were hopeless. Thus I have tried some simple π + effective $\tau P = +$ meson fits. On 105 data points we had satisfactory fits for $\alpha_0 = .2$ and $.4$ with $\chi^2 \approx 160$ and all the disagreement at lower energies. For $\alpha_0 = .69$ (P') χ^2 was about 20 higher.

It is perhaps significant that this is the only reaction, out of those I have considered, which prefers nonconspiracy as it is also the one that, due to a lack of direct resonances, has least absorptive corrections.

(b) Charge exchange $K^+n \to K^{0*}p$ $K^-p \to \bar{K}^{*0}n$

For the exchanged poles I will consider, it requires $\rho - A_2$ interference to produce a difference between the cross sections for the two charge exchange reactions and this will be a small effect. Thus from isospin conservation the π is much larger than for $K^+p \to K^{*+}p$ and the previously dominant T = 0 mesons do not contribute. For example, even at 10 Gev the π and combined $\tau P = +$ contributions to σ_{total} are roughly equal.

As in $\pi^-p \to \rho^0 n$, ρ_{00} is rather small and so, unlike $K^{*+}p$, conspiracy is definitely favoured. The ρ and A_2 both give rather small contributions due to their weak $N\bar{N}$ coupling but the insufficient data and the effect of the $\tau P = +$ conspirator obscure any attempt to find a preference for one or the other.

The shape of $d\sigma/dt$ at 4.1 and 5.5 Gev is rather broader than expected theoretically (indeed all three charge states prefer a larger scale factor (.25) for the π than $\pi N \to \rho N$ but this may be an effect of the nearer threshold) while the cross section at 10 Gev is about 30% lower than expected.

The variation of the density matrix elements with t is so different at 4.1 and 5.5 Gev that no simple theory could fit them.

(c) $\underline{K^- p \to K^{*-} p}$

This charge state contains more data and a larger energy range than the other two and accordingly I have attempted more fits (70) than in any of the other reactions I have considered. ρ_{10} is negative for small t and although conspiratorial fits are satisfactory they prefer a smaller ratio $\gamma_1'/\gamma_0' \Big|_{t=0}$ than for $\pi N \to \rho N$ even when you take into account the different threshold positions. However the data is compatible with as large a conspiracy as in $\pi N \to \rho N$.

As we mentioned before the energy dependence of σ_{total} does not suggest the high intercept of the P'. Finding the π parameters from a fit to all the data we subtracted off the π and then fitted the remainder to a form proportional to $s^{\alpha_{effective}}$ finding

$$0 > t > -.3 \qquad \alpha_{effective} = .12 \pm .05$$

$$-.3 > t > -.9 \qquad \alpha_{effective} = -.4 \pm .06$$

where we averaged over the given t intervals to reduce the error. On dropping the accurate data in the 2 to 3 Gev range the value of $\alpha_{\text{effective}}$ in $0 > t > -.3$ was unaltered but the value for the second range changed to $-.7 \pm .12$.

We tried fits to π and an effective $\tau P = +$ meson of even signature with various intercepts and slopes. High values of α_0 ($\geq .4$) were only compatible if they had steep (1.5) slopes but the best fit occured with $\alpha_0 = .2$ and $\alpha_0' = 1.25$ which had a χ^2 of 530 on 180 data points. On adding a conspirator with a small slope (.5) which gave a significant contribution for large t, the necessity of associating steep slopes with high intercepts disappeared and the best fit occured with $\alpha_0 = .4$, $\alpha_0' = 1$ and a χ^2 of 400.

On dropping the data between 2 and 3 Gev the amount of π necessary dropped by some 20%. (This was like $\pi N \rightarrow \rho N$ where the lower energy data needed more $\tau P = -$ than the π provided). Also as the most accurate experiments were now in the middle of the energy range the fits could pivot on these and on varying the intercept between .1 and .7 χ^2 only varied by 20 with a minimum of 280 for $\alpha_0 = .4$ (and 120 data points).

We may conclude that the reaction is probably dominated by a P' type Regge pole whose parameters are rather sensitive to the method of analysis employed but whose preferred average intercept is nearer .4 than .69.

(d) <u>All Charge States</u>

We then tried a few runs on the combined data. This was probably not very useful as the separate charge states analyses had suggested very different π parameters for the three cases. Thus $K^{*+}p$ did not want conspiracy while $K^{*-}p$ although consistent with no conspiracy needed a π helicity 1 coupling of the opposite sign to $K^{*+}p$. Finally $\bar{K}^{*0}n$ definitely wanted conspiracy. We included nothing in our fits to resolve these discrepancies but $d\sigma/dt$ was fitted reasonably well with the $\bar{K}^{*0}n$ too large theoretically at the higher energies. The residue at the pole agreed well with that expected from the K^* width. (We had similar agreement for $\pi N \rightarrow \rho N$ although the width seems less well determined experimentally).

On 320 data points our χ^2 varied from 1040 for π, P' and A_2 exchange to 820 for π, c, P', ω and the D meson. We added the D meson in an attempt to lower the theoretical ρ_{1-1} at low energies and also I hoped it might reduce the amount of π necessary leaving, as the D meson is T = 0, a smaller predicted charge exchange cross section. It succeeded in the first aim but did not have a large enough contribution near t = 0 for the second hope to be realised.

In the above fits the contribution of the $\omega \sim$ one fifth that of P' and one would expect it to be small as the near equality of the K^{*-} and K^{*+} cross sections suggest little P', ω interference which is of opposite sign in these two reactions.

Due to the above mentioned discrepancies ρ_{10} which usually gave a small contribution to χ^2 now gave as much as the other density matrix elements.

The difference between K^* and ρ production is illustrated in figures 4.6 and 4.7.

4.7 Double Resonance Production

(i) Constraints

In Section 4.5 on N^* production we only had $\tau P = +$ exchange. We must now consider $\tau P = -$ exchange. This has at the lower threshold 2 constraints

$$\begin{aligned} \sqrt{3}\ (\gamma'_{\frac{1}{2}\frac{1}{2}} - \gamma'_{-\frac{1}{2}\frac{1}{2}}) &= \gamma'_{3/2\ \frac{1}{2}} - \gamma'_{-3/2\ \frac{1}{2}} \\ \sqrt{3}\ (\gamma'_{3/2\ \frac{1}{2}} + \gamma'_{-3/2\ \frac{1}{2}}) &= \gamma'_{\frac{1}{2}\frac{1}{2}} + \gamma'_{-\frac{1}{2}\frac{1}{2}} \end{aligned} \qquad (4.7.1)$$

where all amplitudes $\sim 1/[t - (m_2 - m_4)^2]^{\frac{1}{2}}$.

There are at the top thresholds four constraints which we as usual ignore. (The difference in the number of constraints at the two thresholds is because the lighter particle is a fermion according to our earlier discussion about the change in the effective parity for ℓ' states).

Experimentally $\tau P = -$ mesons appear to have less spin flip than the $\tau P = +$ which may be connected with the reduced number of constraints.

(ii) General Discussion

These reactions are interesting as they provide opportunities to test factorization as the spin structure at each vertex should be the same as in the single resonance production processes.

$\pi^+ p \rightarrow \rho^0 N^{*++}$ has been considered in detail by T. W. Rogers. We may remark here that ρ_{10} is negative as one expects at the very least from factorization and our $\pi N \rightarrow \rho N$ fits. There is such difficulty with the normalization and the behaviour of $d\sigma/dt$ near $t = 0$ that it is difficult to carry the factorization tests further.

$\pi^+ p \rightarrow \omega^0 N^{*++}$ M2),S5) has ρ and B exchange with about 50% of each at 4 Gev. From the density elements the amount of ρ is seen to increase by 8 Gev in agreement with one's expectations. In accordance with this situation is the dip in $d\sigma/dt$ at $t = 0$ where the ρ meson contribution vanishes. I have not had time to see if the coupling structure for the ρ meson determined from $\pi N \rightarrow \pi N^*$ is in quantitative agreement with this although it is encouraging that ρ_{33} does seem to be about 50% the πN^* value and increases with energy.

The only reaction of this kind, that we have made quantitative fits to, is $K^+ p \rightarrow K^{*0} N^{*++}$.

(iii) $K^+ p \rightarrow K^{*0} N^{*++}$

Like the charge exchange reaction in single resonance (K^*) production this isolates the π exchange contribution as being dominant. Some $\tau P = +$ exchange is however necessary and ρ

and A_2 are available. Both improve the fit obtained with π alone: ρ by decreasing the theoretical value of ρ_{00} near $t = 0$ and A_2 by increasing the cross section for large t.

ρ_{10} is always negative and the π parameters necessary for the $K\bar{K}^*$ vertex are in rough accordance with those found in $K^{*-}p$ and $K^{*0}n$ production. The available data does not enable one to distinguish conspiracy as even at 5 Gev the physical region boundary is still at $t = -.05$ and so we have no data at small t. There is no agreement with the positive ρ_{10} of $K^{*+}p$ which we tentatively associated with the lack of direct resonances in the K^+p system. As there is only one $K^{*+}p$ experiment incompatible with negative ρ_{10}, perhaps $K^+p \rightarrow K^{+*}p$ will eventually turn out to agree with the other three reactions supporting negative ρ_{10}.

Conspiracy, from the discussion of Section 4.3, would suggest $d\sigma/dt$ vanishing at $t = 0$. There is no evidence in the published data for a turnover in $d\sigma/dt$ and in my fits without conspiracy I find good agreement with the expected π residue at its pole. This contrasts with $\pi^+p \rightarrow \rho^0N^{*++}$ and indeed whereas the Born terms for this and $K^+p \rightarrow K^0N^{*++}$ differ by a factor 3 the experimental cross sections are roughly equal.

Again one should be able to enforce the ρ and A_2 couplings from the πN^* and KN^* analyses respectively. However it will be less interesting than for ω^0N^{*++} as the combined ρ, A_2 contribution is only about 20% that of the π.

Table of Experimental Data Used

Reaction	Reference	Lab. momentum	No. of events	No. of $d\sigma/dt$ values	No. of sets of density matrix element values
$\pi^+p \rightarrow \pi^0N^{*++}$	P.L. 7, 125 (1963)	1.59	115	11	0
	P.L. 13, 341 (1964)	2.79	70	12	0
	P.R. 136, B195 (1964)	3.54	100	20	0
	P.R. 138, B897 (1965)	4	180	14	4
	P.L. 19, 608 (1965) and P.L. 22, 533 (1966)	8	?	8	1
$K^+p \rightarrow K^0N^{*++}$	P.R. 142, 913 (1966)	1.96	290	7	1
	John Hopkins University Preprint	2.26	240	7	2
	N.C. 36, 1101 (1965)	2.97	180	10	3
	N.C. 46, 539 (1966)	3.5	180	5	0
	N.C. 46, 539 (1966)	5	?	4	0
$K^+p \rightarrow K^{0*}N^{*++}$	P.L. 6, 62 (1963)	1.96	280	9	0
	N.C. 39, 417 (1965)	2.97	500	11	5
	N.C. 46, 539 (1966)	3.5	650	5	4
	N.C. 46, 539 (1966)	5	500	4	3

Reaction	Reference	Lab. momentum	No. of events	No. of $d\sigma/dt$ values	No. of sets of density matrix element values
$K^- p \rightarrow K^{*-} p$	P.R.L. 16, 485 (1966)	2.1	1500	9	9
	P.R.L. 16, 485 (1966)	2.45	570	3	3
	P.R.L. 16, 485 (1966)	2.64	2150	13	13
	P.L. 12, 352 (1964)	2.97	310	5	3
	P.L. 14, 338 (1965)	3.5	160	20	0
	Argonne Preprint	4.1	1000	18	4
	Argonne Preprint	5.5	600	18	4
	Unpublished	6	350	25	0
	Unpublished	10	?	13	0
$K^+ p \rightarrow K^{*+} p$	P.R. 142, 913 (1966)	1.96	170	6	1
	John Hopkins University Preprint	2.26	220	8	2
	P.R.L. 15, 737 (1965)	2.3	250	25	2
	N.C. 36, 1101 (1965)	2.97	180	10	3
	N.C. 46, 539 (1966)	3.5	430	5	4
	N.C. 46, 539 (1966)	5	?	5	1
$K^+ n \rightarrow K^{*0} p$	P.R.L. 15, 737 (1965)	2.3	750	25	3

Reaction	Reference	Lab. momentum	No. of events	No. of $d\sigma/dt$ values	No. of sets of density matrix element values
$K^-p \rightarrow \bar{K}^{*0}n$	Argonne Preprint	4.1	135	18	4
	Argonne Preprint	5.5	100	18	4
	Unpublished	10	?	9	1
$\pi^-p \rightarrow \rho^-p$	UCRL 16877	2.05	250	20	0
	P.R. 152, 1183 (1967)	2.14	620	10	3
	UCRL 16877	2.36	360	20	0
	P.R. 153, 1423 (1967)	2.7	1000	30	9
	UCRL 16877 average from 2.05 → 3.22	≃ 2.72	2200	0	12
	P.R. 145, 1128 (1966)	2.88	720	5	4
	UCRL 16877	3.22	630	20	0
	Purdue Preprint	4.2	450	30	3
	P.L. 24, 112 (1967)	8	160	6	5
	Unpublished	11	?	0	2
$\pi^+p \rightarrow \rho^+p$	P.R. 145, 1072 (1966)	2.08	850	30	0
	P.R. 142, 896 (1966)	2.9	530	10	1
	P.R. 138, B897 (1965)	4	175	14	4
	P.L. 19, 608 (1965) and P.L. 22, 533 (1966)	8	?	10	1

Reaction	Reference	Lab. momentum	No. of events	No. of $d\sigma/dt$ values	No. of sets of density matrix element values
$\pi^- p \rightarrow \rho^0 n$	UCRL 16877	2.05	430	20	0
	UCRL 16877	2.36	500	20	0
	P.R. 153, 1423 (1967)	2.7	2200	30	6
	UCRL 16877 average from 2.05 → 3.22	≏ 2.72	3500	0	10
	P.R. 145, 1128 (1966)	2.88	1180	5	0
	UCRL 16877	3.22	920	20	0
	N.C. 31, 729 (1964)	4	150	7	0
	Orsay Preprint	8	160	13	0

Figure 4.1

$\pi^+p \to \pi^0 N^{*++}$ at 4 Gev. (As in all the figures $d\sigma/dt$ is plotted on a logarithmic scale). A fit to ρ and ρ' exchange. The solid line represents the ρ contribution and the dashed line the total contribution.

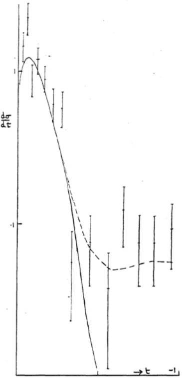

Figure 4.1

Figure 4.2

$K^+p \rightarrow K^0N^{*++}$ at 2.97 Gev. A fit to A_2 only. Notice the characteristic difference between this and the ρ cross section of the previous diagram.

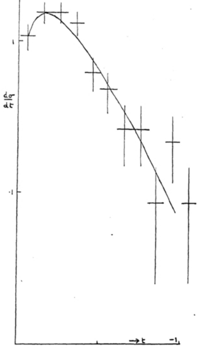

Figure 4.2

Figure 4.3

$\pi^- p \to \rho^- p$ at 2.7 Gev, from a fit to all the production data with π, ω and conspirator (c) exchange. The solid line is the total contribution and the dashed line the ω and c ($\tau P = +$) contribution. The disagreement on the first point on this and the next diagram is attributed to the forward scanning bias.

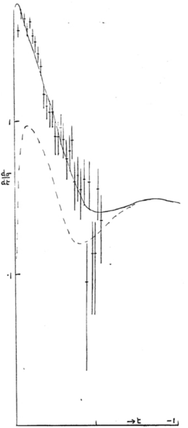

Figure 4.3

Figure 4.4

$\pi^- p \rightarrow \rho^- p$ at 8 Gev (solid lines) and
$\pi^+ p \rightarrow \rho^+ p$ at 8 Gev (dotted lines).
From the same fit as the previous diagram with non-interfering ω and c giving the same theoretical cross section for these two reactions. Again the solid and dashed lines are the total and ω + c contributions respectively.

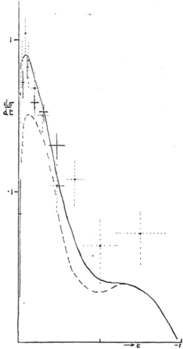
1
·1
$\frac{d\sigma}{dt}$
→ t
-1

Figure 4.5

Density matrix elements for $\pi^- p \rightarrow \rho^- p$ at 2.7 Gev from fits to all the $\pi\rho$ data. The solid line is a fit to π, ω and A_2 and the dashed line a conspiratorial fit to π, A_1, c, ω, A_2. Notice the characteristic differences in ρ_{10} and the dips in ρ_{1-1} due to the ω trajectory passing through zero.

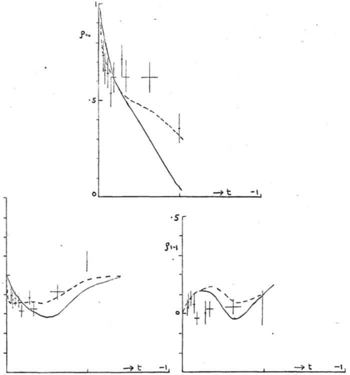

Figure 4.5

Figure 4.6

$K^- p \rightarrow K^{*-} p$ at 2.64 Gev from a fit to all the K^* production data with π, D, c, ω and P' exchange. Again the solid line is the total and the dashed line the c, ω and P' contribution.

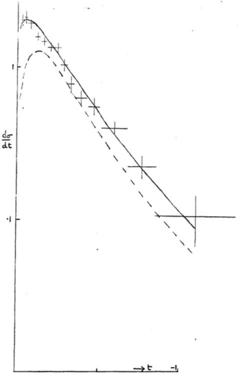

Figure 4.6

Figure 4.7

The density matrix elements from the same reaction and the same fit as the previous diagram. In ρ_{10} and ρ_{1-1} one sees the π for small t and the D for large t as the dominant $\tau P = -$ contribution.

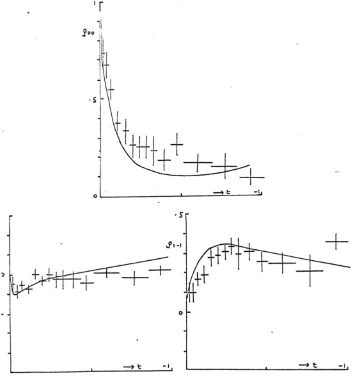

Figure 4.7

Erratum

Two mistakes have been found.

(i) In subsection 4.3 (i) it was not emphasized that the improvement in the position of the cut in s following from using z^{α} not s^{α} only occured for special mass values. Perhaps a better method is to replace $(e^{-i\pi\alpha} + \tau)s^{\alpha}$ by $e^{-i\pi\alpha} \times (s - s_{threshold})^{\alpha} + \tau(u_{threshold} - u)^{\alpha}$ but this leads to ghosts for certain integral values of α .

(ii) In Section 4.6 the ω parameters do not agree with those following from factorization and the elastic scattering data. This analysis of this latter data suggests that all the ω residue functions vanish at $t \simeq -.13$. Fits to $\pi N \to \rho N$ which enforce this behaviour agree well with the high energy data with one important exception. This is the accurate 4.2 Gev $\pi^- p \to \rho^- p$ data where neither ρ_{00} shows the expected rise nor ρ_{1-1} the expected dip at $t \simeq -.13$. However recent $\pi^- p \to \rho^0 n$ data at 4.2 and 8 Gev confirm the view that the dominant $\tau P = +$ contribution to $\pi N \to \rho N$ is T = 0 exchange. This should be the ω as from SU_3 the $\phi\pi\rho$ coupling vanishes.

CHAPTER 5

Electromagnetic Corrections to the Strong Interactions

5.1 Introduction

The topics to be discussed in this chapter bear no relation to the previous work in this thesis. Indeed, for these topics, we will avoid the complications due to spin, and will consider only spinless non-identical particles.

There are many excellent accounts in the literature of the theory of combining the strong and electromagnetic interactions. However they use rather different, and in some cases unfashionable, methods. We can separate four approaches.

(i) Low-energy

Here potential[H3)] and N/D[N1)] methods may be used. The nonrelativistic problem of the N/D method has been solved by Cornille and Martin[C2)]. This will provide a good basis for any N/D approach as an N/D calculation is only expected to be reliable at low energies. We will consider this in Section 5.4, which is on Dashen's[D2)] calculation of the p-n mass difference, where we will relate his method to these standard[C2)] results.

(ii) High-energy Elastic Scattering at $t = 0$

By this we mean the theory[B3),R1),S6)] necessary to extract the "pure nuclear" amplitude from experimental measurements. We will consider it in Section 5.3 and translate the previous methods into on-mass shell language. Also we compare it with other situations (e.g. the absorptive model) where one is faced with the problem of combining two potentials.

(iii) General Relativistic Theory

This is expounded in the massive work by Yennie, Frautschi and Suura[Y1]. Here it is shown how one can extract the infra-red divergent factors from matrix elements in such a way that experimental quantities are finite. They also prove that under certain circumstances (e.g. large angle scattering but not unfortunately[S6] under the conditions of (ii)) this gives the dominant radiative corrections at high energy.

(iv) Rigorous Results

In (iii) the infra-red divergence was treated by using the standard field theory of a massive photon whose mass λ tends to zero at the end of the calculation. In this limit, and working to all orders in e^2, the amplitude for the production of a finite number of photons is zero. However summing over all possible numbers of photons gives finite experimental quantities which can usually be calculated, as shown in (iii), from the result to first order in e^2. In a treatment which gives the photon a zero mass from the start, it is unsatisfactory not to have a finite amplitude (as opposed to finite cross sections) and so one can follow Chung[C3),F7] and define scattering amplitudes between states containing an infinite number of photons. Although it is very pleasing to treat the electromagnetic interaction to all orders in e^2, it seems unlikely that any practical schemes will be based on such an approach. Thus Section 5.2 suggests that the analyticity of the amplitude, to all orders in e^2, is unsatisfactory whereas, to any finite order in e^2, it can be treated by the methods usually applied for non-zero mass particles. So it would seem sufficient to treat the amplitude to first order in e^2, adding in the corrections due to higher order terms, when they are enhanced by the long-range nature of the Coulomb force. (This would be necessary, for instance, at threshold and at $t = 0$ in elastic scattering). We shall adopt this pragmatic approach in the following considerations.

(v) Definitions

In order to discuss the best estimate of the "pure nuclear" scattering amplitude we may define some amplitudes.

The nonrelativistic scattering amplitudes is

$$f = \frac{1}{8\pi \sqrt{s}} \quad T ,$$

where T is as defined in the appendix to Chapter 2. We define the Coulomb scattering amplitude f_c, with no strong interactions present, by

$$f_c = \frac{1}{p} \sum_{\ell} (2\ell + 1)\, e^{i\delta_\ell^C} \sin \delta_\ell^C \, P_\ell(\cos\theta_s) \qquad (5.1.1)$$

with phase-shifts δ^C.

Similarly introduce the strong interaction amplitude f_s with phase δ^S and the combined amplitude f_{c+s} with phase δ^{C+S}.

Define $\bar{\delta}$ by

$$\delta_\ell^{C+S} = \bar{\delta}_\ell + \delta_\ell^C \qquad (5.1.2)$$

and put $f_{c+s} = f_c + f_2$ where

$$f_2 = \frac{1}{p} \sum_{\ell} (2\ell + 1)\, e^{2i\delta_\ell^C} e^{i\bar{\delta}_\ell} \sin \bar{\delta}_\ell \, P_\ell(\cos\theta_s) \qquad (5.1.3)$$

f_2 might be our first guess at the "nuclear" amplitude but as we will see later a better choice under some circumstances is f_1 defined by

$$f_1 = \frac{1}{p} \sum_{\ell} (2\ell + 1)\, e^{i\bar{\delta}_\ell} \sin \bar{\delta}_\ell \, P_\ell(\cos\theta_s) \qquad (5.1.4)$$

Nonrelativistically f_1 has an infra-red convergent perturbation series and it may be interesting to note that it may be found from

$$\left\langle \begin{matrix}\text{in strong}\\ \text{in Coulomb}\end{matrix} \;\middle|\; \begin{matrix}\text{strong out}\\ \text{Coulomb in}\end{matrix} \right\rangle \qquad (5.1.5)$$

i.e. it is the scattering matrix generated by the strong potential where in both the initial and final states one takes, as basis states, Coulomb "in states", rather than the plane wave states used when there is no electromagnetic interaction. Of course we find f_{C+s} by taking out boundary conditions for both potentials in the ket.

Relativistically we have the extra infra-red divergence associated with photon emission, and f_1 still has this divergence.

We will also need the relation[R1)]

$$f_1 = f_2 - 2ip \int f_c^* \; f_2 \; \frac{d\Omega}{4\pi} \tag{5.1.6}$$

We will compare the analyticity of f_1 and f_2 in Section 5.2 where we use potential theory as a guide.

In Sections 5.3 and 5.4 we consider the methods of (ii) and (i) respectively.

I would like to thank J.-K. Storrow for discussions on these problems and his work with Landshoff on the more rigorous aspects.

5.2 Nonrelativistic Analyticity

We will consider the analyticity of f_1 and f_2 in non-relativistic potential theory. This will not be done rigorously but, as we shall find a rather unpleasant behaviour from our own limited treatment, it seems unlikely that either relativity or a fuller nonrelativistic theory will make this any better.

The relativistic and nonrelativistic results are manifestly similar to first order in e^2, as long as one takes care of

relativistic crossed diagrams by permuting s, t and u in the argument below. In particular the distinction between s and t disappears relativistically and, for instance, one can obtain the same result for the nature of the singularity of 
(⁓ = a photon) from my nonrelativistic result ((i) below), or from inserting a one photon, nucleon intermediate state in t channel unitarity.

(i) Analyticity in t

Working to first order in the strong interaction coupling, but to all orders in the electromagnetic interaction, we may calculate[N1]

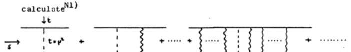

which is (for a zero-mass photon)

$$f_1 = f^2 M \;\; e^{-\pi\eta} \;\Gamma(1+i\eta)\;\Gamma(1-i\eta)\;\frac{\left[\mu - 2ip\right]^{2i\eta}}{\left[\mu^2 + 4p^2\right]^{i\eta + 1}} \qquad (5.2.1)$$

$$ {}_2F_1\;(1+i\eta, 1-i\eta,\; 1,\; \frac{2p^2}{\mu^2 + 4p^2}\;\;(1 + \cos\theta)\;)$$

$$f_2 = f^2 M \;\; e^{-\pi\eta}\;\;\left[\Gamma(1+i\eta)\right]^2\;\;\frac{\left[\mu - 2ip\right]^{2i\eta}}{\mu^{2i\eta + 2}} \qquad (5.2.2)$$

$$ {}_2F_1\;(1+i\eta,\; 1+i\eta,\; 1;\; t/\mu^2)$$

where

$$\eta = \frac{M\, e^2}{2p} \qquad (5.2.3)$$

. The pole at $t = \mu^2$ has been joined by an infinite number of cuts starting there. In f_2, we see from (5.2.2) that this gives a behaviour $(t - \mu^2)^{-1-2i\eta}$ to the amplitude. We note that:

(a) The dispersion integral over the discontinuity of such a function does not converge unless provided with predetermined subtractions. This is done automatically by using a photon mass $\lambda^2 \to 0$ but in fact presents no difficulty[S7].

(b) The pole is somewhat obscured by the cuts and relativistically one must be careful about the definition of the electromagnetic mass and coupling constant changes. This is again specified by separating the pole and the cut with a photon mass λ^2.

(c) To first order in e^2 the amplitude $f_2 \sim \frac{\ln x}{x}$ $(x = t - \mu^2)$ and the Landau curve of  has degenerated into the pair of lines $t = \mu^2$ and $p^2 = 0$.

(d) The result that the singularity on the Landau curve of  due to  is only logarithmically worse than the original singularity of , extends to case when we have any number of strong lines. Thus, as in the non-coulomb case, the singularity on the Landau curve improves by a power ½, up to logarithms, each time we add a strong line.

The diagrams, such as 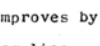, are enhanced to be larger than $O(\alpha)$ by the long range nature of the coulomb force. Although one may not be able to calculate the detailed coulomb corrections one can hope to estimate this enhancement.

In the analyticity approach, this enhancement manifests itself as the rather singular cut we have just discussed. One can therefore decide that the task of evaluating large coulomb corrections reduces to exhibiting functions which do not have such singular cuts.

As from (5.2.1) we find that $f_1 \sim$ original pole term + a term $\propto \ln (t - \mu^2)$ we have a reason for believing f_1 to be a better estimate than f_2 of the "nuclear" amplitude.

These results have been generalized to the relativistic case by Storrow[L2].

(ii) Analyticity in s

(a) Threshold Behaviour

Cornille and Martin[C2] have shown that

$$\frac{e^{i \bar{\delta}_\ell} \sin \bar{\delta}_\ell}{C^2 \, p \, \Pi_\ell} \tag{5.2.4}$$

has a bounded right hand cut determined by a suitable form of unitarity (5.4.1). Here

$$\begin{aligned} C^2 &= 2\pi\eta / (e^{2\pi\eta} - 1) \\ \Pi_\ell &= \prod_{\lambda=1}^{\ell} \left(p^2 + \frac{M^2 e^4}{4\lambda^2}\right) \end{aligned} \tag{5.2.5}$$

We can now try to investigate the analyticity of the full amplitudes by summing their partial wave series (5.1.3) (5.1.4). We obtain a different result from the non-coulomb case because the partial wave amplitude no longer has a factor $p^{2\ell}$ to cancel the $1/2p^2$ in $\cos\Theta = 1 + t/2p^2$. So we find that for general fixed t, f_1 and f_2 have an essential singularity as $p^2 \to 0$ while f_1/c^2 has satisfactory analyticity regarded as a function of s and $\cos\Theta$. However for the particular case $t = 0$ in elastic scattering ($\cos\Theta = 1$) we may write a fixed t dispersion relation.

(b) Difference between f_1 and f_2

f_2 may not be numerically very like the nuclear amplitude (see Section 5.3) but it does at least have expected crossing and analyticity properties.

f_1 is defined especially w.r.t. the s-channel, and so cannot have easy $s \leftrightarrow u$ crossing properties. Also it has some unexpected s singularities below threshold which normally only appear on unphysical sheets. Thus from (5.1.6) we see that f_1 is not only singular when f_2 is but also when a t or u singularity of f_2 enters the domain of integration in (5.1.6)

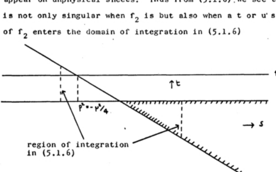

This is just like a K-matrix or the left-hand cut of a partial wave amplitude and the singularity begins at the same point $p^2 = -\mu^2/4$. The discontinuity is trivially evaluated and determines the singularity to be logarithmic. In the language of (i) the cost of removing the singular t discontinuity is this mild s singularity plus a similar remaining logarithmic t singularity. According to the philosophy of (i), both are negligible away from the cut, unless one was using f_1 in a dispersion relation working to an accuracy of $O(\alpha)$.

We would like to point out a relation between this unphysical singularity and (5.1.5) which shows f_1 to be specified by a mixed $i\epsilon$ prescription i.e. the ket has opposite boundary conditions for the coulomb and strong interactions. Thus in a Lippmann-Schwinger formalism we have to first order in the electromagnetic interaction but to all orders in the strong interactions

$$f_2 - f_s = 2f_s\, G\, f_c + f_s\, G\, f_c\, G\, f_s \qquad (5.2.6)$$

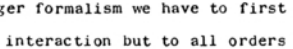

where G is the usual Greens function $\propto \frac{1}{q^2 - k^2 - i\epsilon}$

while

$$f_1 - f_s = f_s\, (G + G^*)\, f_c + f_s\, G\, f_c\, G\, f_s \qquad (5.2.7)$$

which has a principal value integral in the first term which removes the infra-red divergence at the cost of unsatisfactory analyticity.

The crossing and $p^2 = -\mu^2/4$ difficulty do not occur in f_1 for the leading Regge term in f_s at high energies.

Finally we note that f_1 is also singular when the t singularities of f_c enter the domain of integration. This indeed is its most important unexpected singularity and occurs at $p^2 = -\lambda^2/4$ i.e. $p^2 = 0$ in the limit $\lambda^2 = 0$. For the partial wave amplitude it is customary[C2] (cf. (5.2.4)) to draw the cut from 0 to ∞ and not to $-\infty$ as one expects. One then divides by a factor C^2 in order to ensure that the discontinuity over the new cut is given by unitarity. We will come across this again in Section 5.4.

5.3 Isolation of the Purely Nuclear Amplitude

It is customary to identify f_1 with the "nuclear" amplitude and we must now see under what circumstances this is true. It is certainly not true at low energies, as we see from Section 5.2, and we shall indicate at the end of this section reasons for doubting its usefulness at very high energies.

Using f_2 has taken account of graphs containing no strong vertices. In order to isolate the amplitude most like that when there is no electromagnetism (e.g. the amplitude which obeys SU_2), we will lay no claim to estimate graphs such as  which are $O(\alpha)$ but will try to estimate

 which is enhanced above O(α) by the long range nature of the coulomb force. There is a one to one correspondence between these latter graphs and infra-red divergent graphs.

Only for a long range force is  dominant over 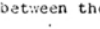 as for a perturbing force of the same range as the strong force they are of course identical.

One can discuss these problems with any of the classical approaches to high energy scattering[B3),I1),R1)] and Rix and Thaler[R1)] have noted the relation to the Feynman graph formalism[Y1)]. However in order to relate the problem to fashionable schemes, we will use an on-mass shell method.

(i) Nonrelativistic

The difference between f_1 and f_2 has been written out graphically in (5.2.6) and (5.2.7) showing how f_1 still has significant, albeit O(α), differences from f_s.

Work to first order in α and write

$$f_2 = f_s + \delta f$$

when unitarity gives

$$\text{Im } \delta f = 2p \int \frac{d\Omega}{4\pi} \left(\text{Re} f_s \, f_c + \text{Re}(f_s^* \, \delta f) \right) \qquad (5.3.1)$$

(a) Approximate Im δf by the first term in (5.3.1) and generate Re δf by a fixed t dispersion relation.

(b) Assume the integrand has no left-hand cut so that we find

$$\delta f \doteq 2ip \int f_s f_c \frac{d\Omega}{4\pi} \quad (5.3.2)$$

or

$$f_1 \doteq f_s \; \ldots \quad \text{as desired.}$$

Assumption (a) is justified as (5.3.2) makes the second term of (5.3.1) vanish identically. Assumption (b) is the crucial one in that it contains our long range philosophy which has yet to be used. Thus in Section 5.2 we considered the left-hand cut of (5.3.2) showing that it was for the $p^2 = -\mu^2/4$ singularity a mild logarithmic singularity and not enhanced by the long range force. The most dangerous part of the left-hand cut is that due to the photon pole but it can be treated as mentioned at the end of Section 5.2 by rotating the cut to run from 0 to ∞ and using a modified unitarity relation.

(ii) Estimations of f_1

Take the elastic reaction $1 + 2 \rightarrow 1 + 2$ at $t = 0$ when the particles have charges $z_1 e$ and $z_2 e$.

Then from (5.3.2)

$$f_2 - f_1 = ic \int_{-4p^2}^{0} \frac{dt'}{t' - \lambda^2} \; f_s \; (s,t') \quad (5.3.3)$$

where $c = \eta \; z_1 \; z_2$.

(a) Putting $f_s = f_s(s,0) \; e^{-At'}$ gives[R1)]

$$f_2 - f_1 = ic \log (A \; \lambda^2) \; f_s(s,0) \quad (5.3.4)$$

which, with $A = (R/2)^2$ and R a nucleon radius, gives Bethe's formula[B3] up to numerical factors inside the logarithm and this is consistent with the neglect of terms which are $O(\alpha)$.

(b) Soloviev[S6] puts $f_s = f_s(s,0)$ which is sufficient to remove the infra-red divergence but has little else in its favour for this particular application. Thereby we get

$$f_2 - f_1 = ic \log(\lambda^2/4p^2)\, f_s(s,0) \qquad (5.3.5)$$

which has a different energy dependence from (5.3.4). Of course Soloviev's result is quite sufficient if all one wishes is an infra-red finite answer and is not concerned with estimating radiative corrections.

(iii) Relativistic Analysis

The methods used in (i) and (ii) undergo important modifications when we introduce relativity.

(a) The change in the photon Born term in (ii) is as usual taken care of by replacing η by its relativistic value α/v_{lab}.

(b) In calculating Re δf by a dispersion relation in (i), we must use $\sqrt{s}\ \ \delta f$ to obtain correct relativistic analyticity. Then the extra $\sqrt{s}$ in the analogue of (5.3.2) has a left-hand cut which must be considered as well as that from the integrand. The fact that

$$P \int_{4m^2}^{\infty} \frac{\sqrt{s'}\ ds'}{p(s' - s)}$$

is non-zero whereas

$$P \int_{4m^2}^{\infty} \frac{ds'}{p(s'-s)} = 0$$

for $s > 4m^2$ is related to the fact that whereas nonrelativistically the infra-red divergent factor is pure imaginary, relativistically we have a real part cancelling with photon emission diagrams in experimental quantities.

(c) Thus to obtain consistent results we must add to (5.3.1) intermediate states containing one photon and any strongly interacting particles. This is not only due to diagrams such as

but also those like

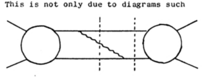

which have no infra-red divergence themselves whereas their 2-particle and 2-particle + photon discontinuities are separately divergent.

(5.3.1) becomes

$$\text{Im}\, \delta f^{\,f \leftarrow i} \simeq I_1 + I_2 + I_3 \quad . \qquad (5.3.6)$$

where

$$I_1 = \int d\Omega_2 (\text{Re}\, f_s^{f \leftarrow i} f_c^{i \leftarrow i} + \text{Re}\, f_s^{f \leftarrow i} f_c^{f \leftarrow f})$$

$$I_2 = \sum_n \int d\Omega_2 \,\text{Re} \left\{ \delta f^{f \leftarrow n} f_s^{*n \leftarrow i} + f_s^{*f \leftarrow n} \delta f^{n \leftarrow i} \right\}$$

and I_3 is the same as I_2 except that the intermediate state n has an extra photon. I_3 can be estimated[Y1] by making a pole approximation in the variable s_{12} defined below

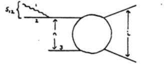

to get

$$I_3 \simeq \alpha \int d\Omega_2 \, \mathrm{Re}(f_s^{*f \leftarrow n} \quad f_s^{n \leftarrow i}) \cdot \left\{ \widetilde{B}^{\,f \leftarrow i} - \widetilde{B}^{\,n \leftarrow i} - \widetilde{B}^{\,f \leftarrow n} \right\} \tag{5.3.7}$$

where the function $\widetilde{B}$ is as defined in Yennie, Frautschi and Suura[Y1].

If we try to solve (5.3.6) in the form $\delta f = \gamma f$, there is, for our elastic t = 0 case, cancellation between I_2 and I_3, and we recover (5.3.4) or (5.3.5) for the coefficient of $\ln \lambda^2$. But we want to know whether to take (5.3.4) or (5.3.5) with their different quantities multiplying λ^2 to make it dimensionless. Here there is a real difficulty as this means we must estimate $\widetilde{B}$ which in reference[Y1] would lead to a result like (5.3.5). Although this estimate is presumably wrong I do not see how to obtain the same cut-off A in I_1 and I_3.

This may be a real difficulty as the term in $\delta f \propto \ln \lambda^2$

. represents a perturbation $d\alpha$ in the Regge pole at $j = \alpha$ we put in (5.3.4). This can be shown as, ignoring signature, a perturbed Regge pole gives an asymptotic behaviour $\delta f \sim \gamma f_s$ where

$$\mathrm{Re}\,\gamma \sim \log s \quad d\alpha(t)$$
$$\mathrm{Im}\,\gamma \sim -\pi \quad d\alpha(t)$$

However the rest of (5.3.4) with $A \sim \log s$ represents a cut at $j = \alpha$ + photon spin $- 1 = \alpha$ with a singular residue. Now it is well known that cannot have a cut in the j plane and so one may be sceptical about (5.3.4).

For the elastic $t = 0$ case $\widetilde{B}^{\,i \leftarrow i}$ is asymptotically negligible due to s-u cancellation and the trouble only occurs for $n \neq i$ in (5.3.7) and so perhaps (5.3.4) holds to higher energies than in the inelastic case.

The mechanism of the cancellation of the cut in  is probably best examined in a Feynman graph formalism as in Rothe[R2].

Finally we note a relation to another theory - the absorptive model - which is meant to correspond to a cancelled cut in the j plane.

Identify forces as below

Absorptive Model		Coulomb
strong	⟷	Coulomb
π exchange	⟷	strong

as entries on the first line are important only in elastic reactions while those on the second are thus the only inelastic forces. This mismatching of the short and long range forces in unimportant as diagrams such as 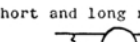 are symmetric and either force may be regarded as added "externally" to the other.

5.4 N/D Equations

We will now consider how one can include electromagnetic forces in an N/D equation. We will first treat the problem nonrelativistically pointing out the equivalence between Dashen and Frautschi's method[D1)] and that of Cornille and Martin[C2),N1)]. Finally we will consider relativistic effects. For convenience we will only treat s waves and let a_x be the $\ell = 0$ partial wave of the various amplitudes f_x introduced in Section 5.1.

(i) Nonrelativistic Treatment

When one considers the N/D equation for the long range coulomb perturbation it is natural, from a nearest singularity philosophy, to suppose that the left-hand cut of $a_{c+s} - a_s$ can be well approximated by the longest range force, namely single photon exchange. However, as we have seen in similar situations in the previous sections, this is incorrect and leads to infra-red divergences for one must also consider, for instance,  whose cut has moved up to coincide with that due to  . As we have said, using f_1 estimates  to some extent and so one may distinguish three approaches.

(a) Take $\delta a = a_{c+s} - a_s$ and include as its left-hand cut 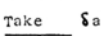 plus any diagram used in the original N/D calculation of a_s with an extra photon added i.e. if a_s had only the Born term  as its left-hand cut we would take 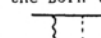 +  for the left-hand cut of $a_{c+s} - a_s$.

The formula of Dashen[D1] for the change δs_B in the bound state mass^2 on adding the coulomb perturbation is found as follows. Write $a_s = N/D$ and letting a_s have a pole $R/s - s_B$ we find

$$\frac{1}{2\pi i}\int_c \frac{D^2\ \delta a\ ds}{(s - s_B)} = D'^2(s_B)\ \delta s_B R \qquad (5.4.1)$$

where c is any counter clockwise contour surrounding $s = s_B$. The integrand has no right-hand cut and so we can convert c into an integral over the left-hand cut. It is easy (see (iii)) to prove (5.4.1) is non-infra-red divergent due to cancellation between  and 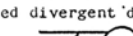 .
This is true even when, as above, we calculate a_s approximately from  and δa from  +  .
This is because the infra-red divergence of  is a function of s with no left-hand cut times  .

So its left-hand cut involves only $\mathrm{Im}\, a_s \Big|_{\mathrm{l.h.c.}}$, and not $\mathrm{Re}\, a_s$, and it is $\mathrm{Im}\, a_s$ that is calculated exactly in an N/D equation.

The change δR in the residue may be considered similarly using the equation

$$\frac{1}{2\pi i}\int_C \frac{D^2\,\delta a\,ds}{(s-s_B)^2} = D'^2(s_B)\,\delta R + \delta s_B\, D'(s_B)\, D''(s_B) R \quad (5.4.2)$$

However δR has an instrinsic infra-red divergence which is removed by specifying, for instance, that one should take the residue in f_1.

In his actual calculation[D2)], as opposed to the theory[D1)], Dashen uses a version of this method with, however, a rather dubious estimate of  .

(b) The second way of tackling the problem is to take $a_1 - a_s$ and only include  as the left-hand cut. This is the method advocated by Dashen and Frautschi[D1)].

(c) An entirely equivalent prescription to (b) is that based on the rigorous theory of Cornille and Martin[C2)]. Namely form $a'_{new} = a_1/C^2$ where C^2 is given by (5.2.5) and rotate the one photon left-hand cut to run from 0 to $+\infty$. Then we have

$$\mathrm{Im}\,\frac{1}{a_{new}}\Bigg|_{\mathrm{new\ r.h.c.}} = -\,p\,C^2 \qquad (5.4.3)$$

and we get the method (b) on assuming a_{new} has the same left-hand cut as a_s.

In order to estimate the error in the approximation (b) or (c) one need only refer to the work of Noyes and Wong[N1] where they explicitly evaluate the residual left-hand cut contribution of 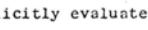 in a_{new}.

(ii) Example

In figure 5.1 we plot estimates of δs_B for Paton's[P2] example of the s-wave exponential potential. We have taken a potential of strength $- a/\mu^2 = 5$ (in Paton's[P2] notation) and give results for N = 1 or 2 where in the unperturbed problem we have taken up to the Nth Born terms. Three different ways have been used for the perturbed problem.

(α) All graphs included which contain one "photon" line and up to N strong lines. This is essentially the method (a).

(β) The naive method using graphs with one "photon" line and up to N - 1 strong lines. This is infra-red divergent.

(γ) As (β) but the graph containing N strong lines and an external "photon" is estimated as in the method (b) or (c).

From the figure (γ) may appear as good as (α) but this is probably a spurious effect as, in this model, all the higher order terms omitted in (α) are positive. Thus (γ) by over-estimating 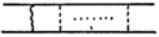 may be accidentally better.

To estimate the error due to a bad unperturbed solution note that with $s_B = - q_B^2$ we have the following values of q_B/μ.

exact		.74
approximate calculation	N = 3	.67
	2	.51
	1	.215

Similar results are obtained from calculations for δR. However, if one calculates the quantity on the right-hand side of (5.4.2) which is more rapidly convergent than δs_B in (5.4.1), the estimates (α), (β), (γ) become more nearly equal. But for low N, they are still in disagreement with the exact result showing the rapid convergence of the perturbed problem cannot overcome a bad unperturbed solution.

(iii) Relativistic Treatment

The modifications necessary are very similar to Section 5.3(iii). We will first indicate how one can exhibit the cancellation of the infra-red divergence in δS_B and then state which terms cancel among themselves.

In (5.4.1) we rewrite

$$\int_c = \int_{l.h.c.} + \int_{r.h.c.}$$

as an integral over the left- and right-hand cuts. Relativistically $\int_{r.h.c.}$ is non-zero due to the presence of photon emission diagrams. In the $\int_{l.h.c.}$ we replace δa by $\delta a'$ where

$\delta a = \delta a'$ + the perturbed pole terms whose parameters we are trying to find.

We now turn the $\int_{l.h.c.}$ into an integral over the right-hand cut giving

$$2\pi i\, D'^2(s_B)\ \delta s_B\ R = \int_{r.h.c.} \frac{ds}{s-s_B} \left\{ -\,\mathrm{Im}(\delta a'\, D^2) \right. \qquad (5.4.4a)$$

$$\left. +\ \mathrm{Im}(\delta a\, D^2) \right\} \qquad (5.4.4b)$$

This equation is less tautological than it appears as in (5.4.4a) $\delta a'$ is usually evaluated as $\delta a_{l.h.c.}$ (the integral over the left-hand cut of δa) while (5.4.4b) is evaluated from unitarity and has contributions only from photon emission diagrams. We have written $\delta a'$ rather than $\delta a_{l.h.c.}$ as then the infra-red divergences will cancel term by term in the integrand. (5.4.4) also allows a trivial extension to the new form of the strip approximation[J4)] where unitarity is only enforced for threshold $\leqslant s \leqslant$ strip boundary.

Infra-red divergent terms in (5.4.4) are; in (5.4.4a),

(α) $\delta a'$ is the partial wave projection of an infra-red divergent part of δf;

(β) The one photon Born term has an infra-red divergent partial wave projection;

while in (5.4.4b),

(γ) The photon emission contributions to unitarity are infra-red divergent.

(α) has contributions from 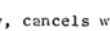 and  which are proportional to 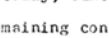 times a function with a real and imaginary part. The imaginary part, which is all that is present nonrelativistically, cancels with (β). The real part combines with the remaining contributions to (α), namely

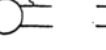   and  to

cancel with (γ).

We finish with four disconnected remarks on the relativistic case.

(a) The difference of

$$p\sqrt{s} = \sqrt{(s - (m_N + m_\pi)^2)\,(s - (m_N - m_\pi)^2)}$$

from its threshold value

$$\sqrt{(s - (m_N + m_\pi)^2)\, 4\, m_N\, m_\pi}$$

and in particular the left-hand cut of $p\sqrt{s}$ need photon emission diagrams to obtain cancellation of the infra-red divergence. This could suggest that photon emission diagrams are important at quite low energies for $\pi N \rightarrow \pi N$.

(b) The cancellation of the infra-red divergence will no longer occur for approximations to a_s as happened in the non-relativistic case. Thus the infra-red divergent part of

 will involve not only $\mathrm{Im}\, a_s \Big|_{\text{l.h.c.}}$ but also

Re a_s.

(c) Dashen's method calculates δs_B from an assumption about the strong interactions: namely that the particle is a bound state. The canonical field theory method[C4] calculates the mass change assuming the special form of the electromagnetic interaction. All graphs of this latter approach, for example,

where ------ is the bound state, occur in Dashen's method but are suppressed at high energy due to the two extra propagators p_1 and p_2 not present in the field theory method.

(d) Again one can treat the change δR in the coupling constant in the same way as δs_B but I think this is less useful for the reasons mentioned in Section 5.2 (i) (b).

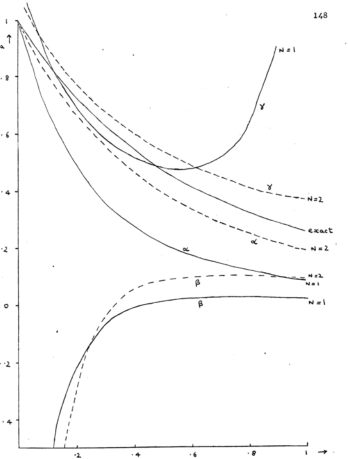

Figure 5.1

Figure 5.1

$\delta s_B / \delta a$ v. the ratio K of the unperturbed range μ to the perturbed range. δa is the change in the coupling strength and the other notation is explained in Section 5.4(ii).

REFERENCES

A1. M. Andrews and J. Gunson, J. Math. Phys. 5, 1391 (1964)

B1. A. Bialas and B. E. Y. Svensson, Nuovo Cimento, 42, 672 (1966)

B2. Bateman Manuscript Project (McGraw-Hill, 1953)

B3. H. A. Bethe, Ann. Phys. (U.S.A.) 3, 190 (1958)

C1. P. A. Carruthers and J. P. Krisch, Ann. Phys. (U.S.A.) 33, 1 (1965)

C2. H. Cornille and A. Martin, Nuovo Cimento, 26, 298 (1962)

C3. V. Chung, Phys. Rev. 140, B1110 (1965)

C4. W. N. Cottingham, Ann. Phys. (U.S.A.) 25, 424 (1963)

D1. R. F. Dashen and S. C. Frautschi, Phys. Rev. 135, B1190 (1964)

D2. R. F. Dashen, Phys. Rev. 135, B1196 (1964)

F1. G. C. Fox, "Methods for constructing invariant amplitudes free from kinematic singularities and zeros".

F2. D. Z. Freedman and J. M. Wang, "O(4) Symmetry and Regge pole theory".

F3. D. Z. Freedman and J. M. Wang, Phys. Rev. 153, 1596 (1967)

F4. J. Franklin, Phys. Rev. 152, 1437 (1966)

F5. G. C. Fox and E. Leader, Phys. Rev. Letters, 18, 628 (1967)

F6. D. Z. Freedman, C. E. Jones and J. M. Wang, Phys. Rev. 155, 1645 (1967)

F7. M. Froissart (seminar)

G1. M. L. Goldberger and K. M. Watson, Collision Theory (Wiley, 1964)

G2. M. L. Goldberger, M. T. Grisaru, S. W. MacDowell and D. Y. Wong, Phys. Rev. 120, 2250 (1960)

G3. E. Gotsman and Y. Frishman, Phys. Rev. 140, B1151 (1965)

G4. M. L. Goldberger and C. E. Jones, Phys. Rev. 150, 1269 (1966)

H1. Y. Hara, Phys. Rev. 136, B507 (1964)

H2. K. Hepp, Helv. Phys. Acta, 37, 55 (1964)

H3. J. Hamilton and W. S. Woolcock, Phys. Rev. 118, 291 (1960)

I1. M. M. Islam, "On Bethe's formula for Coulomb-Nuclear Interference".

J1. M. Jacob and G. C. Wick, Ann. Phys. (U.S.A.) 7, 404 (1959)

J2. J. D. Jackson and H. Pilkuhn, Nuovo Cimento, 33, 906 (1964)

J3. R. J. Jabbur and D. Griffiths, "Interference effects in rho meson decay".

J4. C. E. Jones, Nuovo Cimento, 40, 761 (1965)

K1. A. Kotanski, Acta Phys. Polon. 29, 699 (1966)

K2. A. Kotanski, Acta Phys. Polon. 30, 629 (1966)

L1. E. Leader and R. Omnes, "On the removal of singularities in the Regge asymptotic behaviour".

L2. P. V. Landshoff and J. K. Storrow, Cambridge preprint.

L3. E. Leader, Cambridge preprint HEP 67-6.

M1. I. Muzinich, J. Math. Phys. 5, 1481 (1964)

M2. D. R. O. Morrison, Report to Stony Brook Conference, 1966.

N1. H. P. Noyes and D. Y. Wong, Phys. Rev. 126, 1866 (1962)

O1. R. Odorico, "The use of helicity amplitudes in superconvergent sum rules".

P1. R. J. N. Phillips, "Is there a pion conspiracy".

P2. J. Paton, Nuovo Cimento, 43A, 100 (1966)

R1. J. Rix and R. M. Thaler, Phys. Rev. 152, 1357 (1966)

R2. H. J. Rothe, UCRL 17068.

S1. H. P. Stapp, Phys. Rev. 125, 2139 (1962)

S2. H. P. Stapp, UCRL 17429.

S3. A. R. Swift, J. Math. Phys. 6, 1472 (1965)

S4. A. R. Swift, Phys. Rev. Letters, 18, 813 (1967)

S5. N. Schmitz in C.E.R.N. 65-24.

S6. L. D. Soloviev, JETP (Sov. Phys.) 22, 205 (1966)

S7. L. D. Soloviev, Nuclear Phys. 64, 657 (1965)

T1. T. L. Trueman and G. C. Wick, Ann. Phys. (U.S.A.) 26, 322 (1964)

T2. J. R. Taylor, J. Math. Phys. 7, 181 (1966)

T3. R. W. Tucker, Cambridge preprint HEP 67-4.

T4. T. L. Trueman, Phys. Rev. Letters, 17, 1198 (1966)

T5. R. L. Thews, Phys. Rev. 155, 1624 (1967)

W1. L. L. Wang, Phys. Rev. 142, 1187 (1966)

W2. D. N. Williams, UCRL 11113.

W3. G. C. Wick, Ann. Phys. (U.S.A.) 18, 65 (1962)

W4. S. Weinberg, Phys. Rev. 133, B1318 (1964)

W5. S. Weinberg, Phys. Rev. 134, B882 (1964)

Y1. D. R. Yennie, S. C. Frautschi, H Suura, Ann. Phys. (U.S.A.) 13, 379 (1961)